

# Ionic Hydrogenation of Pyridinium and Azetidinium Cations

Zheren Jim Yang

Submitted in partial fulfillment of the requirements for the degree of  
Doctor of Philosophy in the Graduate School of Arts and Sciences

COLUMBIA UNIVERSITY  
2017

© 2017

Zheren Jim Yang

All Rights Reserved

## Abstract

### Ionic Hydrogenation of Pyridinium and Azetidinium Cations

Zheren Jim Yang

Research described herein seeks to study the reactivity of CpRu(P-P)H with pyridinium and azetidinium cations. For the former, we wish to determine if a previously established methodology for the regioselective reduction of a particular pyridinium cation may be extended to other pyridinium cations and if the methodology may be improved with the introduction of a pendant amine in the diphosphine. Our studies have shown that this methodology could not be extended to pyridinium cations having substituents on the pyridinium ring. For the latter, we seek to establish the reactivity of CpRu(P-P)H with azetidinium cations and compare these results to what the Norton Group has previously established in studies concerning aziridinium cations. Our studies have shown that opening of azetidinium is about six orders of magnitude slower compared to the opening of aziridinium.

## TABLE OF CONTENTS

List of Schemes	iv
List of Figures	vii
List of Tables	viii
List of Abbreviation	ix

### Chapter 1: Introduction

1.1. Overview	1
1.1.1. Inner-sphere hydrogenation of C=N bonds	1
1.1.2. Outer-sphere hydrogenation of C=N bonds using bifunctional catalysts	2
1.2. Stepwise ionic hydrogenation	4
1.2.1. Catalytic ionic hydrogenation	7
1.2.2. Ionic hydrogenation by Frustrated Lewis Pairs	11
1.3. Acid/base chemistry of transition metal dihydrogen and dihydride complexes	14
1.3.1. Effect of intramolecular amines on metal dihydrogen complexes	15
1.4. Goals of the research project	17
References	18

### Chapter 2: Ionic Hydrogenation of Pyridinium Cations

2.1. Previous efforts on the reduction of pyridinium cations	20
2.2. Attempt to ascertain the scope of the two-step hydride transfer	23
2.3. Addressing the catalyst deactivation using P <sub>2</sub> N <sub>2</sub> chelating ligands	27
2.3.1. Background of P <sub>2</sub> N <sub>2</sub> ligands	27

2.3.2.	Preparation of half-sandwich Group-8 metal hydride complexes bearing P <sub>2</sub> N <sub>2</sub> ligand	30
2.3.2a.	Half-sandwich hydride complexes bearing P <sub>2</sub> N <sub>2</sub> ligand	31
2.3.2b.	Intramolecular deprotonation and proton shuttling	34
2.3.2c.	Electrochemical properties	36
2.3.2d.	Half-sandwich Group-8 P <sub>2</sub> N <sub>2</sub> hydrides as electrocatalysts for the oxidation of dihydrogen	38
2.3.3.	Ionic hydrogenation of pyridinium cation with Cp*Ru(P <sub>2</sub> N <sub>2</sub> )H	40
2.4.	Experimental Procedures	45
	References	50
	Appendix	52

### Chapter 3: Ionic Hydrogenation of Azetidinium Cations

3.1.	Relevance of ring opening of azetidines and azetidinium cations	53
3.1.1.	General trends for nucleophilic ring opening of azetidinium cations	54
3.1.1a.	Nucleophilic ring opening of C2-substituted azetidinium cations	55
3.1.1b.	Effect of C2 aromatic substituent on the ring opening of azetidinium cations	58
3.1.1c.	Mechanism of nucleophilic ring opening	61
3.1.1d.	Ring opening of azetidinium cations by metal hydrides	62
3.1.1e.	Leaving groups that facilitate intramolecular substitution reaction in azetidinium cations	63
3.1.1f.	Kinetic studies of nucleophilic ring opening of azetidinium	63
3.1.2.	Ring opening of azetidinium via the generation of an ylide	65

3.2.	Previous studies of hydride transfer to aziridinium cation	67
3.2.1.	Regioselectivity and kinetics of ring opening of aziridinium cations	67
3.2.2.	Catalytic hydrogenation of aziridinium cations	68
3.2.3.	Single electron transfer to aziridinium cation 3.31d	69
3.3.	Opening of an azetidinium cation by a transition metal hydride	71
3.3.1.	Preparation of novel azetidinium cation	71
3.3.2.	Hydride transfer to azetidinium cation from CpRu(dppm)H	73
3.3.2.1.	Reaction order of hydride transfer to azetidinium cation from ruthenium hydride	74
3.3.2.2.	Temperature dependence of the rate constant of hydride transfer to azetidinium cation	77
3.3.4.	Ring opening of azetidinium by a catalytic amount of ruthenium hydride	80
3.3.5.	Hydride transfer to azetidinium cation from other hydride sources	82
3.3.6.	Reduction potential of azetidinium cation and single-electron transfer to azetidinium cation	83
3.4.	Experimental Procedures	88
	References	94

## List of Schemes

### Chapter 1:

Scheme 1.1	Inner-sphere hydrogenation of alkenes	1
Scheme 1.2	Inner-sphere hydrogenation of imines	2
Scheme 1.3	Hydrogenation of imines catalyzed by Shvo's Catalyst	4
Scheme 1.4	Stepwise ionic hydrogenation effected by $\text{CF}_3\text{COOH}$ and $\text{Et}_3\text{SiH}$	5
Scheme 1.5	Ionic hydrogenation catalyzed by $\text{Cp}(\text{CO})_2(\text{PR}_3)\text{MH}$	7
Scheme 1.6	Ionic hydrogenation of iminium cations catalyzed by $\text{CpRu}(\text{P-P})\text{H}$	8
Scheme 1.7	A catalytic hydrogenation of alkenes which calculations show to proceed via an ionic mechanism	9
Scheme 1.8	Iridium hydride catalyzed ionic hydrogenation of quinolines and iminium cations formed from tetrahydroquinolines	10
Scheme 1.9	Activation of dihydrogen by Frustrated Lewis Pairs (FLPs)	12
Scheme 1.10	Hydrogenation of an imine catalyzed by a FLP	13
Scheme 1.11	Heterolytic cleavage of a ruthenium dihydrogen complex having a pendant amine	16

### Chapter 2:

Scheme 2.1	Two step transfer of hydride from $\text{Cp}^*\text{Ru}(\text{dppf})\text{H}$ to a pyridinium cation	21
Scheme 2.2	Catalytic cycle for the reduction of a pyridinium cation by $\text{Cp}^*\text{Ru}(\text{dppf})\text{H}$	22

Scheme 2.3	Hydride transfer from [(PPh <sub>3</sub> )CuH] <sub>6</sub> to a pyridinium cation	23
Scheme 2.4	Self-disproportionation reaction of ruthenium hydride radical cation	25
Scheme 2.5	Preparation of P <sub>2</sub> N <sub>2</sub> ligands from primary phosphines	28
Scheme 2.6	Oxidation of formate ion by a Ni(P <sub>2</sub> N <sub>2</sub> ) <sub>2</sub> complex	30
Scheme 2.7	Preparation of CpFe(P <sub>2</sub> N <sub>2</sub> )Cl	32
Scheme 2.8	Preparation of CpFe(P <sub>2</sub> N <sub>2</sub> )Cl having substitution on Cp ring	32
Scheme 2.9	Conversion between CpFe(P <sub>2</sub> N <sub>2</sub> )Cl, CpFe(P <sub>2</sub> N <sub>2</sub> )H, and [CpFe(P <sub>2</sub> N <sub>2</sub> )(H <sub>2</sub> )] <sup>+</sup>	33
Scheme 2.10	Intramolecular deprotonation of [CpFe(P <sub>2</sub> N <sub>2</sub> )(H <sub>2</sub> )] <sup>+</sup>	34
Scheme 2.11	Half-sandwich iron dihydrogen complex without pendant amine is unable to incorporate deuterium to form [CpFe(P-P(HD))] <sup>+</sup>	35
Scheme 2.12.	Catalytic cycle for the oxidation of H <sub>2</sub> by CpM(P <sub>2</sub> N <sub>2</sub> )H	39

### Chapter 3:

Scheme 3.1	Nucleophilic ring opening of azetidinium cation having electron withdrawing groups on C2	56
Scheme 3.2	Regioselective nucleophilic ring opening of an azetidinium cation having a quaternary C2	57
Scheme 3.3	Preference for chloride ion to attack C2 of an N-acyl azetidinium cation instead of the acyl group	57
Scheme 3.4	Ring opening of an <i>in situ</i> generated azetidinium cation having a phenyl substituent on C2	59



Scheme 3.5	Ring opening of an <i>in situ</i> generated spirocyclic, C2 aryl-substituted azetidinium cation	60
Scheme 3.6	An example of ring opening of azetidinium via a S <sub>N</sub> 2 mechanism	62
Scheme 3.7	Ring expansion of an azetidine to a pyrrolidine via the formation and subsequent opening of an azetidinium cation generated from intramolecular substitution reaction	63
Scheme 3.8	Comparison of the rate of ring opening of an aziridinium cation to the rate of ring opening of a corresponding azetidinium cation	64
Scheme 3.9	Expansion of an azetidinium to a pyrrolidine via the generation of an azetidinium ylide	65
Scheme 3.10	Opening of an azetidinium and the concomitant formation of an epoxide generated via the formation of an azetidinium ylide	66
Scheme 3.11	Expansion of an azetidinium ylide to a pyrrolidine via a radical mechanism	67
Scheme 3.12	Regioselectivity of hydride transfer to various aziridinium cations from CpRu(dppm)H	68
Scheme 3.13	Catalytic hydrogenation of aziridinium cations by CpRu(dppm)H	69
Scheme 3.14	Preparation of an unsubstituted spirocyclic azetidinium	72
Scheme 3.15	Synthesis of novel azetidinium cation 3.39	73
Scheme 3.16	Catalytic hydrogenation of azetidinium by CpRu(dppm)H	82
Scheme 3.17	Two-step reduction of azetidinium cation 3.39 by Cp* <sub>2</sub> Co and 1,4-cyclohexadiene	86

## List of Figures

### Chapter 1:

Figure 1.1	Various Noyori-type catalysts	3
Figure 1.2	P <sub>2</sub> N <sub>2</sub> ligand and a metal complex containing two P <sub>2</sub> N <sub>2</sub> ligands	17

### Chapter 2:

Figure 2.1	Two conformers of 1,2-dihydropyridines	26
Figure 2.2	Spectra of <sup>31</sup> P-coupled and <sup>31</sup> P-decoupled <sup>1</sup> H NMR spectra of Cp* <sub>2</sub> Ru(P <sup>Ph</sup> <sub>2</sub> N <sup>Bn</sup> <sub>2</sub> )Cl	42

### Chapter 3:

Figure 3.1	Site of nucleophilic ring opening of azetidinium cation having quaternary C2	56
Figure 3.2	<sup>1</sup> H NMR spectra of the hydride signal of CpRu(dppm)H in the reaction mixture of aziridinium cation 3.31d and CpRu(dppm)H at various temperatures	70
Figure 3.3	A representative plot of a kinetic run.	76
Figure 3.4	Pseudo-first-order rate constant of reaction between CpRu(dppm)H and azetidinium vs [CpRu(dppm)H]	77
Figure 3.5	Eyring Plots of reaction between CpRu(dppm)H and azetidinium	79
Figure 3.6	<sup>1</sup> H NMR of azetidinium cation 3.39 and Cp* <sub>2</sub> Ru(dppf)H	84
Figure 3.7	Cyclic voltammetry of azetidinium cation 3.39	85

## List of Tables

### Chapter 2

Table 2.1	Potential of Ru <sup>III/II</sup> for various ruthenium hydrides	21
-----------	--	----

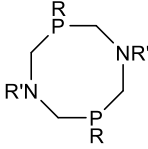
### Chapter 3

Table 3.1:	Reaction of various metal hydrides with azetidinium 3.39	83
------------	--	----

Table 3.2	Summary of the relevant electrochemical potentials of various hydrides and cations	87
-----------	--	----

## List of Abbreviations

Ar	aromatic group
Bn	Benzyl
BPh <sub>4</sub> <sup>-</sup>	tetraphenylborate anion
C <sub>5</sub> F <sub>4</sub> N	2,3,5,6-tetrafluoropyridine
COD	Cyclooctadiene
Cp	η <sup>5</sup> -cyclopentadienyl
Cp*	η <sup>5</sup> -pentamethylcyclopentadienyl
DBN	1,5-diazabicyclo[4.3.0]non-5-ene
DBU	1,8-diazabicyclo[5.4.0]undec-7-ene
DIBAL	diisobutylaluminium hydride
DMAP	Dimethylaminopyridine
DMSO	Dimethylsulfoxide
dppe	1,2-bis(diphenylphosphino)ethane
dppf	1,1'-bis(diphenylphosphino)ferrocene
dppm	1,1-bis(diphenylphosphino)methane
dppp	1,3-bis(diphenylphosphino)propane
EPR	electron paramagnetic resonance
Et <sub>3</sub> N	Trimethylamine
Fc	ferrocene
Fc <sup>+</sup>	ferrocenium cation
FLP	Frustrated Lewis Pairs
HAT	hydrogen atom transfer
<i>i</i> Pr	isopropyl
<i>k</i>	rate constant
K <sub>eq</sub>	equilibrium constant
LiHMDS	lithium bis(trimethylsilyl)amide
MeCN	acetonitrile
MeOH	methanol
M-H	metal-hydrogen bond
[M(H) <sub>2</sub> ]	metal dihydride
[M(H <sub>2</sub> )]	metal dihydrogen
Ms	mesyl group

NBD	norbornadiene
NHC	n-heterocyclic carbene
NMR	nuclear magnetic resonance
OTf	triflate group
P <sub>2</sub> N <sub>2</sub>	
PCy <sub>3</sub>	tricyclohexylphosphine
PhF	fluorobenzene
P–P	chelating bisphosphine ligand
PPh <sub>3</sub>	triphenylphosphine
PPY	4-pyrrolidinopyridine
PR <sub>3</sub>	tertiary phosphine
SET	single-electron transfer
<i>t</i> Bu	<i>tert</i> -butyl
TEMPO	(2,2,6,6-tetramethylpiperidin-1-yl)oxyl
THF	tetrahydrofuran
TMP	2,2,6,6-tetramethylpiperidine
Tol	toluene group
Ts	tosyl group

## Acknowledgement

I would like to express my gratitude to Professor Jack Norton, who has kindly, patiently, and tirelessly provided guidance and advice during my time at Columbia, both in his capacity initially as the Director of Graduate Studies and later as my research advisor. I am grateful for having received the opportunity to study organometallic chemistry under his guidance. His encouragements during the past eight years, both when I was physically at Columbia and when I was writing this dissertation while working full time, are greatly appreciated.

I am grateful to Professor Gerard Parkin and the late Professor Nicholas Turro for serving on my research committee. Their suggestions during my second year and ORP defenses were particularly insightful. I would also like to thank Professors Rachel Austin and Xavier Roy for serving on my dissertation committee and for their comments and suggestions. I would like to thank Professor Ruben Gonzalez for helping me with navigating the requirements of the graduate program when I left to start working full time.

I could not have completed my studies without the assistance and camaraderie of the past and present members of the Norton Group, and I would like to thank Dr. James Camara, Dr. Jiawei Chen, Dr. Tobias Dahmen, Dr. Michael Eberhart, Dr. Deven Estes, Dr. John Hartung, Dr. Yue Hu, Dr. Kathleen Kristian, Jonathan Kuo, Dr. Gang Li, Dr. Ling Li, Dr. Shuo Li, Dr. Jason Polisar, Dr. Mary Pulling, Dr. Anthony Shaw, and Dr. Travis Valdez. In particular, I would like to thank Dr. Anthony Shaw for introducing me to the experimental aspect of organometallic chemistry and Dr. Jason Polisar for his help with the studies on azetidinium cations and for serving on my dissertation committee.

I would like to thank Dr. John Decatur for help with NMR experiments, in particular with setting up procedure to acquire  $^{31}\text{P}$ -decoupled  $^1\text{H}$  NMR spectra. I would like to thank Dr. Yasuhiro Itagaki for assistance with mass spec. experiments.

Finally, I would like to thank my family for the unwavering and unconditional support I received.

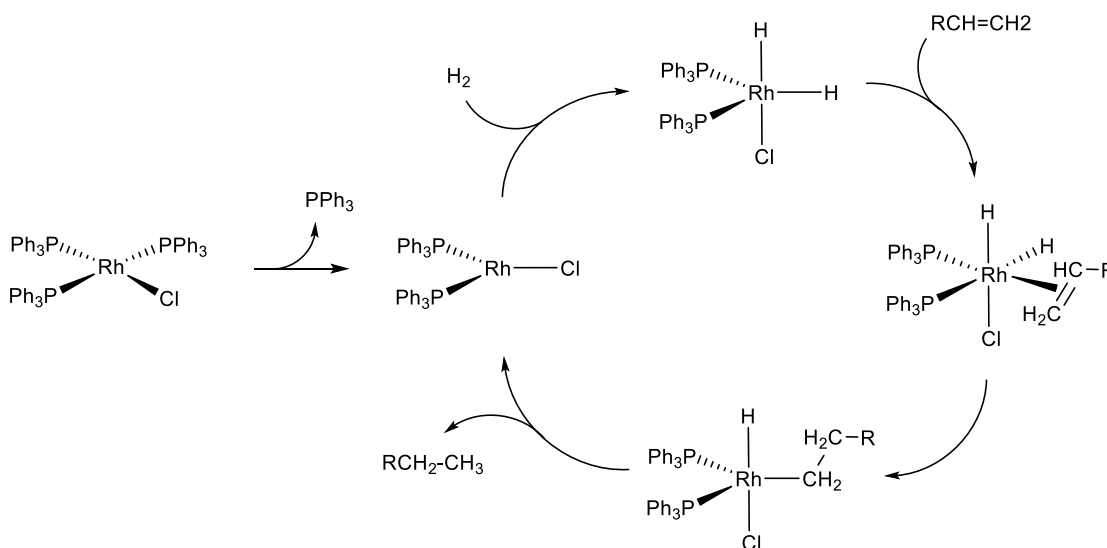
## Chapter 1. Introduction

### 1.1. Overview

The work described in this dissertation is concerned with the reduction of pyridinium and azetidinium cations by half-sandwich ruthenium hydrides of the formula CpRu(P-P)H via an ionic mechanism. Central to this transformation are the methods of C=N bond reduction, ionic hydrogenation, other ligands in half-sandwich ruthenium hydrides, and the effect these ligands have on the stability of and interconversion between hydride, dihydrogen, and dihydride complexes. This chapter will provide a general overview of these concepts.

#### 1.1.1 Inner-sphere Hydrogenation of C=N Bonds

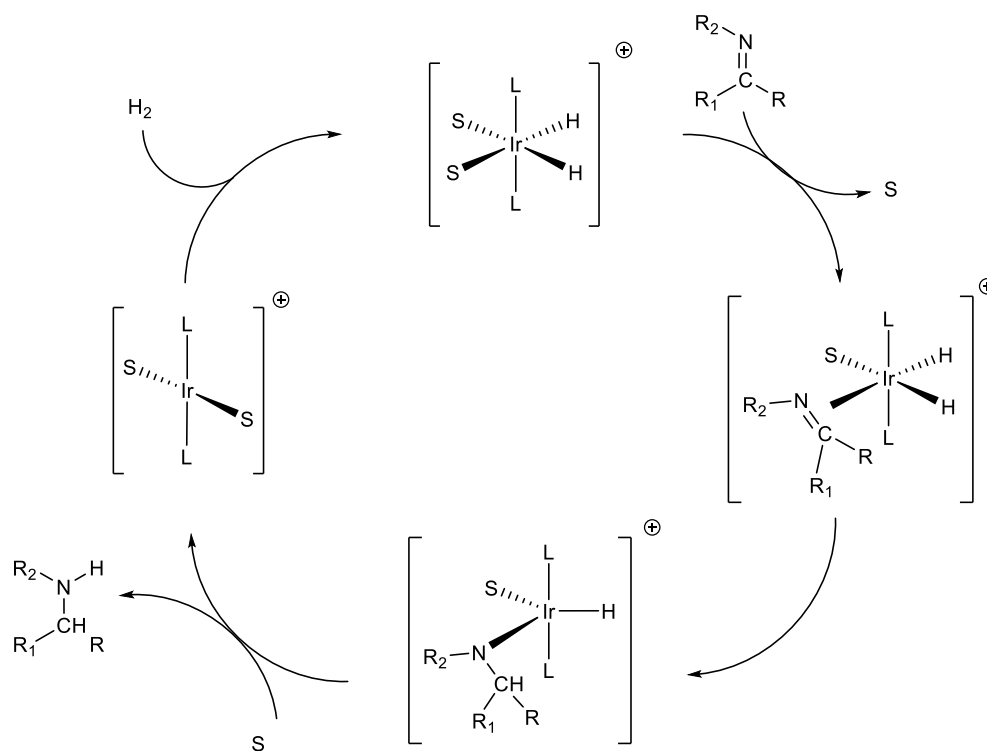
Most homogenous hydrogenations of alkenes effected by transition metal hydride complexes proceed via an inner-sphere mechanism, where an  $\eta^2$ -bound alkene inserts into an M-H bond. Subsequent reductive elimination of the resulting alkyl ligand with the remaining hydride ligand yields the alkane product.<sup>1</sup> Well-known examples of this type of hydrogenation include work pioneered by Wilkinson et al (Scheme 1.1).<sup>1a</sup>



**Scheme 1.1.** Inner-sphere hydrogenation of alkenes.



Examples of inner-sphere hydrogenation of C=N bonds are fewer,<sup>1a, 2</sup> and this has been attributed to, *inter alia*, the less favorable  $\eta^2$  binding of C=N bonds required in such mechanisms, as  $\eta^1$  binding through the lone pair of the nitrogen is generally preferable.<sup>1a</sup> Nonetheless, pre-catalysts such as  $\text{IrCl}(\text{PPh}_3)_3$ ,  $[\text{Ir}(\text{PPh}_3)_2(\text{NBD})]^+$ , and their rhodium analogues, all of which are better known for their roles as pre-catalysts for inner-sphere alkene hydrogenation similar to that shown in Scheme 1.1, are believed to effect the hydrogenation of imines in which an  $\eta^2$ -bound imine inserts into an M-H bond (Scheme 1.2).<sup>2-3</sup>



**Scheme 1.2.** Inner-sphere hydrogenation of imines.

### 1.1.2 Outer-Sphere Hydrogenation of C=N Bonds Using Bifunctional Catalysts

Subsequent reports have demonstrated the efficacy of outer-sphere hydrogenation for the hydrogenation of imines, where the substrate may be coordinated to the ligands of metal complex but not directly to the metal center.<sup>1a</sup> Metal complexes effecting such transformations

are often bifunctional and have separate functional groups for the donation of proton and hydride. Usually, the hydride is directly bound to the metal center while the proton is bonded to an electronegative element as part of a hydroxyl or amino group located on a ligand close to the metal center. Two of the most well-known bifunctional complexes that can catalyze the hydrogenation of imines are the Noyori type catalyst (**Fig. 1.1**), where the protic hydrogen is part of an amino group on a ligand, and the active half **1.1a** of the dimeric Shvo's Catalyst **1.1**.<sup>1,4</sup>

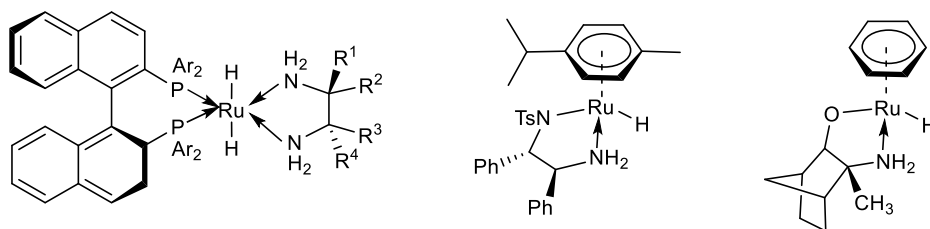
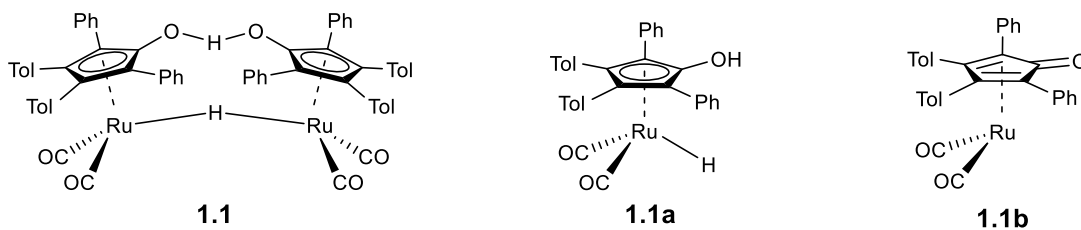


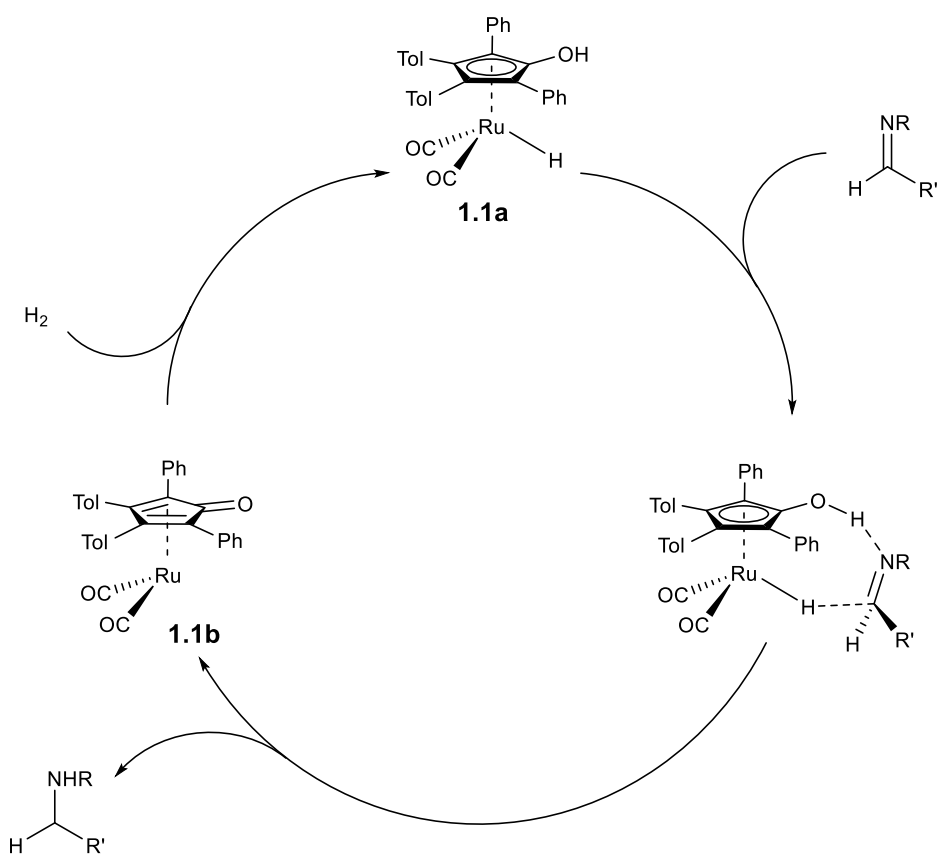
**Fig. 1.1.** Various Noyori type catalysts.

Shvo's Catalyst **1.1** dissociates into its monomeric halves **1.1a** and **1.1b** in solution, where complex **1.1a** effects the hydrogenation of substrates (Scheme 1.3).<sup>5</sup> After donating its protic and hydridic hydrogens, **1.1a** is transformed into complex **1.1b**, which may be converted back to the active hydrogenation catalyst **1.1a** under H<sub>2</sub> gas or from sources of H<sub>2</sub> such as isopropyl alcohol via transfer hydrogenation.<sup>5</sup>



The mechanism of hydrogenation by the ruthenium hydride **1.1a** has been an issue of contention with two schools of thoughts; one a concerted, outer-sphere mechanism and the other an inner-sphere mechanism with a ring-slippage to accommodate coordination of the substrate.<sup>5-6</sup>

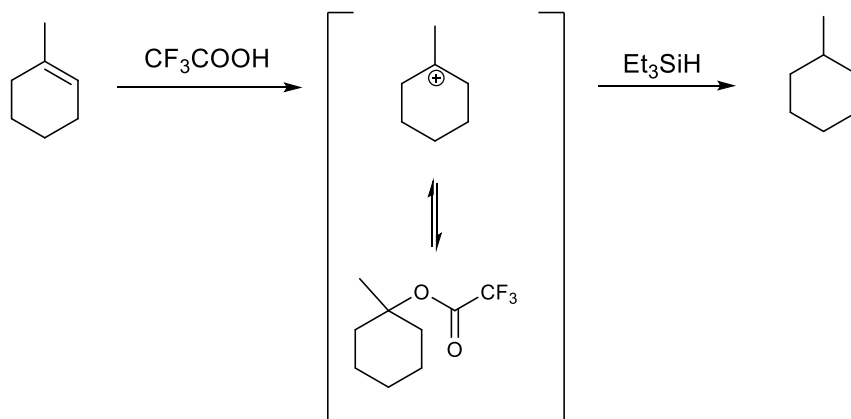
Kinetic isotope studies by Casey et al. and computational studies have supported the concerted, outer-sphere mechanism.<sup>1a, 5</sup> Computational studies further suggest that bond formation in the transition state is asynchronous: this asynchronicity is particularly pronounced when the substrate is an electron-rich imine, and may lead to a step-wise transfer.<sup>6</sup> The transformations effected by these bifunctional catalysts may be considered as *ionic*, as they involve the transfer of ionic constituents of dihydrogen; however, as elaborated more fully below, an ionic mechanism can also be one in which the substrate is never coordinated to the metal complex.



**Scheme 1.3.** Hydrogenation of imines catalyzed by Shvo's Catalyst.

## 1.2. Stepwise Ionic Hydrogenation

While ionic hydrogenation is defined as the transfer of H<sub>2</sub> as its charged components (*i.e.* a proton and a hydride),<sup>1b, 4b</sup> reactions where the transfers of proton and hydride are not concerted are of particular interest to the research of the Norton Group. The earliest reports of ionic hydrogenation as a stoichiometric reaction involved branched alkenes or styrene, as these molecules form stabilized carbocations upon protonation;<sup>7</sup> in contrast, no hydrogenation product is observed when unbranched alkenes are subjected to the same reaction conditions.<sup>7</sup> The protonation of 1-methylcyclohexene generates a mixture of the tertiary 1-methylcyclohexyl cation and its adduct with trifluoroacetate, where the two species are in a rapidly maintained equilibrium (Scheme 1.4). Subsequent addition of a silane transforms the tertiary cation into the alkane product.

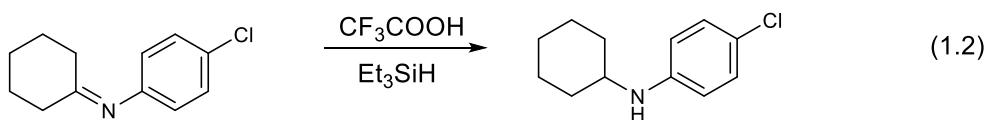
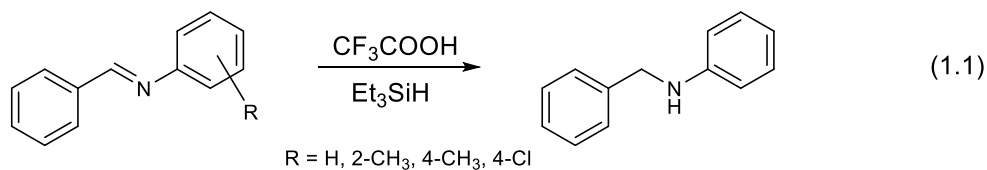


**Scheme 1.4.** Stepwise ionic hydrogenation effected by  $\text{CF}_3\text{COOH}$  and  $\text{Et}_3\text{SiH}$ .

One of the key requirements for the proton and hydride donors is that the rate of reaction between the reagents to yield dihydrogen should be slower than the rate of proton transfer to the branched alkene.<sup>1b, 8</sup> While the formation of dihydrogen may be suppressed by lowering reaction temperature, the usage of trifluoroacetic acid with triethylsilane is the most optimal as the two reagents do not react.<sup>7</sup> Another advantage offered by this pairing of proton and hydride donors is

chemoselectivity, as functional groups such as carboxylic acids, esters, nitriles, and aromatic rings are not reduced.

Although trifluoroacetic acid and triethylsilane may be utilized to effect the reduction of C=O bonds, different products are obtained depending on the nature of the substrate: aliphatic ketones are reduced to a mixture of alcohols and ethers, while aromatic ketones are deoxygenated to the corresponding hydrocarbon.<sup>7b</sup> The application of the two reagents to the reduction of imines has limited scope, as the combination fails to reduce most aliphatic imines.<sup>7b</sup> Aromatic imines such as N-benzylidene-4-methylaniline (eq. 1.1) and N-cyclohexylidene-4-chloroaniline (eq. 1.2) may be reduced to the corresponding amines, though the conditions for reduction of the latter require both elevated temperature and prolonged reaction time in comparison to the conditions for reduction of the former.<sup>1b, 8</sup>

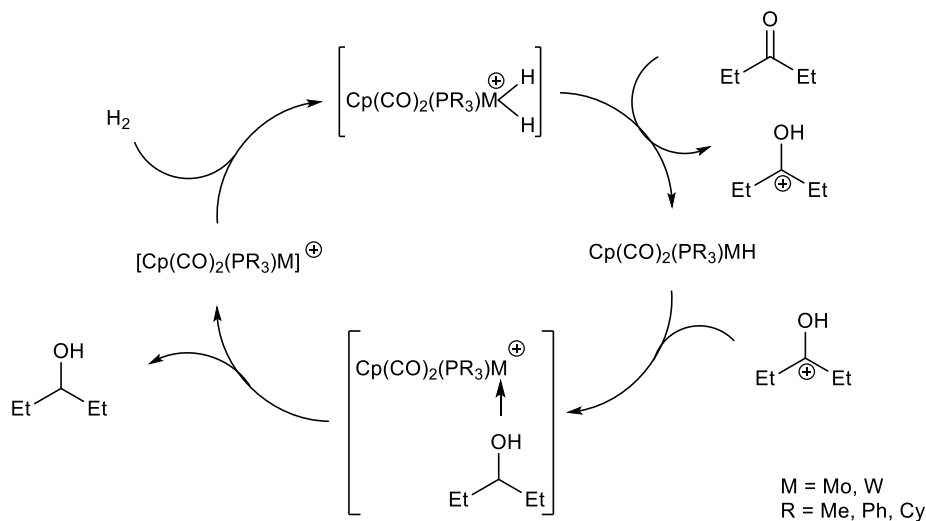


Subsequent development in the area of stoichiometric ionic hydrogenation involved the pairing of a Brønsted acid with various other types of hydride donors. The combination of a strong acid with either a germanium or a tin hydride effects the deoxygenation of a tertiary alcohol, where the reaction proceeds via a tertiary carbocation.<sup>9</sup> Hydrides of transition metals such as tungsten and molybdenum have been shown to effect the stoichiometric hydrogenation of ketones, aldehydes, and epoxides when the substrates are first activated by a Brønsted acid,<sup>10</sup> and similar processes have been reported for rhenium<sup>11</sup> and ruthenium hydrides.<sup>12</sup> One advantage of using transition metal hydrides is their ability to form a dihydrogen or dihydride

complex upon protonation, as opposed to releasing dihydrogen as many silanes do. For example,  $\text{Cp}(\text{CO})_2(\text{PR}_3)_3\text{MH}$  forms a dihydride complex  $[\text{Cp}(\text{CO})_2(\text{PR}_3)_3\text{MH}_2]^+$  when treated with triflic acid.<sup>8</sup>

### 1.2.1. Catalytic Ionic Hydrogenation

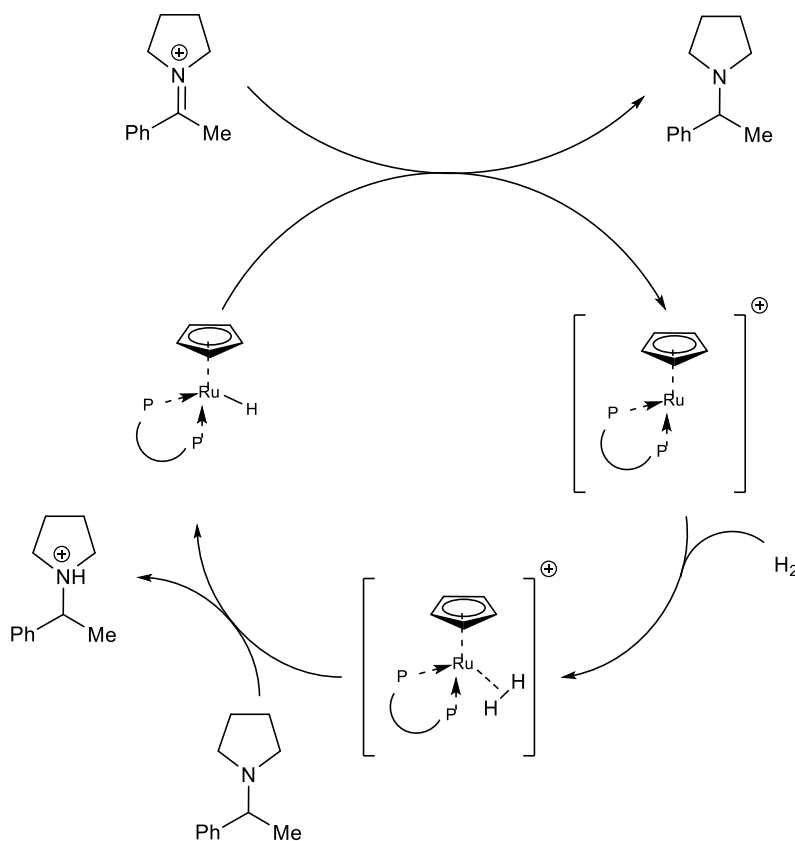
As the dihydride  $[\text{Cp}(\text{CO})_2(\text{PR}_3)_3\text{MH}_2]^+$  is sufficiently acidic to protonate a ketone substrate (while generating  $\text{Cp}(\text{CO})_2(\text{PR}_3)_3\text{MH}$ ), and as this dihydride may be obtained by treating the coordinatively unsaturated  $[\text{Cp}(\text{CO})_2(\text{PR}_3)_3\text{M}]^+$  with  $\text{H}_2$ , ionic hydrogenation may be effected without adding a Brønsted acid for the initial protonation of the substrate, making  $\text{Cp}(\text{CO})_2(\text{PR}_3)_3\text{MH}$  a *catalyst* for ionic hydrogenation (Scheme 1.5).<sup>8</sup> Though the turnover rate for the catalytic cycle is slow due to the slow dissociation of the alcohol product from the metal, this represents one of the first examples of catalytic ionic hydrogenation.<sup>8</sup>



**Scheme 1.5.** Ionic hydrogenation catalyzed by  $\text{Cp}(\text{CO})_2(\text{PR}_3)_3\text{MH}$

At about the same time, the Norton Group was studying the ionic hydrogenation of iminium and aziridinium cations catalyzed by half-sandwich ruthenium hydrides of the formula  $\text{CpRu}(\text{P-P})\text{H}$  (Scheme 1.6), where P-P represents a chelating diphosphine with the phosphorus

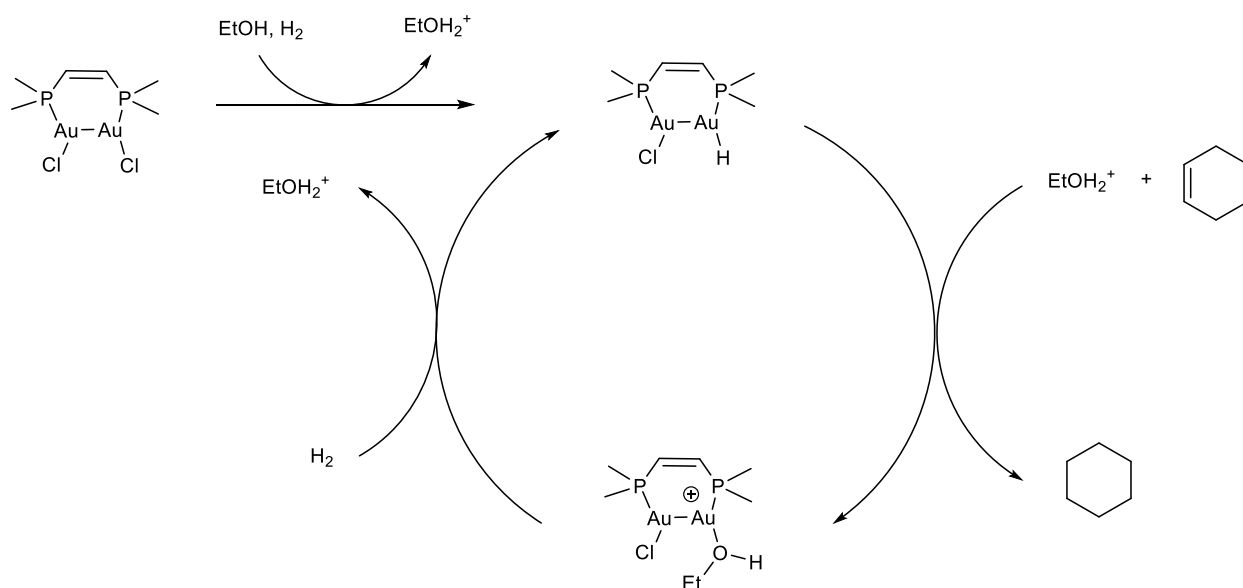
atoms connected by an alkyl linkage.<sup>13</sup> The bite angle of chelating diphosphine around the metal influences the rate of hydride transfer: the rate of hydride transfer decreases about an order of magnitude when an additional carbon is introduced into the alkyl linkage connecting the phosphorus atoms.<sup>13b</sup> As hydride transfer is the rate-limiting step in the catalytic cycle, the overall turnover rate is affected by the choice of diphosphine,<sup>13a</sup> with CpRu(dppm)H having the fastest turnover.<sup>13b</sup> One difference between the catalytic cycle of Scheme 1.4 and that of Scheme 1.5 is the base that deprotonates the dihydrogen/dihydride to regenerate the metal hydride: the ketone substrate is sufficiently basic to deprotonate the  $[\text{Cp}(\text{CO})_2(\text{PR}_3)\text{MH}_2]^+$ , while  $[\text{CpRu}(\text{P}-\text{P})(\text{H}_2)]^+$  must be deprotonated by the amine product as the activated iminium substrate cannot.



**Scheme 1.6.** Ionic hydrogenation of iminium cations catalyzed by CpRu(P-P)H

In 2013, Crabtree et al. noted the relative scarcity of reports on catalytic outer-sphere ionic hydrogenation.<sup>14</sup> Computational tools have helped to determine whether a reaction

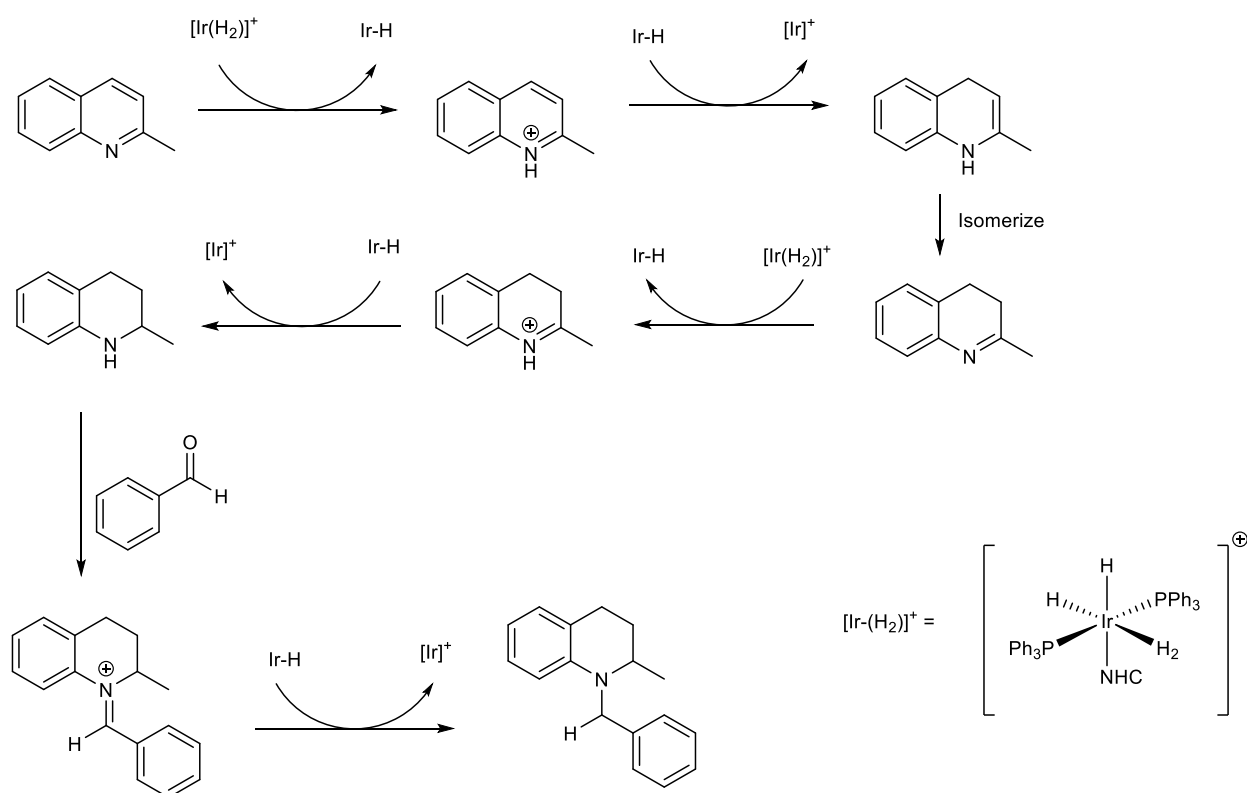
operates via an ionic mechanism. One study has determined that the hydrogenation of alkenes and imines by an Au(I) hydride generated *in situ* proceeds via an ionic mechanism (Scheme 1.7).<sup>15</sup> The authors suggested that the bimetallic gold(I) chloride complex can heterolytically activate dihydrogen when dissolved in a protic solvent such as ethanol, which generates one gold hydride and one molecule of EtOH<sub>2</sub><sup>+</sup>. Studies from the authors suggested that the alkene substrate is first protonated by EtOH<sub>2</sub><sup>+</sup> and subsequently receives a hydride from the *in situ* generated gold hydride. One molecule of ethanol then coordinates to the resulting unsaturated metal center, and the pair of gold hydride and protonated solvent may be regenerated in the presence of dihydrogen.<sup>15b</sup> Another computational study demonstrated that the mechanism of hydrogenation may change with the substrate, with the hydrogenation of carbonyls occurring via an ionic mechanism and the hydrogenation of alkenes proceeding via the insertion of the substrate into a Ru-H bond.<sup>16</sup>



**Scheme 1.7.** A catalytic hydrogenation of alkenes which calculations show to proceed via an ionic mechanism



One recent development in stepwise ionic hydrogenation is the reduction of C=N bonds by an *in-situ* generated iridium dihydrogen complex developed by Crabtree et al (Scheme 1.8), which reduces quinolines to tetrahydroquinolines.<sup>14</sup> When the reaction takes place in the presence of benzaldehyde, the iridium complex can reduce the iminium cation formed from the condensation of the tetrahydroquinoline product with the benzaldehyde (Scheme 1.8).<sup>14</sup> After the iridium transfers a proton and a hydride, the resulting 16-e<sup>-</sup> cationic complex can take up dihydrogen, which regenerates the dihydrogen complex. While the authors did not elaborate on how the iridium dihydrogen complex is deprotonated in the catalytic reduction of the *in-situ* generated iminium cation, it would appear that the final amine product is responsible for the regeneration of the iridium hydride.

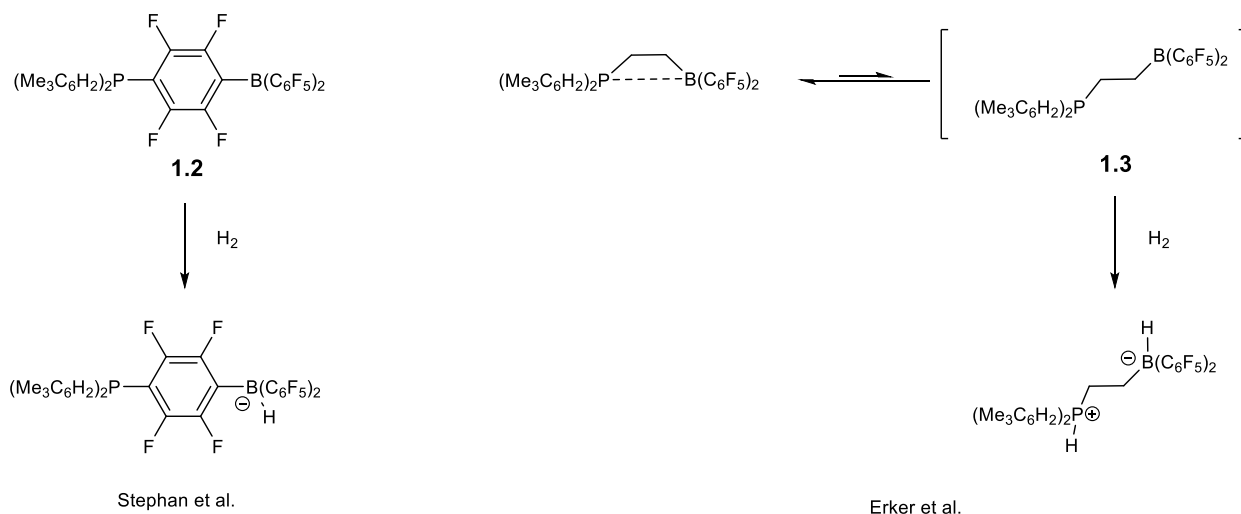


**Scheme 1.8.** Iridium hydride catalyzed ionic hydrogenation of quinolines and iminium cations formed from tetrahydroquinolines

Another recent report demonstrated that  $\text{Cp}(\text{CO})_2(\text{PMe}_3)\text{MoH}$  (of Scheme 1.5, *vide supra*) may be regenerated via transfer hydrogenation from formic acid instead of regeneration via uptake of  $\text{H}_2$ .<sup>17</sup> Like Brønsted acids in the stoichiometric reaction discussed in § 1.2, formic acid protonates carbonyl substrates, and subsequent hydride transfer from the metal yields the product alcohol. One advantage of this transfer hydrogenation route is that the formate ion generated by the initial deprotonation coordinates to the metal, and subsequent elimination of  $\text{CO}_2$  regenerates the hydride.

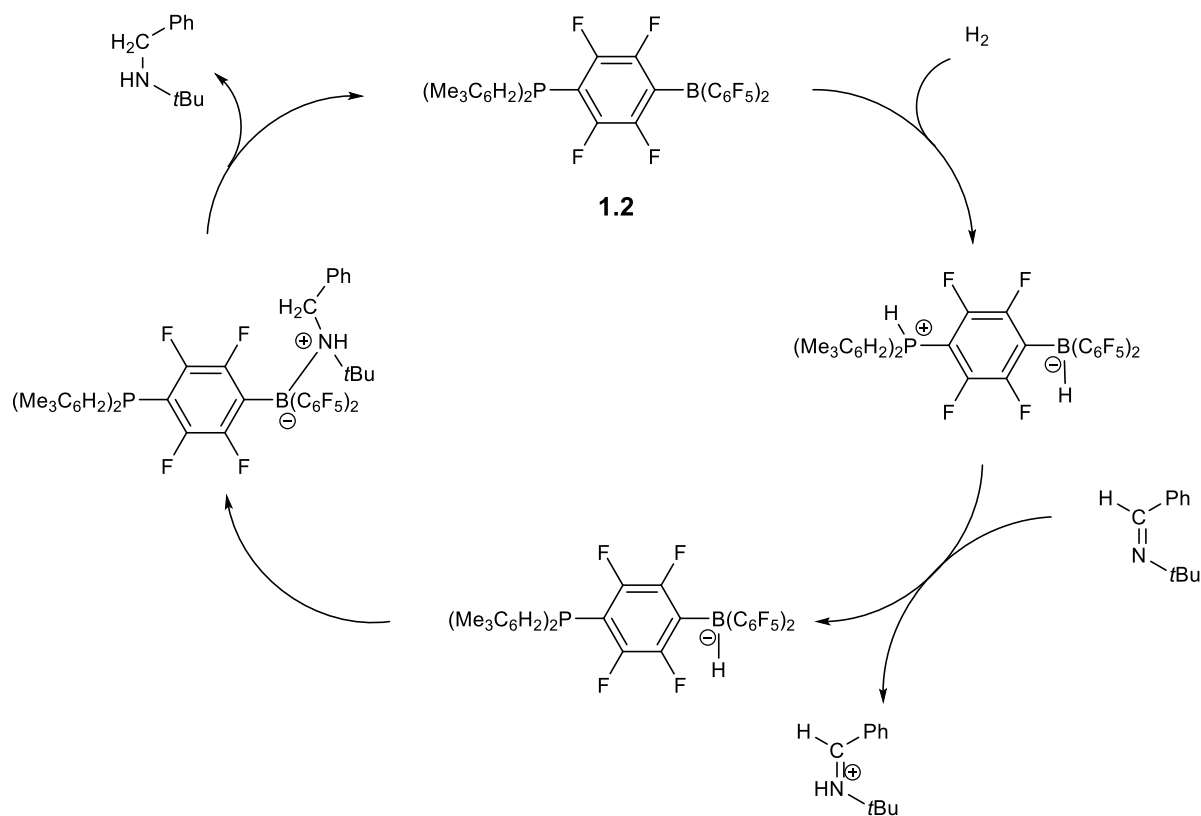
### 1.2.2. Ionic Hydrogenation by Frustrated Lewis Pairs

A recent development in the area of catalytic ionic hydrogenation is the usage of Frustrated Lewis Pairs (FLPs) as hydrogenation catalysts.<sup>18</sup> A FLP (e.g. **1.2** and **1.3** in Scheme 1.9) is defined as a combination of a bulky Lewis acid and a bulky Lewis base, where steric congestion prevents the irreversible formation of a Lewis adduct. One example of an intermolecular FLP is that of  $\text{P}(t\text{Bu})_3$  and  $\text{B}(\text{C}_6\text{F}_5)_3$ ; examples of intramolecular FLPs include the molecules synthesized by Stephan et al. (**1.2**) and Erker et al (**1.3**) in their seminal contributions to this new area of research.<sup>18a, b, 19</sup> FLPs may be tuned to activate small molecules such  $\text{CO}$ ,  $\text{CO}_2$ , and  $\text{H}_2$ , and their activation of  $\text{H}_2$  results in a hydrogenated FLP (Scheme 1.9) that can serve as a hydrogenation catalyst. Though the Erker FLP exists as a four-membered ring at room temperature due to dative interaction between the phosphorus and boron atoms, this FLP can heterolytically activate  $\text{H}_2$  at room temperature, presumably by going through the open-chain isomer.<sup>19</sup> The activation of  $\text{H}_2$  by main-group compounds is particularly remarkable as this was previously the domain of transition metal complexes.<sup>18b</sup>



**Scheme 1.9.** Activation of dihydrogen by FLPs.

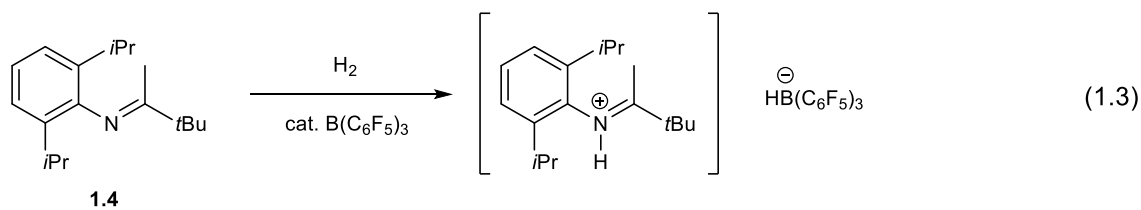
The reversible activation of  $\text{H}_2$  is particularly relevant to ionic hydrogenation as hydrogenated FLPs can serve as both hydride donors and proton donors (Scheme 1.10).<sup>18a, b</sup> Both the Stephan FLP **1.2** and the Erker FLP **1.3** are effective at the catalytic reduction of nitrogen-containing moieties such as bulky imines and aziridines. Stephan et al. have proposed that the catalytic cycle for the hydrogenation of imines by FLPs proceeds according to Scheme 1.9. In this catalytic cycle, transfer of a proton from the hydrogenated FLP to the imine to form an activated iminium cation has to occur before the hydride transfer.<sup>20</sup> This conclusion is supported by the observation that the zwitterionic phosphonium borate [(Cy<sub>3</sub>P)-(C<sub>6</sub>F<sub>4</sub>)-BH(C<sub>6</sub>F<sub>5</sub>)<sub>2</sub>], which contains a hydride donor but not a proton donor, cannot effect the stoichiometric hydrogenation of imines.<sup>20</sup> After the hydride transfer step (Scheme 1.10), the nitrogen of the product amine forms a Lewis adduct with the borane, and the product amine has to dissociate from the adduct before the FLP can take on another  $\text{H}_2$  to regenerate the active catalyst.



**Scheme 1.10.** Hydrogenation of an imine catalyzed by a FLP.

As the strength of the dative bond in the borane-amine adduct is inversely related to the steric congestion about the amine nitrogen, less sterically hindered amines are less likely to dissociate to regenerate the FLP. Catalytic hydrogenation effected by the Stephan FLP (Scheme 1.9) takes place at 80-120 °C in order to promote this dissociation; however, catalytic hydrogenation using the Erker FLP proceeds at room temperature.

One corollary from the heterolytic activation of H<sub>2</sub> by *intermolecular* FLP is that the pairing of certain imines with a Lewis acid should result in H<sub>2</sub> activation to form an iminium hydridoborate, and this is observed for bulky imines such as **1.4** (eq. 1.3).<sup>18a, b, 21</sup> The heterolytic cleavage of H<sub>2</sub> results in the formation of an activated iminium cation, which can be reduced by the hydridoborate. As such, the substrate to be reduced can take on the role of Lewis base played by the phosphines in the intramolecular FLPs.



### 1.3. Acid/base Chemistry of Transition Metal Dihydrogen and Dihydride Complexes

The various examples of transition-metal-catalyzed ionic hydrogenation discussed above involve the transformation between metal hydrides, coordinatively unsaturated complexes formed after hydride transfer, and metal dihydrogen or dihydride complexes formed when the coordinatively unsaturated complexes take up H<sub>2</sub>. Metal dihydrogen or dihydride complexes are particularly important in the catalytic cycle as the hydride is regenerated only after the deprotonation of the dihydrogen or dihydride.

Metal dihydrogen complexes are stable only within a range of electron density at the metal center. While low electron density leads to poor back donation and even liberation of H<sub>2</sub>, high electron density increases the occupation of the antibonding σ\* orbital and results in the formation of the corresponding dihydride complex.<sup>22</sup> For example, protonation of CpRu(dppm)H leads solely to the formation of dihydrogen complex [CpRu(dppm)(H<sub>2</sub>)]<sup>+</sup> while protonation of Cp\*Ru(dppm)H produces a mixture of 2:1 ratio of [CpRu(dppm)(H<sub>2</sub>)]<sup>+</sup> to [CpRu(dppm)(H)<sub>2</sub>]<sup>+</sup>.<sup>22b</sup> The dihydrogen complex is often the kinetic product of protonation, while formation of the *trans*-dihydride is driven by thermodynamic stability.<sup>23</sup>

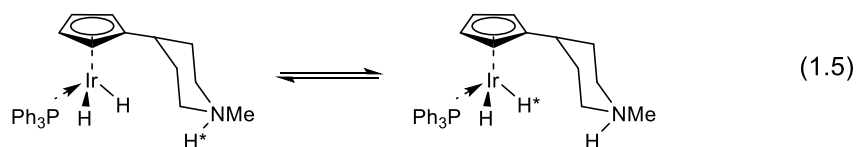
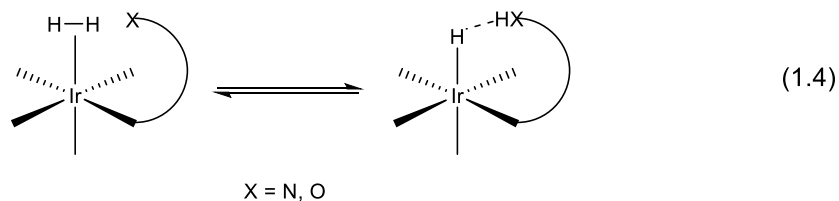
While initial studies proposed that the isomerization process for both Cp- and Cp\*-based dihydrogen complexes is an intramolecular one as the rate of isomerization is first order with respect to the concentration of the dihydrogen complex,<sup>36,37</sup> subsequent studies have shown that this generalization is not true for Cp-based dihydrogen complexes.<sup>22a, 23c, 24</sup> At least in the case

of  $[\text{CpRu}(\text{dppe})(\text{H}_2)]^+$ , isomerization to  $[\text{CpRu}(\text{dppe})(\text{H})_2]^+$  has been shown to proceed via an initial deprotonation of the dihydrogen complex followed by protonation of the metal center at a position *trans* to the metal hydride.<sup>22a, 25</sup> Although the isomerization of the dihydrogen  $[\text{CpRu}(\text{dppe})(\text{H}_2)]^+$  to the corresponding dihydride  $[\text{CpRu}(\text{dppe})(\text{H})_2]^+$  complex is reversible,<sup>26</sup> the equilibrium strongly favors the dihydride complexes  $[\text{Cp}^*\text{Ru}(\text{dppe})(\text{H})_2]^+$  and  $[\text{Cp}^*\text{Ru}(\text{dppf})(\text{H})_2]^+$  over the respective dihydrogen complexes.<sup>23c, 27</sup> Because the dihydride complexes  $[\text{Cp}^*\text{Ru}(\text{dppe})(\text{H})_2]^+$  and  $[\text{Cp}^*\text{Ru}(\text{dppf})(\text{H})_2]^+$  are harder to deprotonate compared to their corresponding dihydrogen complexes, isomerization to the dihydride complex reduces catalyst loading in catalytic hydrogenation reactions.<sup>13c, 22a, 27</sup>

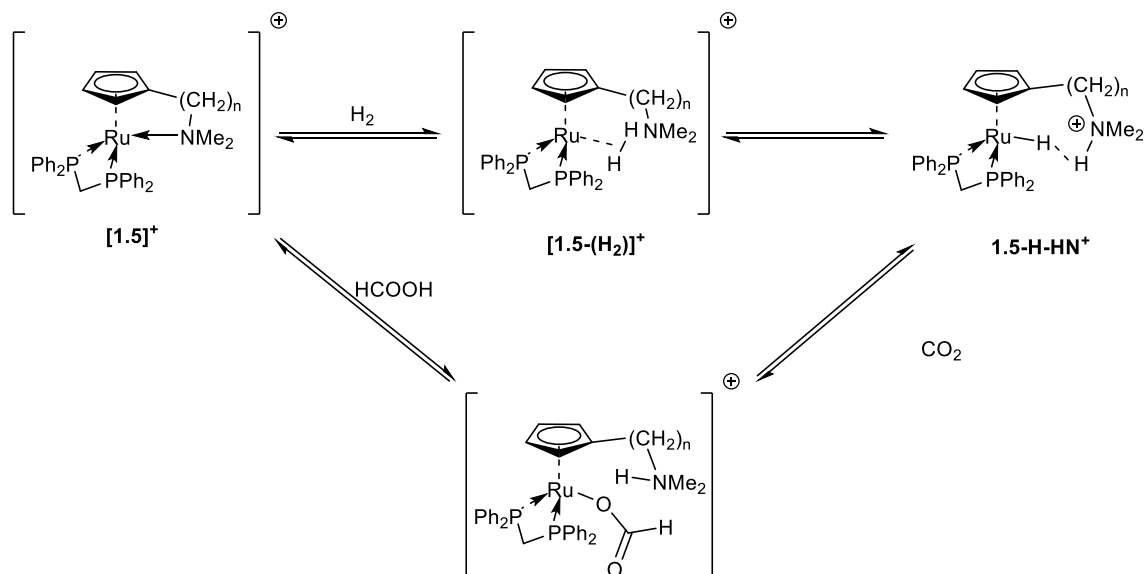
### 1.3.1. Effect of Intramolecular Amines on Metal Dihydrogen Complexes

One potential drawback of the catalytic cycle that the Norton Group has developed for the hydrogenation of quaternary nitrogen substrates is the reliance on the product amine to effect the deprotonation of the dihydrogen complex; in situations where the product amine cannot deprotonate the dihydrogen complex, an external base has to be used to convert the dihydrogen complex into the metal hydride.<sup>27</sup>

One possible solution is the use of an intramolecular base to deprotonate the dihydrogen complex. One iridium complex has a pendant base attached to its ligands, and the pendant base can reversibly deprotonate a bound dihydrogen (eq. 1.4).<sup>28</sup> Another iridium complex having a pendant amine attached to the Cp ring has been shown to be able to scramble the protons attached to the metal and the proton on the amine (eq. 1.5).<sup>29</sup>



Subsequent work has tethered a pendant amine to the Cp ring via an alkyl linkage, and the amine can coordinate to the ruthenium center to form complex **[1.5]<sup>+</sup>**.<sup>28c</sup> Under hydrogenation conditions, molecular dihydrogen displaces the pendant amine to form a dihydrogen complex **[1.5-(H<sub>2</sub>)<sup>+</sup>**, which can be heterolytically activated by the pendant amine to yield a metal hydride having protonated pendant amine **1.5-H-HN<sup>+</sup>** (top path of Scheme 1.11).



**Scheme 1.11.** Heterolytic cleavage of a ruthenium dihydrogen complex having a pendant amine

Ruthenium-amine complex **[1.5]<sup>+</sup>** can also be treated with formic acid to yield a ruthenium-formate complex that can undergo subsequent decarboxylation to yield **1.5-H-HN<sup>+</sup>**

(bottom path of Scheme 1.11). That the pendant amine may be protonated by the formic acid suggests that proton exchange between pendant amine and an external base may be possible.

Recently, DuBois et al. have developed a class of cyclic diphosphines known as  $P_2N_2$  ligands (**Fig. 1.2**), which incorporates amines into the linkage between the phosphorus atoms. When coordinated to metals,  $P_2N_2$  ligands can facilitate proton transfer from the metal center to an external base. More details on  $P_2N_2$  ligands and their applications will be discussed in Chapter 2.

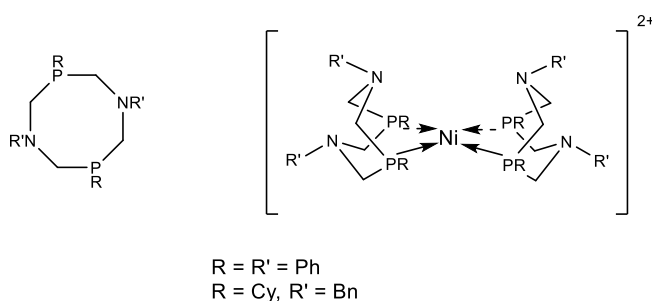


**Fig. 1.2.**  $P_2N_2$  ligand and a metal complex containing two  $P_2N_2$  ligands.

#### 1.4. Goals of the Research Project

The goals of the research project are directed to better understanding of the reactivity of  $CpRu(P-P)H$  with pyridinium and azetidinium cations. For the former, we seek to determine if a previously established methodology for reducing one pyridinium cation<sup>27</sup> may be extended to other cations and if the methodology may be improved. For the latter, we seek to establish the reactivity of  $CpRu(P-P)H$  with azetidinium cations and compare these results to what the Norton Group has previously established in studies concerning aziridinium cations.<sup>13d</sup>



## References

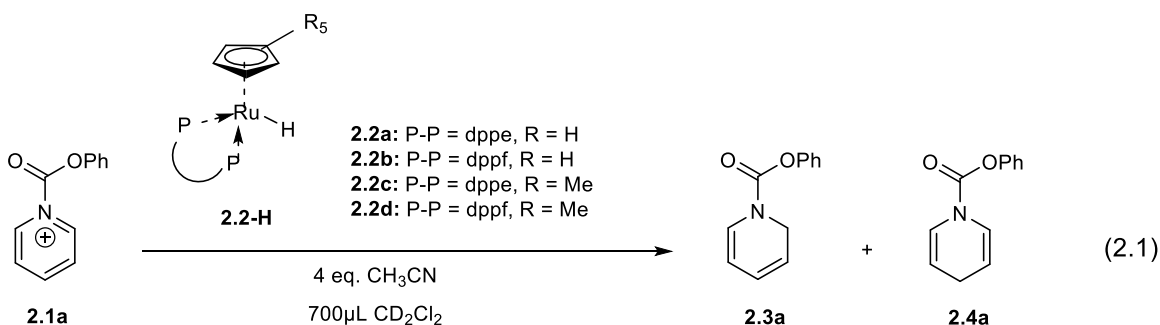
1. (a) Comas-Vives, A.; Ujaque, G.; Lledós, A., Inner- and Outer-Sphere Hydrogenation Mechanisms: A Computational Perspective. In *Adv. Inorg. Chem.*, Rudi van, E.; Jeremy, H., Eds. Academic Press: 2010; Vol. Volume 62, pp 231; (b) Bullock, R. M., Ionic Hydrogenations. In *The Handbook of Homogeneous Hydrogenation*, Wiley-VCH Verlag GmbH: 2008; pp 153.
2. Herrera, V.; Muñoz, B.; Landaeta, V.; Canudas, N. *J. Mol. Catal. A: Chem.* **2001**, *174*, 141.
3. (a) Fabrello, A.; Bachelier, A.; Urrutigoity, M.; Kalck, P. *Coord. Chem. Rev.* **2010**, *254*, 273; (b) Landaeta, V. R.; Muñoz, B. K.; Peruzzini, M.; Herrera, V.; Bianchini, C.; Sánchez-Delgado, R. A. *Organometallics* **2006**, *25*, 403.
4. (a) Wang, C.; Villa-Marcos, B.; Xiao, J. *Chem. Commun.* **2011**, *47*, 9773; (b) Chakraborty, S.; Guan, H. *Dalton Trans.* **2010**, *39*, 7427.
5. Conley, B. L.; Pennington-Boggio, M. K.; Boz, E.; Williams, T. J. *Chem. Rev.* **2010**, *110*, 2294.
6. Comas-Vives, A.; Ujaque, G.; Lledós, A. *Organometallics* **2008**, *27*, 4854.
7. (a) Kursanov, D. N.; Parnes, Z. N.; Bassova, G. I.; Loim, N. M.; Zdanovich, V. I. *Tetrahedron* **1967**, *23*, 2235; (b) Kursanov, D. N.; Parnes, Z. N.; Loim, N. M. *Synthesis* **1974**, *1974*, 633.
8. Bullock, R. M. *Chem. Eur. J.* **2004**, *10*, 2366.
9. Carey, F. A.; Tremper, H. S. *Tetrahedron Lett.* **1969**, *10*, 1645.
10. (a) Gaus, P. L.; Kao, S. C.; Youngdahl, K.; Darensbourg, M. Y. *J. Am. Chem. Soc.* **1985**, *107*, 2428; (b) Gibson, D. H.; El-Omrani, Y. S. *Organometallics* **1985**, *4*, 1473; (c) Song, J.-S.; Szalda, D. J.; Bullock, R. M. *Organometallics* **2001**, *20*, 3337; (d) Song, J.-S.; Szalda, D. J.; Bullock, R. M.; Lawrie, C. J. C.; Rodkin, M. A.; Norton, J. R. *Angewandte Chemie International Edition in English* **1992**, *31*, 1233.
11. Bakhmutov, V. I.; Vorontsov, E. V.; Antonov, D. Y. *Inorg. Chim. Acta* **1998**, *278*, 122.
12. Geraty, S. M.; Harkin, P.; Vos, J. G. *Inorg. Chim. Acta* **1987**, *131*, 217.
13. (a) Magee, M. P.; Norton, J. R. *J. Am. Chem. Soc.* **2001**, *123*, 1778; (b) Guan, H.; Iimura, M.; Magee, M. P.; Norton, J. R.; Janak, K. E. *Organometallics* **2003**, *22*, 4084; (c) Guan, H.; Iimura, M.; Magee, M. P.; Norton, J. R.; Zhu, G. *J. Am. Chem. Soc.* **2005**, *127*, 7805; (d) Guan, H.; Saddoughi, S. A.; Shaw, A. P.; Norton, J. R. *Organometallics* **2005**, *24*, 6358.
14. Manas, M. G.; Graeupner, J.; Allen, L. J.; Dobereiner, G. E.; Rippy, K. C.; Hazari, N.; Crabtree, R. H. *Organometallics* **2013**, *32*, 4501.

15. (a) Gonzalez-Arellano, C.; Corma, A.; Iglesias, M.; Sanchez, F. *Chem. Commun.* **2005**, 3451; (b) Comas-Vives, A.; Ujaque, G. *J. Am. Chem. Soc.* **2013**, *135*, 1295.
16. Chaplin, A. B.; Dyson, P. J. *Organometallics* **2007**, *26*, 4357.
17. Neary, M. C.; Parkin, G. *Chemical Science* **2015**, *6*, 1859.
18. (a) Stephan, D. W.; Greenberg, S.; Graham, T. W.; Chase, P.; Hastie, J. J.; Geier, S. J.; Farrell, J. M.; Brown, C. C.; Heiden, Z. M.; Welch, G. C.; Ullrich, M. *Inorg. Chem.* **2011**, *50*, 12338; (b) Stephan, D. W.; Erker, G. *Angew. Chem. Int. Ed.* **2015**, *54*, 6400; (c) Stephan, D. W. *Chem. Commun.* **2010**, *46*, 8526.
19. Spies, P.; Erker, G.; Kehr, G.; Bergander, K.; Frohlich, R.; Grimme, S.; Stephan, D. W. *Chem. Commun.* **2007**, 5072.
20. Welch, G. C.; Prieto, R.; Dureen, M. A.; Lough, A. J.; Labeodan, O. A.; Holtrichter-Rossmann, T.; Stephan, D. W. *Dalton Trans.* **2009**, 1559.
21. Chase, P. A.; Jurca, T.; Stephan, D. W. *Chem. Commun.* **2008**, 1701.
22. (a) Belkova, N. V.; Epstein, L. M.; Filippov, O. A.; Shubina, E. S. *Chem. Rev.* **2016**, *116*, 8545; (b) Jia, G.; Lau, C.-P. *Coord. Chem. Rev.* **1999**, *190–192*, 83.
23. (a) Chinn, M. S.; Heinekey, D. M. *J. Am. Chem. Soc.* **1990**, *112*, 5166; (b) de los Ríos, I.; Jiménez Tenorio, M.; Padilla, J.; Puerta, M. C.; Valerga, P. *Organometallics* **1996**, *15*, 4565; (c) Belkova, N. V.; Dub, P. A.; Baya, M.; Houghton, J. *Inorg. Chim. Acta* **2007**, *360*, 149.
24. Belkova, N. V.; Collange, E.; Dub, P.; Epstein, L. M.; Lemenovskii, D. A.; Lledós, A.; Maresca, O.; Maseras, F.; Poli, R.; Revin, P. O.; Shubina, E. S.; Vorontsov, E. V. *Chem. Eur. J.* **2005**, *11*, 873.
25. Silantyev, G. A.; Filippov, O. A.; Tolstoy, P. M.; Belkova, N. V.; Epstein, L. M.; Weisz, K.; Shubina, E. S. *Inorg. Chem.* **2013**, *52*, 1787.
26. (a) Jia, G.; Lough, A. J.; Morris, R. H. *Organometallics* **1992**, *11*, 161; (b) Jia, G.; Morris, R. H. *J. Am. Chem. Soc.* **1991**, *113*, 875.
27. Shaw, A. P.; Ryland, B. L.; Franklin, M. J.; Norton, J. R.; Chen, J. Y. C.; Hall, M. L. *J. Org. Chem.* **2008**, *73*, 9668.
28. (a) Park, S.; Lough, A. J.; Morris, R. H. *Inorg. Chem.* **1996**, *35*, 3001; (b) Peris, E.; Lee, J. C.; Rambo, J. R.; Eisenstein, O.; Crabtree, R. H. *J. Am. Chem. Soc.* **1995**, *117*, 3485; (c) Chu, H. S.; Lau, C. P.; Wong, K. Y.; Wong, W. T. *Organometallics* **1998**, *17*, 2768.
29. Mar Abad, M.; Atheaux, I.; Maisonnat, A.; Chaudret, B. *Chem. Commun.* **1999**, 381.

## Chapter 2. Ionic Hydrogenation of Pyridinium Cations.

### 2.1. Previous efforts on the reduction of pyridinium cations.

Dr. Anthony Shaw, a former doctoral student in the Norton Group, previously reported the reduction of pyridinium cation **2.1a** by a series of half-sandwich ruthenium hydrides **2.2a-H** through **2.2d-H** of the general formula CpRu(P-P)H (eq. 2.1).<sup>1</sup> The distribution of the product isomers depends on the ruthenium hydride used. For the reduction effected by **2.2a-H** through **2.2c-H**, the product is a mixture of 1,2-dihydropyridine **2.3a** and 1,4-dihydropyridine **2.4a**; for the reduction effected by **2.2d-H**, the product is solely the 1,4-dihydropyridine **2.4a**.

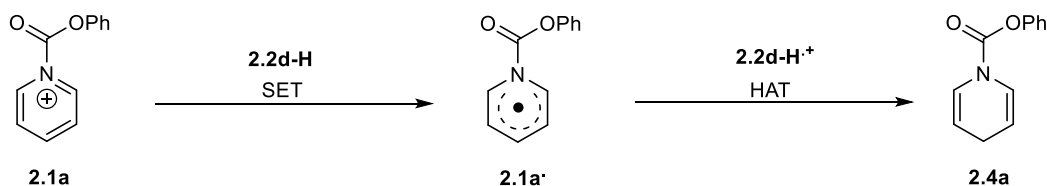


The product distribution of the reaction correlates well with the oxidation potential of the hydride effecting the reduction (Table 2.1). Hydride Cp\*Ru(dppf)H **2.2d-H**, having the highest oxidation potential of the four hydrides (-0.63 V vs. Fc/Fc<sup>+</sup> in CH<sub>2</sub>Cl<sub>2</sub>), transfers hydride exclusively to the  $\gamma$ -carbon of the pyridinium ring, yielding solely 1,4-dihydropyridine **2.4a**. On the other hand, hydride **2.2a-H**, having the lowest oxidation potential of the four hydrides (-0.16 V vs Fc/Fc<sup>+</sup> in CH<sub>2</sub>Cl<sub>2</sub>), gives a ratio **2.3a:2.4a** of 52:48. Hydrides **2.2b-H** (-0.31 V) and **2.2c-H** (-0.51 V), having oxidation potential between those of **2.2a-H** and **2.2d-H**, give ratios **2.3a:2.4a** of 30:70 and 4:96, respectively.

Ruthenium Hydride	Potential of Ru <sup>III/II</sup> (vs Fc <sup>+</sup> /Fc in CH <sub>2</sub> Cl <sub>2</sub> )	Ratio of <b>2.3a</b> to <b>2.4a</b>
<b>2.2a-H</b>	-0.16 V	52:48
<b>2.2b-H</b>	-0.31 V	30:70
<b>2.2c-H</b>	-0.51 V	4:96
<b>2.2d-H</b>	-0.63 V	0:100

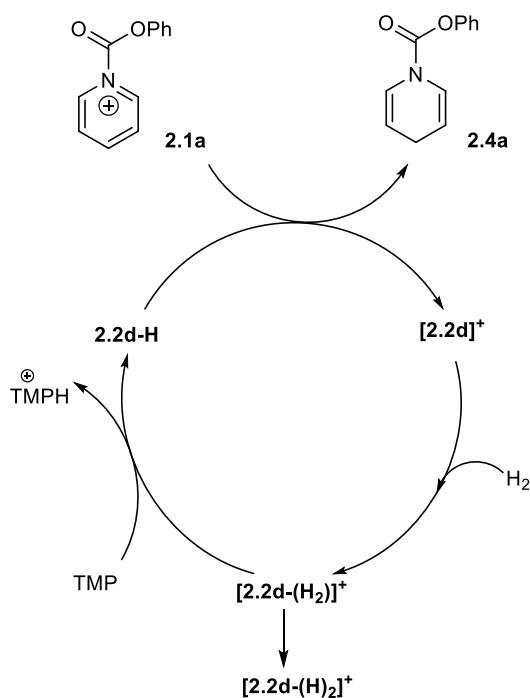
Table 2.1.

That a mixture of pyridinium cation **2.1a** and Cp\*Ru(dppf)H **2.2d-H** gives an EPR signals provides additional evidence that the hydride transfer involved the production of a paramagnetic species, implying that the hydride transfer is a two-step process: an initial single electron transfer (SET) followed by hydrogen atom transfer (HAT) (Scheme 2.1). One of the goals of the present research is to determine if this reactivity pattern may be generalized to substituted pyridinium cations (§ 2.2).



**Scheme 2.1**

The reduction of pyridinium cation **2.1a** by Cp\*Ru(dppf)H **2.2d-H** may be catalytic with H<sub>2</sub> as the ultimate reductant (Scheme 2.2). A coordinatively unsaturated, 16e<sup>-</sup> complex [Cp\*Ru(dppf)]<sup>+</sup> [**2.2d**]<sup>+</sup> is formed after **2.2d-H** transfers hydride, and a dihydrogen complex [Cp\*Ru(dppf)(H<sub>2</sub>)]<sup>+</sup> [**2.2d-(H<sub>2</sub>)**]<sup>+</sup> is formed after the uptake of dihydrogen by [**2.2d**]<sup>+</sup>. Similar to Scheme 1.5 in Chapter 1, the dihydrogen complex has to be deprotonated in order to regenerate the hydride; however, unlike Scheme 1.5, the product amine of Scheme 2.2, 1,4-dihydropyridine **2.4a**, is not basic enough to deprotonate [**2.2d-(H<sub>2</sub>)**]<sup>+</sup>. Therefore, tetramethylpiperidine (TMP), a strong base, has to be used.

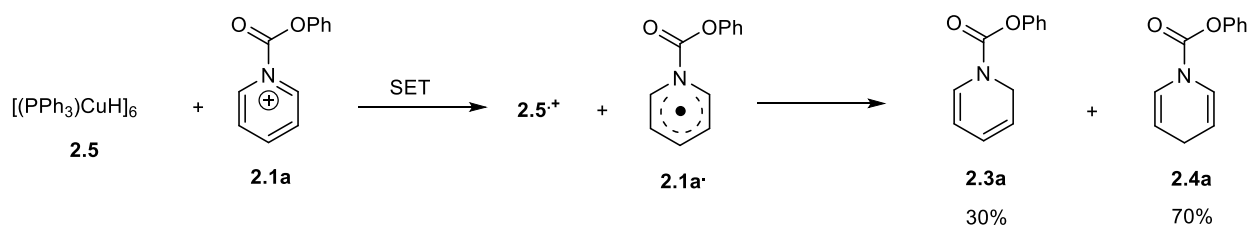


### Scheme 2.2

One complication in this catalytic cycle is that dihydrogen complex  $[\mathbf{2.2d-(H_2)}]^+$  irreversibly isomerizes to the corresponding dihydride complex  $[\mathbf{2.2d-(H)_2}]^+$ , reducing the amount of catalyst as the reaction proceeds. While the rate of this competing reaction may be reduced by maintaining the temperature of the catalytic reaction at 10 °C,<sup>1</sup> a preferable approach would be to deprotonate the dihydrogen more efficiently, which represents another goal of the present research (§ 2.3).

In work subsequent to the studies described in § 2.2, Dr. Michael Eberhart, another former Norton Group doctoral student, has shown that a higher reduction potential for hydride does not necessarily imply that two-step hydride transfer is ubiquitous.<sup>2</sup> Stryker's Reagent,  $[\text{PPh}_3\text{CuH}]_6$  **2.5**, is a hexameric hydride having a reduction potential more negative than that of  $\text{Cp}^*\text{Ru}(\text{dppf})\text{H}$  **2.2d-H**; yet when pyridinium cation **2.1a** is treated with **2.5**, a mixture of 1,2-dihydropyridine **2.3a** and 1,4-dihydropyridine **2.4a** is produced. Stopped-flow experiments on

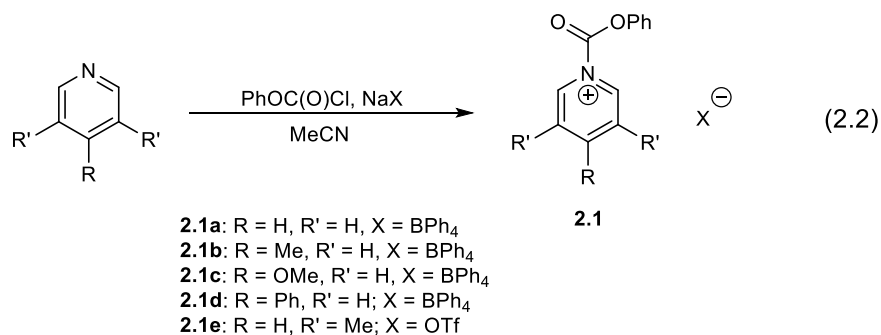
the reaction between **2.1a** and **2.5** indicates that electron transfer from **2.5** indeed occurred, but this might not be the sole mechanism of hydride transfer (Scheme 2.3).<sup>2</sup>



**Scheme 2.3**

## 2.2. Attempt to ascertain the scope of the two-step hydride transfer

I prepared pyridinium cations **2.1b-2.1e** utilizing procedures similar to established method used for the preparation of pyridinium **2.1a**: substituted pyridines were treated with phenylchloroformate in the presence of a sodium salt yielding the desired pyridinium salts (eq. 2.2).<sup>1, 3</sup> Tetraphenylborate was the counterion for pyridinium **2.1b-2.1d**, and triflate was the counterion for pyridinium **2.1e**. This procedure was not successful for the acylation of pyridines having substituents on the  $\alpha$ -carbon; attempts to prepare the salts of 2,6-dimethylpyridine and 2-methylpyridine failed, presumably because of steric hindrance.

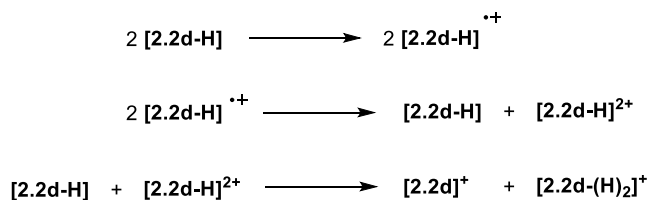


In contrast to the reaction between the unsubstituted pyridinium cation **2.1a** and Cp\*Ru(dppf)H **2.2d-H**, which yielded solely 1,4-dihydropyridine **2.4a** (eq. 2.1), neither 1,2-dihydropyridine nor 1,4-dihydropyridine was detected in the <sup>1</sup>H NMR spectrum when **2.1b-2.1e**

were treated with **2.2d-H**. The disappearance of the doublet peak assigned to the hydrogen atom on the  $\alpha$ -carbons of the pyridinium ring ( $\sim\delta$  9.37 for all pyridinium cations studied) and the disappearance of the upfield triplet peak corresponding to the hydride of **2.2d-H** led to the conclusion that both the pyridinium cation and the hydride were consumed during the reaction.

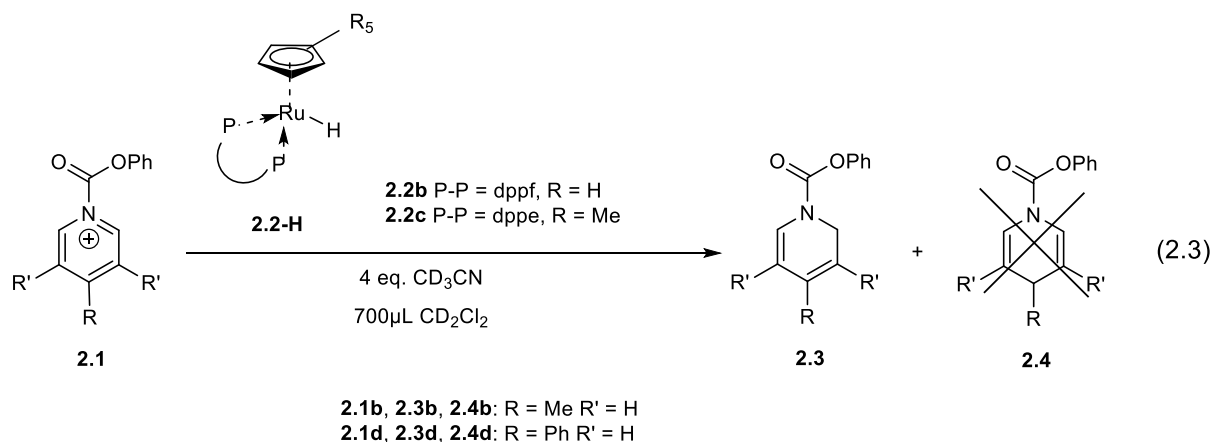
Although I was unable to identify the organic products in any of the reactions, I was able to identify the inorganic products in two reactions. Before I introduced the various pyridinium cations into a solution of hydride **2.2d-H** in  $\text{CD}_2\text{Cl}_2$ , I took a  $^1\text{H}$  NMR spectrum of **2.2d-H**. The integration of the upfield hydride signal was standardized by comparing it to the integration of the residual  $\text{CDHCl}_2$  peak at  $\delta$  5.32. After the completion of each reaction, another  $^1\text{H}$  NMR spectrum was taken.

In the reactions between hydride **2.2d-H** and either cation **2.1b** or **2.1e**, the presence of the dihydride  $[\text{Cp}^*\text{Ru}(\text{dppf})(\text{H})_2]^+$  [**2.2d-(H)<sub>2</sub>**]<sup>+</sup>, indicated by the broad upfield dihydride peak, was unambiguous. In particular, the amount of [**2.2d-(H)<sub>2</sub>**]<sup>+</sup> produced in the reaction between **2.2d-H** and **2.1b** was 96% of the theoretical amount in the reaction shown in Scheme 2.4. In the reactions between **2.2d-H** and either **2.1c** or **2.1d**, only trace amount of [**2.2d-(H)<sub>2</sub>**]<sup>+</sup> was detected in the respective  $^1\text{H}$  NMR spectra, suggesting a different mechanism for the consumption of hydride **2.2d-H**. The almost quantitative conversion of hydride **2.2d-H** to the dihydride complex [**2.2d-(H)<sub>2</sub>**]<sup>+</sup> in the reaction between **2.2d-H** and **2.1b** suggests an initial single electron transfer followed by self-disproportionation, which has been previously observed in other half-sandwich ruthenium hydrides.<sup>4</sup>



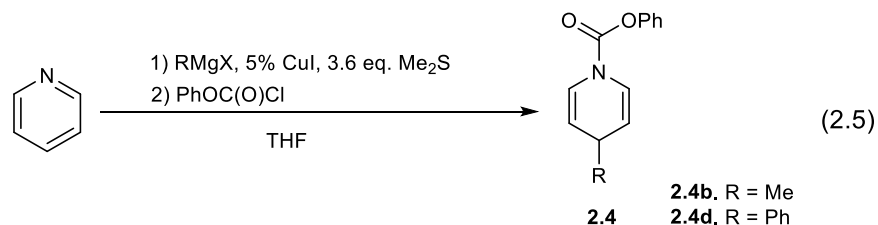
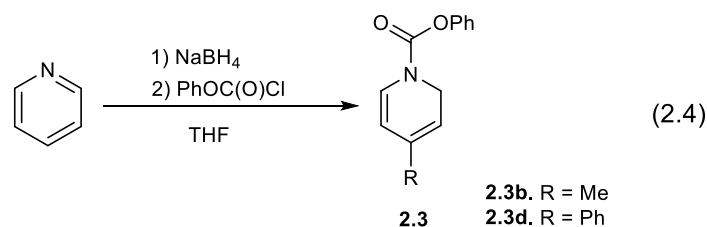
#### Scheme 2.4

I next studied if CpRu(dppf)H **2.2b-H** or Cp\*Ru(dppe)H **2.2c-H** could effect the transfer of hydride to pyridinium cations **2.1b** and **2.1d**. Both hydrides **2.2b-H** and **2.2c-H** regioselectively transferred hydride to the  $\alpha$ -carbon of the pyridinium ring of **2.1b** and **2.1d**, yielding the 1,2-dihydropyridine products with no trace of any 1,4-dihydropyridine product (eq. 2.3). This is in contrast to the reaction between the unsubstituted pyridinium cation **2.1a** and either hydride **2.2b-H** or **2.2c-H** as the 1,4-dihydropyridine was the major product.



I prepared 1,2-dihydropyridines **2.3b** and **2.3d** and 1,4-dihydropyridines **2.4b** and **2.4d** according to known procedures: the 1,2-dihydropyridines were prepared by treating the corresponding pyridines with phenyl chloroformate and sodium borohydride in cold THF<sup>5</sup> (eq. 2.4), and the 1,4-dihydropyridines were prepared by treating pyridine with phenyl chloroformate and the Grignard reagent having the desired substituent in the presence of a copper(I) catalyst (eq. 2.5).<sup>6</sup>





The 1,2-dihydropyridines may be differentiated from the 1,4-dihydropyridines as the spectra of the former showed the presence of two conformers at room temperature (**Fig. 2.1**). The  $^1\text{H}$  NMR spectrum of the 1,4-dihydropyridines has a characteristic signal at  $\sim\delta$  6.9-7.0 (doublet of doublet, protons on  $\alpha$ -carbons) and another characteristic signal at  $\sim\delta$  5.0-5.1 (doublet of doublet, protons on  $\beta$ -carbons). Like the  $^1\text{H}$  NMR spectrum of the unsubstituted 1,2-dihydropyridine **2.3a**, NMR spectra of the substituted 1,2-dihydropyridines **2.3b** and **2.3d** showed signals of two conformers at room temperature. The most recognizable signals are one set of signals at  $\sim\delta$  5.3 and  $\sim\delta$  5.1 and another set of signals at  $\sim\delta$  4.5 and  $\sim\delta$  4.3. The ratio of the conformers may be estimated by comparing the integral of the signal at  $\sim\delta$  4.5 and  $\sim\delta$  4.3.<sup>1</sup> For **2.3a**, the ratio is 57:43<sup>1</sup>; for **2.3b**, 56:44; and for **2.3d**, 60:40.

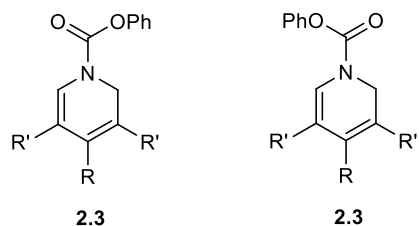
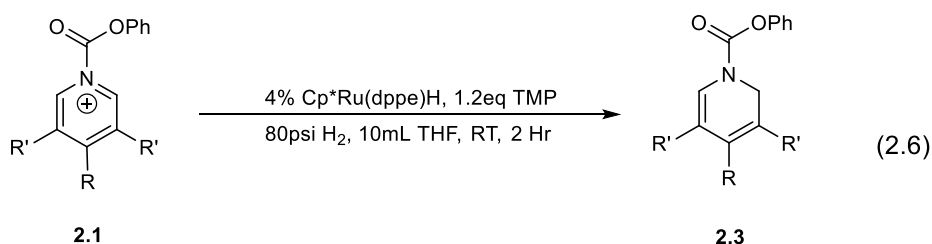


**Fig. 2.1.** Two conformers of 1,2-dihydropyridines **2.3**.

I also attempted the hydrogenation of pyridinium cations **2.1b** and **2.1d** using catalytic amount of hydride **2.2c-H**. The conditions of the reaction were similar to that for catalytic

hydrogenation of pyridinium cation **2.1a**, and the differences were increased catalyst loading (4% vs 2%) and higher reaction temperature (room temperature instead of 10 °C) (eq. 2.6). As in the stoichiometric reactions, 1,2-dihydropyridines were the only products produced. A NMR yield of 71% was obtained for the catalytic hydrogenation of **2.1d** after reaction time of 35 minutes, which would correspond to a turnover frequency (TOF) of 30 hr<sup>-1</sup>; on another attempt, a yield of 73% was obtained after 2 hours. It would appear from these two data points that the reaction was largely completed within the first hour. The NMR yield of the catalytic hydrogenation of **2.1b** was 55%.



**2.1b, 2.3b:** R = Me, R' = H, 55% NMR Yield  
**2.1d, 2.3d:** R = Ph, R' = H, 73% NMR Yield

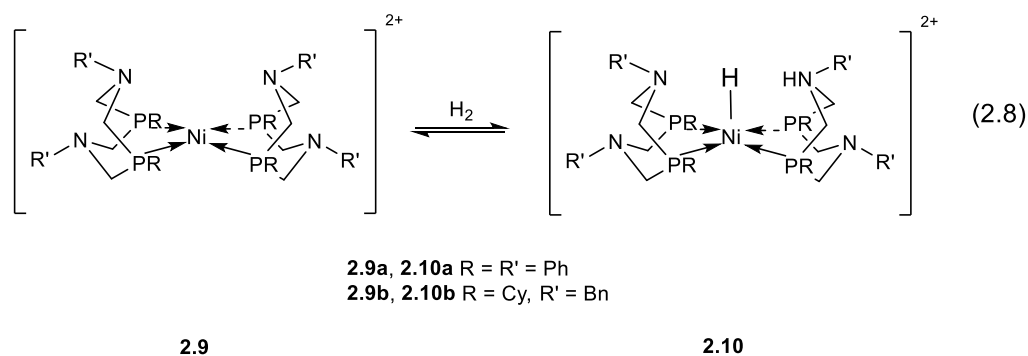
## 2.3. Addressing the catalyst deactivation using P<sub>2</sub>N<sub>2</sub> chelating ligands

### 2.3.1 Background of P<sub>2</sub>N<sub>2</sub> ligands

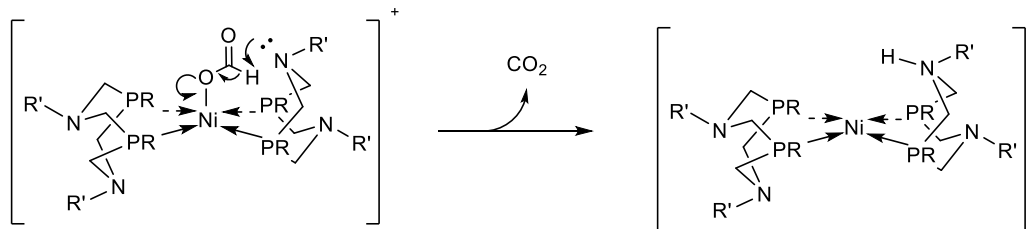
DuBois et al. developed a group of chelating phosphine ligands known as P<sub>2</sub>N<sub>2</sub> ligands (2.6), which may have a variety of alkyl or aromatic substituents on the phosphorus and nitrogen atoms. The P<sub>2</sub>N<sub>2</sub> ligands may be prepared by initially treating a primary phosphine with paraformaldehyde and subsequently treating the condensed product produced in the first step with a primary amine to yield the 8-membered cyclic diphosphines **2.6** (Scheme 2.5).<sup>4a</sup>



In nickel complex **2.9**, which contains two  $P_2N_2$  ligands per complex, each  $P_2N_2$  ligand binds to the metal to form a bicyclic structure. The bottom ring of the bicyclic structure adopts a chair conformation akin to that in complex **2.7**, while the top ring is forced into a boat conformation. The boat conformation adopted by one of the rings is crucial in increasing the rate of proton shuttling from an amine on the  $P_2N_2$  ligand onto the metal center and vice versa (eq. 2.8), and the turnover rate for the oxidation of dihydrogen by complex **2.9b** is  $10\text{ s}^{-1}$ , about 20-1,000 times the turnover rate for complex **2.7**.<sup>8</sup> In addition to being a catalyst for the oxidation of dihydrogen, complex **2.9** is also effective as a catalyst for the formation of dihydrogen from protons.



DuBois et al. also demonstrated that complexes **2.9** are effective as catalysts for the oxidation of formate.<sup>9</sup> After the coordination of the formate ion to the  $Ni^{II}$  metal center of complex **2.9**, the abstraction of the formate hydrogen by an amine on one of the pendant diphosphines liberates  $CO_2$  and leaves a formally  $Ni^0$  complex (Scheme 2.6). Subsequent proton transfer to an external base and double oxidation of the  $Ni^0$  complex completes the catalytic cycle and forms the  $Ni^{II}$  complex **2.9**.



**Scheme 2.6**

### 2.3.2. Preparation of half-sandwich Group-8 metal hydride complexes bearing P<sub>2</sub>N<sub>2</sub> ligand

The class of P<sub>2</sub>N<sub>2</sub> complexes of particular interest to the Norton Group is the half-sandwich metal complexes containing an  $\eta^5$ -cyclopentadienyl ring and a P<sub>2</sub>N<sub>2</sub> ligand as these complexes are structurally similar to the ruthenium complexes **2.2a-H** to **2.2d-H** used in catalytic ionic hydrogenation (§ 2.1, *supra*). We first became aware of P<sub>2</sub>N<sub>2</sub> ligands and metal complexes bearing P<sub>2</sub>N<sub>2</sub> ligands (*e.g.* Ni-complex **2.9**, *supra*) in the fall of 2009, when Dr. Morris Bullock, a colleague of Dr. Mary DuBois at PNWL and a former postdoctoral researcher in the Norton Group, suggested to us that the usage of P<sub>2</sub>N<sub>2</sub> ligands as the chelating phosphine in half-sandwich ruthenium hydrides may address the issue of catalyst deactivation during catalytic hydrogenation (§ 2.1, *supra*).

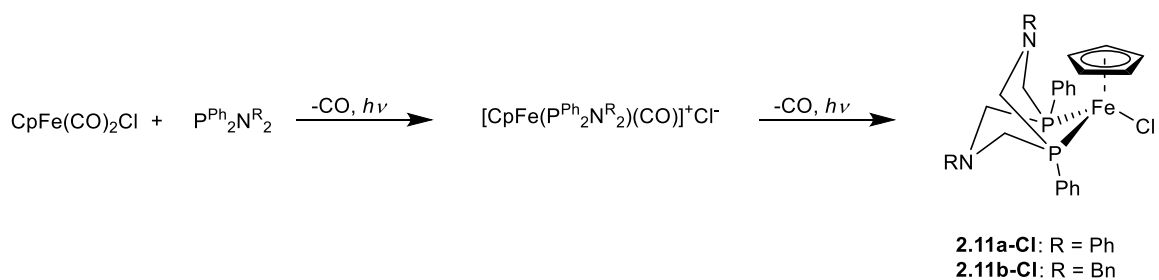
As the amine in the P<sub>2</sub>N<sub>2</sub> ligand had been shown to be capable of removing various types of protons from metal complexes, in particular ones from dihydrogen ligands, we hypothesized that the incorporation of the amine in the diphosphine would speed up the deprotonation of ruthenium-dihydrogen complex to yield the corresponding ruthenium-hydride complex, thus making less competitive the isomerization of the ruthenium-dihydrogen complex to the corresponding ruthenium-dihydride complex.

Unbeknownst to us and Dr. Bullock, Dr. Mary DuBois et al. had begun to study half-sandwich, P<sub>2</sub>N<sub>2</sub>-containing metal complexes at this time. When I informed Dr. Bullock of the

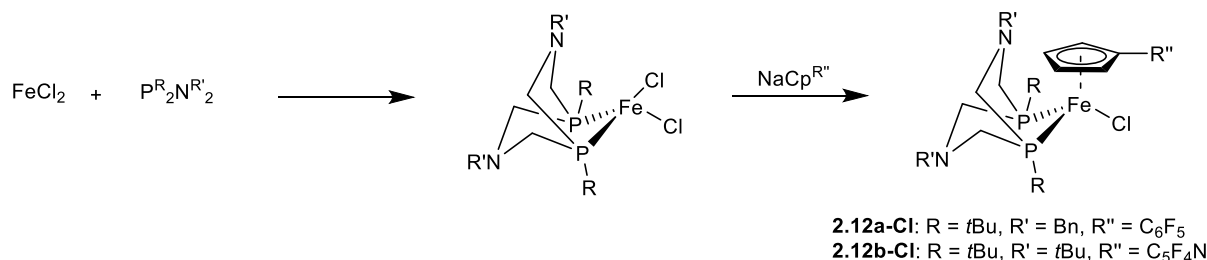
successful isolation of  $\text{Cp}^*\text{Ru}(\text{P}^{\text{Ph}}_2\text{N}^{\text{Bn}}_2)\text{Cl}$  in March of 2010, Dr. Bullock notified us that Dr. Mary DuBois et al. had not only isolated  $\text{Cp}^*\text{Ru}(\text{P}^{\text{Ph}}_2\text{N}^{\text{Bn}}_2)\text{Cl}$  but also prepared  $\text{Cp}^*\text{Ru}(\text{P}^{\text{Ph}}_2\text{N}^{\text{Bn}}_2)\text{H}$ . In the following accounts, I will first provide a general overview of the class of half-sandwich metal complexes bearing  $\text{P}_2\text{N}_2$  ligands and subsequently discuss the application of  $\text{Cp}^*\text{Ru}(\text{P}_2\text{N}_2)\text{H}$  as a catalyst for the hydrogenation of pyridinium cations. Particular attention will be directed to complexes 2.13-Cl and 2.13-H as they represent the same complexes I attempted to synthesize.

### 2.3.2a. Half-sandwich hydride complexes bearing $\text{P}_2\text{N}_2$ ligand

Half sandwich chloride  $\text{P}_2\text{N}_2$  complexes (e.g. **2.11-Cl**, *infra*) represent the starting point for the formation of other complexes such as the hydrido and dihydrogen complexes. For iron  $\text{P}_2\text{N}_2$  complexes, the synthesis for a particular chloride complex depends on the substituent on the cyclopentadienyl (Cp) ligand. Prolonged treatment of  $\text{CpFe}(\text{CO})_2\text{Cl}$  with an equivalent of  $\text{P}^{\text{Ph}}_2\text{N}^{\text{R}_2}$  ligand under photolyzing conditions yields  $\text{CpFe}(\text{P}_2^{\text{Ph}}\text{N}^{\text{R}_2})\text{Cl}$  (**2.11-Cl**); although insufficient duration of photolysis leads to the formation of  $[\text{CpFe}(\text{P}_2^{\text{Ph}}\text{N}^{\text{R}_2})(\text{CO})]^+\text{Cl}^-$ , this complex may be converted to the desired chloride complex with additional photolysis (Scheme 2.7).<sup>10</sup> Preparation of half-sandwich iron complex bearing  $\text{P}_2\text{N}_2$  ligand and substituted Cp ligand requires a different precursor material,  $\text{FeCl}_2$ , which may be initially treated with the desired  $\text{P}_2\text{N}_2$  ligand and subsequently treated with the desired substituted Cp ligand in anionic form to yield  $\text{Cp}^{\text{R}'}\text{Fe}(\text{P}_2^{\text{R}_2}\text{N}^{\text{R}'_2})\text{Cl}$  (**2.12-Cl**) (Scheme 2.8).<sup>11</sup>

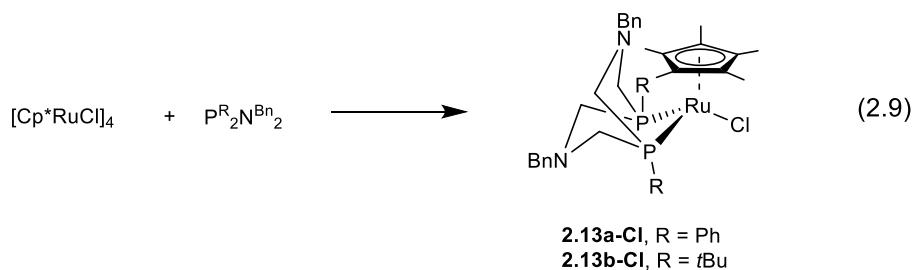


### Scheme 2.7

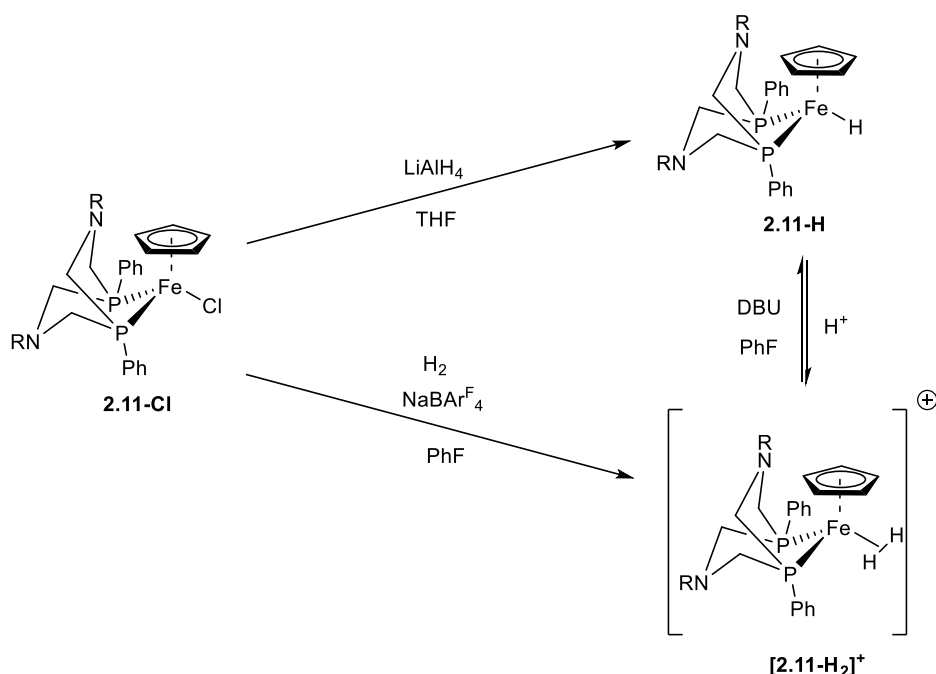


### Scheme 2.8

Half-sandwich ruthenium complexes bearing a single chelating P<sub>2</sub>N<sub>2</sub> ligand may be prepared by treating the oligomeric [Cp\*<sup>\*</sup>RuCl]<sub>4</sub> with an equivalent of the desired P<sub>2</sub>N<sub>2</sub> (eq. 2.9).<sup>11,12</sup>



The interconversions between the chloride, hydride, and dihydrogen complexes of **2.11**, **2.12**, and **2.13** are quite similar: the reduction of the chloride complex by a hydride yields the corresponding hydride complex; the treatment of the chloride complex with H<sub>2</sub> and NaBAR<sup>F</sup><sub>4</sub> yields the dihydrogen complex; and the hydride complex may be reversibly protonated to form the dihydrogen complex (Scheme 2.9, using complexes of **2.11** as examples).



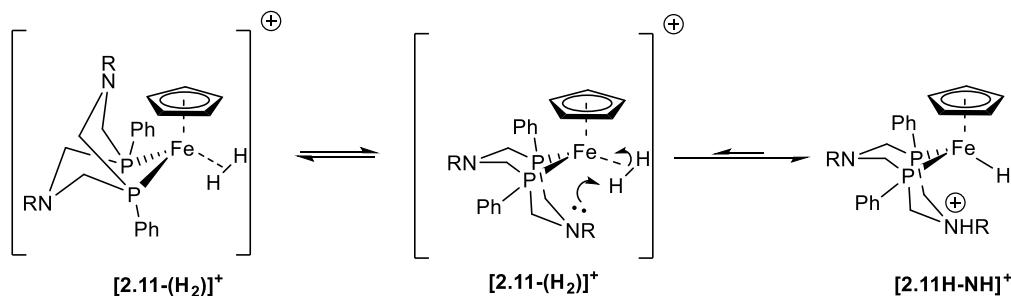
**Scheme 2.9**

Upon coordination to a metal to form complexes of the formula  $CpM(P_2N_2)L$ , the eight-membered  $P_2N_2$  ligand forms a bicyclic structure similar to the conformation adopted by the  $P_2N_2$  ligand in metal complexes bearing two  $P_2N_2$  ligands per molecule (e.g. complex **2.9**, *vide supra*). While the six-membered ring more proximal to the cyclopentadienyl ring ligand will normally adopt a boat conformation, the conformation of the other six-membered ring is influenced by the nature of the ligand L. When L is a ligand having a formal negative charge (e.g. hydride or chloride), the six-membered ring proximal to L adopts a chair conformation in order to minimize repulsion between the ligand and the nitrogen lone pairs in the six-membered ring; in subsequent discussion this conformation will be referred to as the boat-chair conformation. On the other hand, a chair-boat conformation is observed when L is a carbonyl due to the interaction arising between the nitrogen lone pair and the partial positive charge of the carbonyl carbon.<sup>10</sup>



### 2.3.2b. Intramolecular deprotonation and proton shuttling

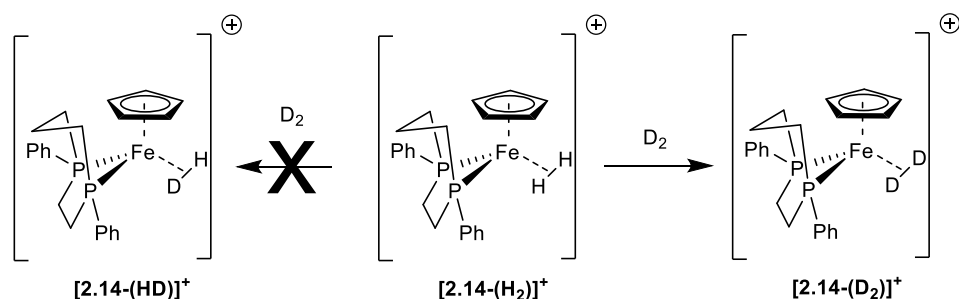
Calculations by DuBois et al. have shown that  $[2.11\text{-H-NH}]^+$ , formed from the heterolytic cleavage of the dihydrogen complex  $[2.11\text{-(H}_2)]^+$  by the amine nitrogen on the  $\text{P}_2\text{N}_2$  ring (Scheme 2.10), is less thermodynamically favorable in comparison to  $[2.11\text{-(H}_2)]^+$ .<sup>10</sup> Though the equilibrium constant for the transformation of  $[2.11\text{-(H}_2)]^+$  to  $[2.11\text{-H-NH}]^+$  is 0.003,  $[2.11\text{-H-NH}]^+$  is nevertheless thermodynamically accessible at room temperature. The relative stability of the dihydrogen complex  $[\text{M}(\text{H}_2)]^+$  and the corresponding intramolecularly protonated hydride complex  $[\text{MH-NH}]^+$  may be altered by changing the substituent on the Cp ring and the nitrogen in the  $\text{P}_2\text{N}_2$  ligand. For example, the intramolecularly protonated hydride complex  $[2.12\text{b-H-NH}]^+$  was calculated to be 0.65 kcal/mol more favorable compared to the dihydrogen complex  $[2.12\text{b-(H}_2)]^+$ ; in fact,  $[2.12\text{b-(H}_2)]^+$  is actually not observed in reaction at room temperature.<sup>13</sup>



**Scheme 2.10**

The proximity of the intramolecular amine to the dihydrogen ligand allows for the facile incorporation of deuterium when a dihydrogen complex is treated with  $\text{D}_2$ , which results in the formation of deuterated dihydrogen complex such as  $[2.11(\text{HD})]^+$ .<sup>10-11, 13</sup> In contrast, when a dihydrogen complex  $[2.14\text{-(H}_2)]^+$  having a nitrogen-less diphosphine is treated with  $\text{D}_2$ , only  $[2.14\text{-(D}_2)]^+$  and  $\text{H}_2$  are observed while the formation of  $[2.14\text{-(HD)}]^+$  is not detected (Scheme 2.11).<sup>10</sup> The ability of the  $\text{P}_2\text{N}_2$  amine to carry out the heterolytic cleavage of dihydrogen is of

interest to our research goals. As discussed previously (§ 2.1, *supra*), slow deprotonation of the dihydrogen complex  $[\text{CpRu}(\text{P-P})(\text{H}_2)]^+$  allows for its isomerization into the corresponding dihydride complex  $[\text{CpRu}(\text{P-P})(\text{H})_2]^+$ . As the dihydride complex cannot be deprotonated in a facile manner, this isomerization reaction represents one route of catalyst deactivation. My primary objective with the  $\text{P}_2\text{N}_2$  ligand is to see whether the incorporation of amines into the backbone of the disphosphine ligand would address the issue of catalyst deactivation.



**Scheme 2.11**

DuBois et al. determined that dihydrogen complexes  $[\mathbf{2.11b-(H_2)}]^+$ ,  $[\mathbf{2.12a-(H_2)}]^+$ , and  $[\mathbf{2.13-(H_2)}]^+$  have  $\text{p}K_a$  values between that of  $[\text{H-DBU}]^+$  and  $[\text{H-Et}_3\text{N}]^+$ .<sup>10-11, 12b, 13</sup> DBU readily deprotonates  $[\mathbf{2.11b-(H_2)}]^+$  while  $\text{Et}_3\text{N}$  fails to do so, thus implying a  $\text{p}K_a$  between 20 and 24 (in  $\text{CH}_3\text{CN}$ ) for this dihydrogen complex. Dihydrogen complex  $[\mathbf{2.12a-(H_2)}]^+$  may be partially deprotonated by  $\text{Et}_3\text{N}$  in  $\text{CH}_3\text{CN}$  and is thus slightly more acidic than  $[\mathbf{2.11b-(H_2)}]^+$ . The ruthenium dihydrogen complexes  $[\mathbf{2.13-(H_2)}]^+$  are the most basic given the electron-donating nature of the  $\text{Cp}^*$  ligand.

DuBois et al. reported that the protonation of hydride  $\mathbf{2.13a-H}$  and  $\mathbf{2.13b-H}$  yielded only their respective dihydrogen complexes  $[\mathbf{2.13a-(H_2)}]^+$  and  $[\mathbf{2.13b-(H_2)}]^+$ , and that the dihydride complexes  $[\mathbf{2.13a-(H)}_2]^+$  and  $[\mathbf{2.13b-(H)}_2]^+$  were not observed in the  $^1\text{H}$  NMR spectra.<sup>12b</sup> While there have yet to be either experimental or computational studies to determine if the dihydrogen complexes  $[\mathbf{2.13-(H_2)}]^+$  are thermodynamically favored over the corresponding dihydride

complexes, the absence of the dihydride complexes is particularly noteworthy for a hydride having a Cp\* ligand.

As observed by Morris et al.<sup>14</sup> and Jia et al.,<sup>15</sup> the protonation of half-sandwich Group-8 metal hydrides (*viz.* CpM(P-P)H) usually results in a mixture of the dihydrogen [CpM(P-P)(H<sub>2</sub>)<sup>+</sup>] and dihydride [CpM(P-P)(H)<sub>2</sub>]<sup>+</sup> complexes. For instance, at equilibrium the ratio of [Cp' Ru(dppe)(H<sub>2</sub>)<sup>+</sup>] to [Cp' Ru(dppe)(H)<sub>2</sub>]<sup>+</sup> is about 3.9:1.<sup>16</sup> When a Cp ligand is replaced by the more electron-donating Cp\* ligand, the dihydrogen complex becomes less thermodynamically stable as higher electron density leads to increased back donation into the H-H σ\* orbital, leading to the formation of the corresponding dihydride.<sup>14a, 15</sup>

Previous studies from the Norton Group showed that the rate of isomerization for the conversion of dihydrogen complex [Cp\* Ru(dppf)(H<sub>2</sub>)<sup>+</sup>] [**2.2d-(H<sub>2</sub>)**]<sup>+</sup> to the corresponding dihydride complex [**2.2d-(H)**]<sub>2</sub><sup>+</sup> is  $1.32(2) \times 10^{-3}$  at 0 °C,<sup>1</sup> which suggests a half-life of about 9 minutes at 0 °C. The rate of isomerization for a similar dihydrogen complex [Cp\* Ru(dppe)(H<sub>2</sub>)<sup>+</sup>] [**2.2c-(H<sub>2</sub>)**]<sup>+</sup> is  $1.53 \times 10^{-3}$  at a lower temperature (-10 °C).<sup>1, 17</sup> While the isomerization of the dihydrogen complex is reversible for certain types complexes,<sup>16</sup> this isomerization is irreversible for [Cp\* Ru(dppf)(H<sub>2</sub>)<sup>+</sup>].<sup>1</sup> Therefore, the usage of Ru<sup>II</sup> hydride complexes whose corresponding dihydrogen complexes may be readily deprotonated avoids one source of catalyst deactivation as discussed above.

### 2.3.2c. Electrochemical properties

The electrochemical behaviors of **2.13-H** and **2.13-Cl** have also been characterized by DuBois et al.<sup>12b</sup> While the substituent on the phosphorus atoms of the P<sub>2</sub>N<sub>2</sub> ligand does not seem to result in different oxidation potential of **2.13a-Cl** and **2.13b-Cl**, the oxidation potentials of

**2.13a-H** differs from that of **2.13b-H**. For the chloride complexes, the potential of the Ru<sup>II/III</sup> couple of both chloride complexes is -0.44 V versus Ferrocenium<sup>+</sup>/Ferrocene (Fc<sup>+</sup>/Fc) in dichloromethane, and the cyclic voltammogram (CV) for both exhibit reversible waves.

DuBois et al. determined the potential of the Ru<sup>II/III</sup> couple of **2.13a-H** to be -0.62 V and the potential of the Ru<sup>II/III</sup> couple of **2.13b-H** to be more negative at -0.84 V. Both experiments were conducted in fluorene. In contrast to the reversible CV for the chloride complexes **2.13a-Cl** and **2.13b-Cl**, the CV of the hydride complexes **2.13a-H** and **2.13b-H** are quasi-reversible and dependent on scan rate. The initial single-electron oxidation of the Ru<sup>II</sup> hydride yields a cationic Ru<sup>III</sup> hydride radical, many of which are known to be highly acidic.<sup>17-18</sup> In addition to the donation of a proton to another molecule such as the starting Ru<sup>II</sup> hydride, the cationic Ru<sup>III</sup> hydride radical could also undergo disproportionation reactions (*i.e.* Scheme 2.4, *supra*). Either the protonation or the disproportionation reaction would consume the cationic hydride radical, thus making it unavailable to be reduced in the returning scan of the CV experiment. DuBois et al. concluded that the protonation of the neutral hydride **2.13-H** by the cationic hydride radical would be the more likely reaction. Faster scanning rates minimize the effects of the aforementioned side reactions, thus making the CV of the hydride complexes reversible at high enough scan rates.

As cationic Ru<sup>III</sup> hydride radicals are already known to be acidic,<sup>18b</sup> and as the nitrogen on the P<sub>2</sub>N<sub>2</sub> ligand further facilitates the removal of proton from the cationic hydride radical, it is unlikely that cationic hydride radical [**2.13-H**]<sup>+</sup> would be a better hydrogen atom donor than it is a proton donor. The implication of this with respect to hydride transfer to pyridinium cation **2.1** is that the two-step mechanism exhibited by **2.2d-H** would be an unlikely one for **2.13-H**. From

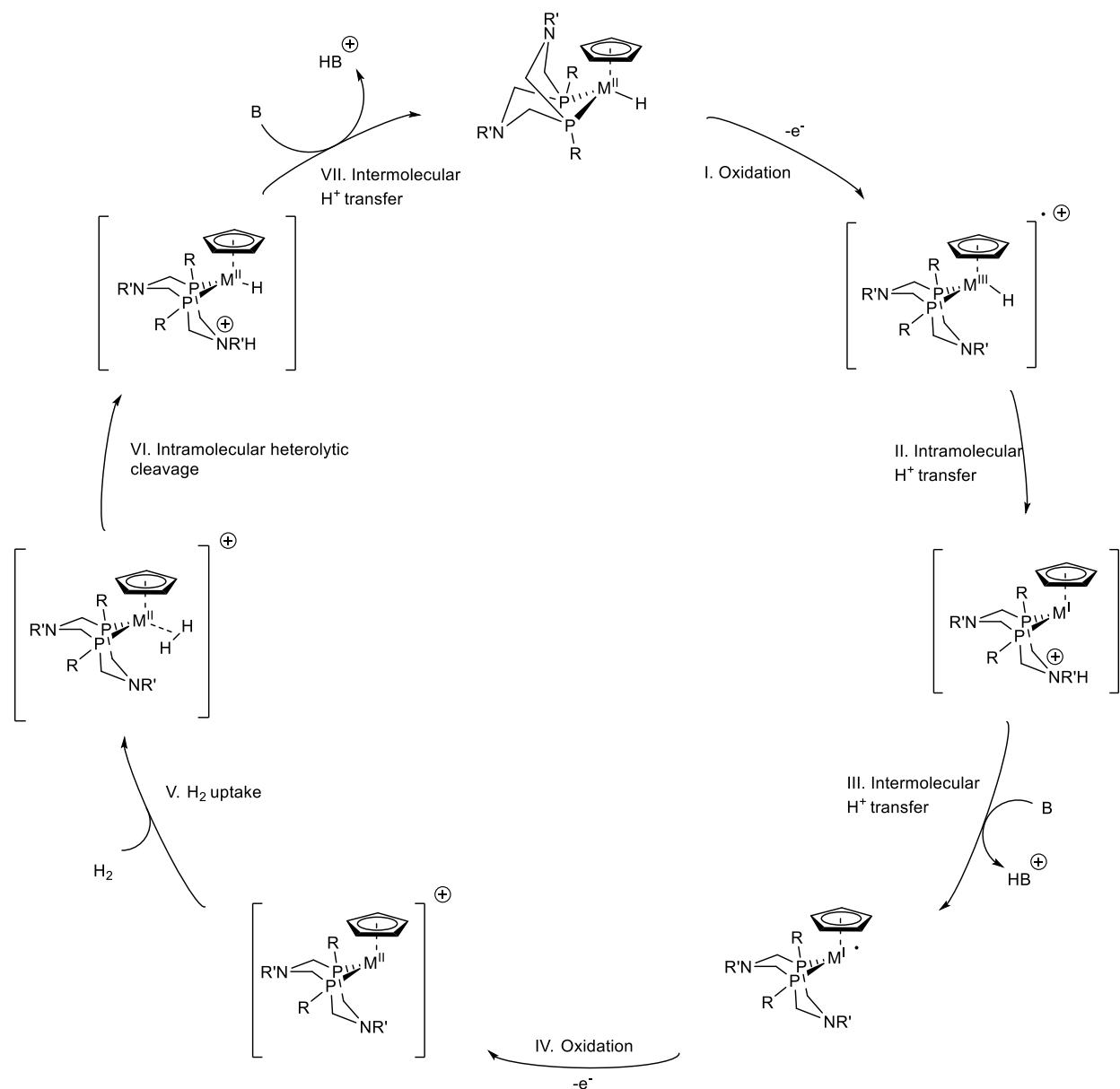
these hindsight knowledge, we were able to conclude that it would be unlikely that either **2.13a-H** or **2.13b-H** would transfer hydride solely to the  $\gamma$ -carbon of the pyridinium cation **2.1**.

### **2.3.2d. Half-sandwich Group-8 P<sub>2</sub>N<sub>2</sub> hydrides as electrocatalysts for the oxidation of dihydrogen**

Scheme 2.12 (*vide infra*) represents the process for the electrocatalytic oxidation of molecular hydrogen by half-sandwich Group-8 complexes bearing P<sub>2</sub>N<sub>2</sub> ligands. Taking the neutral hydride complex as the arbitrary starting point of the cycle, the metal hydride complex undergoes oxidation to form a 17-e<sup>-</sup> cationic M<sup>III</sup>-hydride radical, which, as discussed above in § 2.3.2c, is known to be highly acidic even without the presence of intramolecular bases.<sup>18b</sup> As such, this leads to the facile intramolecular deprotonation of the metal hydride by the tertiary amine nitrogen of the P<sub>2</sub>N<sub>2</sub> ligand. The proton on the ligand amine is then abstracted by an external base, which yields a coordinatively unsaturated, 17-e<sup>-</sup> M<sup>I</sup> complex. The oxidation of this complex to form the coordinatively unsaturated 16-e<sup>-</sup> M<sup>II</sup> complex followed by the uptake of molecular hydrogen yields the metal-dihydrogen complex.

As discussed earlier, deprotonation by the tertiary base of the P<sub>2</sub>N<sub>2</sub> ligand forms the intramolecularly protonated M<sup>II</sup>-hydride complex, which undergoes one more intermolecular proton transfer to return to the starting M<sup>II</sup>-hydride complex. DuBois et al. selected DBU as the external base as its steric bulk prevents it from binding to the metal center of a coordinatively unsaturated complex. As DuBois et al. observed that the tertiary base in the P<sub>2</sub>N<sub>2</sub> ligand may also bind to the metal center of a coordinatively unsaturated complex, complex **2.12b-H** was particularly adept as a catalyst for oxidation of molecular hydrogen as the steric congestion of

the *tert*-butyl groups on the amine of the P<sub>2</sub>N<sub>2</sub> ligand prevents the amine from interacting with the iron center of the complex.



**Scheme 2.12**

The net transformation of steps I-IV of Scheme 2.12 (starting with the oxidation of the neutral hydride) results in the transfer of a proton and two electrons from the metal hydride, which, in effect, is the net transformation of a hydride transfer from a metal hydride complex.

As such, the reactions in steps V-VII of Scheme 2.12 are of particular relevance with respect to catalytic ionic hydrogenation studied by the Norton Group to address the issue of catalyst deactivation (§ 2.1., supra) as these steps shown the heterolytic cleavage of the dihydrogen complex.

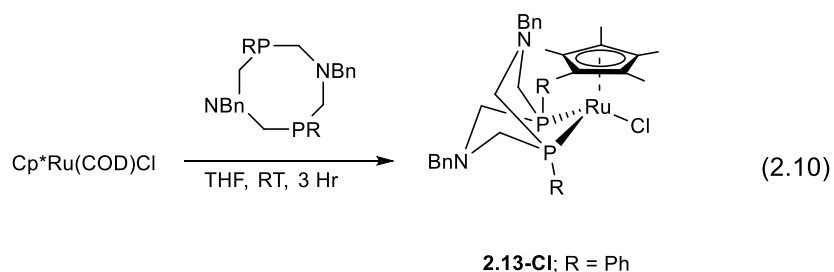
### 2.3.3. Ionic hydrogenation of pyridinium cation with Cp\*Ru(P<sub>2</sub>N<sub>2</sub>)H

As discussed in § 2.3.2 above, there was no literature precedence for the preparation of **2.13-Cl** and **2.13-H** when we began research in the fall of 2009. I modified literature methods used for the preparation of similar half-sandwich ruthenium complexes for the preparation of the chlorido complex **2.13-Cl** and the subsequent reduction to **2.13-H**.

As I had previously prepared ruthenium chlorides **2.2c-Cl** and **2.2d-Cl** according to a method described in the literature<sup>1</sup> by treating Cp\*Ru(PPh<sub>3</sub>)<sub>2</sub>Cl with the respective chelating phosphine in refluxing toluene, I attempted to prepare **2.13-Cl** using similar reaction conditions. When I treated Cp\*Ru(PPh<sub>3</sub>)<sub>2</sub>Cl with P<sup>Ph</sup><sub>2</sub>N<sup>Bn</sup><sub>2</sub> in refluxing toluene, the NMR spectra of the crude product indicated the chelation of P<sup>Ph</sup><sub>2</sub>N<sup>Bn</sup><sub>2</sub>: the <sup>1</sup>H spectrum prominently showed the signature AB splitting pattern (**Fig. 2.2a, *infra***), and the <sup>31</sup>P spectrum showed the presence of free PPh<sub>3</sub> and two new peaks, one larger than the other. However, I was unable to isolate a pure sample of **2.13-Cl** after repeated attempts.

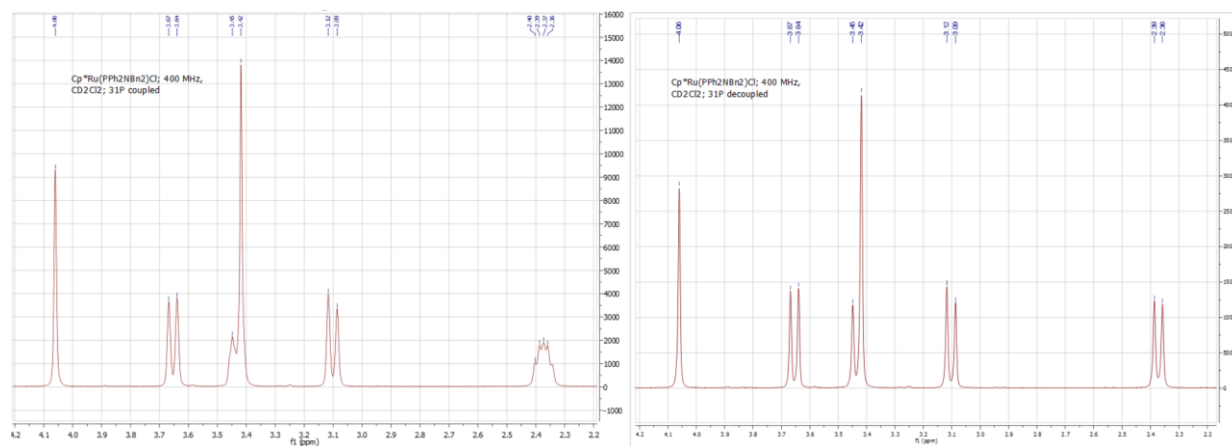
As the removal of the phosphorus-containing byproduct proved difficult, I next attempted to synthesize **2.13-Cl** using a different precursor, Cp\*Ru(COD)Cl, which had previously been used in the literature as a starting material for the preparation of other ruthenium chloride complexes of the formula Cp\*Ru(P-P)Cl, where P-P represents a chelating phosphine.<sup>19</sup> I treated Cp\*Ru(COD)Cl, prepared according to previously described method,<sup>20</sup> with P<sup>Ph</sup><sub>2</sub>N<sup>Bn</sup><sub>2</sub> in

THF at room temperature to obtain **2.13-Cl** (eq. 2.10). Concentration of the reaction mixture led to the formation of a crude orange-colored solid, and pure **2.13-Cl** was obtained by extracting the crude material with pentane followed by slow evaporation of the pentane solution. Both NMR spectra and elemental analysis confirmed that the product obtained was indeed **2.13-Cl**.



The  $^1\text{H}$  NMR spectrum of ruthenium chloride **2.13-Cl** exhibits three sets of doublets and one multiplet (**Fig. 2.2a**, *infra*) for the methylene protons on the  $\text{P}_2\text{N}_2$  ring and two singlet signals for the benzyl protons. One signal corresponding to the benzyl protons overlaps one of the methylene doublets. By decoupling interaction with the phosphorus atoms, the spectrum may be resolved into four sets of doublets (**Fig. 2.2b**, *infra*), which correspond to the four sets of methylene protons on the ring of the  $\text{P}_2\text{N}_2$  ligand. Rotation of the  $\text{Cp}^*$  ring is fast enough that complex **2.13-Cl** contains a plane of symmetry with the ruthenium, the chloride, and the two nitrogen atoms of the  $\text{P}_2\text{N}_2$  ring. As such, there are effectively four different chemical shifts for the methylene protons: each set of methylene protons located in the boat conformation ring (*viz.* the one proximal to the  $\text{Cp}^*$  ligand) form a first pair of diastereotopic protons, and the other set of methylene protons in the chair conformation ring form a second pair of diastereotopic protons. Each pair of diastereotopic protons gives an AB pattern in the  $^1\text{H}$  NMR spectrum. 2D H-H COSY spectrum of **2.13-Cl** (see appendix) established that the most upfield and downfield protons form one AB pattern while the two sets of signals located in the middle form the other AB pattern.





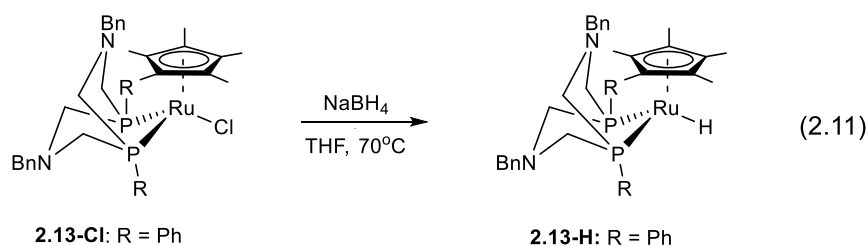
Figs. 2.2a and 2.2b, respectively the  $^{31}\text{P}$  coupled and  $^{31}\text{P}$ -decoupled  $^1\text{H}$  NMR spectra of **2.13-Cl**.

For the AB pattern made of the most upfield and most downfield signals, the average  $\delta$  is 1205.2 Hz, and the value  $\Delta\nu$  is 256.2 Hz, which means that the actual chemical shift values are 948.8 Hz and 1461.6 Hz (or  $\delta$  2.372 and 3.654, respectively) at 400 MHz; the two-bond coupling constant  $J_{\text{H-H}} = 11.2$  Hz. For the AB pattern made of the two signals in the middle, average  $\delta$  is 1307.2 Hz, and  $\Delta\nu$  is 65.9 Hz, which means that the actual chemical shift values are 1241.2 Hz and 1373.2 Hz (or 3.103 and 3.433, respectively) at 400 MHz; the two-bond coupling constant  $J_{\text{H-H}} = 12.4$  Hz. The  $^{31}\text{P}$  spectrum of ruthenium chloride **2.13-Cl** showed a single peak at  $\delta$  31.9. The  $^1\text{H}$  and  $^{31}\text{P}$  spectra of **2.13-Cl** match closely the spectra reported by DuBois et al.<sup>12a</sup>

I initially attempted to prepare  $\text{Cp}^*\text{Ru}(\text{P}^{\text{Ph}}_2\text{N}^{\text{Bn}}_2)\text{H}$  **2.13-H** by treating chloride **2.13-Cl** with lithium triethylborohydride. The  $^1\text{H}$  NMR spectrum of the reaction mixture exhibited an upfield triplet peak ( $\delta$  -12.80,  $J_{\text{P-H}} = 28$  Hz), the chemical shift of which indicated the presence of a transition metal hydride. The observed coupling between the phosphorus atoms and the hydride was expected, as such upfield triplets are observed in the  $^1\text{H}$  spectra of numerous other half-sandwich ruthenium hydrides bearing chelating phosphine ligands. The  $^{31}\text{P}$  NMR spectrum exhibited two signals: a major peak at  $\sim\delta$  45 and a minor peak at  $\sim\delta$  33. As the integral of the

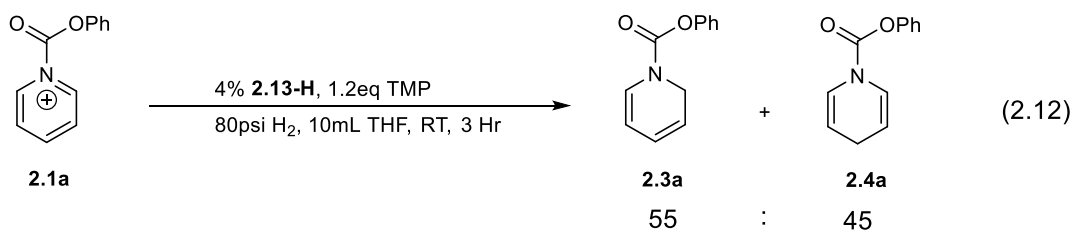
major peak accounted for only 86% of phosphorus nuclei, and as the minor peak is indicative of neither **2.13-Cl** nor **2.13-H**, further purification of the reaction product was needed.

It was at this time that we became aware that DuBois et al. had also synthesized ruthenium hydride **2.13-H** to be used as an electrocatalyst for the oxidation of molecular hydrogen (§ 2.3.2d, *supra*). I adopted the methods of the DuBois group<sup>12b</sup> to obtain **2.13-H** from **2.13-Cl**, using sodium borohydride as the reducing agent (eq. 2.10). A yellow-colored powder was obtained from this reaction.



The reduction of pyridinium cation **2.1a** by **2.13-H** yielded a mixture of 1,2-dihydropyridine **2.3a** and 1,4-dihydropyridine **2.4a**; **2.3a** accounted for ~55% of the product and **2.4a** accounting for the rest of the product. Together, the yield of both dihydropyridine products accounted for ~80% of the starting pyridinium cation **2.1a**. In retrospect, this product distribution of the two isomers was expected as the CV studies of **2.13a-H** by DuBois et al. indicated that its potentials were similar to that of CpRu(dppe)H **2.2a-H**.

I also attempted the reduction of **2.1a** with a catalytic amount of hydride **2.13-H**, using conditions similar to those described in § 2.1, with the exception that the catalyst loading was 4% (eq 2.12). The reaction was completed within three hours, with 87% of the pyridinium cation reduced to one of the two dihydropyridines. The ratio of 1,2-dihydropyridine **2.3a** to 1,4-dihydropyridine **2.4a** was 55:45, which is in line with what we observed for the stoichiometric reduction.



Overall NMR yield of 87%

At this point, as the results of the reduction of pyridinium cation **2.1a** by ruthenium hydride **2.13-H** indicated that **2.13-H** was not capable of reducing **2.1a** in a regioselective manner, and publications from DuBois et al. on **2.13-H** were imminent, I decided not to determine the turnover frequency for the catalytic reaction and terminated further evaluation of **2.13-H** as a catalyst for ionic hydrogenation.

## 2.4. Experimental Procedures

### General Procedures.

All air-sensitive compounds were prepared and handled under an N<sub>2</sub>/Ar atmosphere using standard Schlenk and inert-atmosphere box techniques. *N*-Carbophenoxy pyridinium tetraphenylborate (**2.1a**) was prepared by the method of King et al.<sup>3</sup> CpRu(dppe)H (**2.2a-H**),<sup>21</sup> CpRu(dppf)H (**2.2b-H**),<sup>22</sup> Cp\*Ru(dppe)H (**2.2c-H**),<sup>23</sup> and Cp\*Ru(dppf)H (**2.2d-H**)<sup>24</sup> were prepared according to literature methods. Cp\*Ru(COD)Cl was prepared according to literature method.<sup>20</sup>

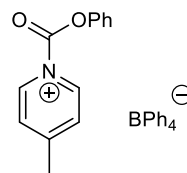
H<sub>2</sub>PPh was prepared by modifying literature method.<sup>25</sup> Instead of carrying out the distillation of crude H<sub>2</sub>PPh under N<sub>2</sub> atmosphere at elevated temperature, the distillation was carried out at lower temperature and reduced pressure by using a pressure controller. **CAUTION:** H<sub>2</sub>PPh is not only malodorous but also pyrophoric at elevated temperatures.

Cp\*Ru(P<sup>Ph</sup><sub>2</sub>N<sup>Bn</sup><sub>2</sub>)H **2.13-H** was prepared according to methods described by DuBois et al.<sup>12b</sup>

CD<sub>3</sub>CN was degassed and stored over 3 Å activated molecular sieves. CD<sub>2</sub>Cl<sub>2</sub> was dried over 3 Å activated molecular sieves, degassed by three freeze-pump-thaw cycles, and stored in an inert atmosphere glovebox. CH<sub>2</sub>Cl<sub>2</sub> was dried and deoxygenated by two successive columns (activated alumina, Q5 copper catalyst). THF was distilled from sodium/benzophenone under an N<sub>2</sub> atmosphere. <sup>1</sup>H NMR spectra taken in CD<sub>3</sub>CN and CD<sub>2</sub>Cl<sub>2</sub> are referenced to the corresponding residual solvent peaks: δ 1.94 and δ 5.32, respectively.

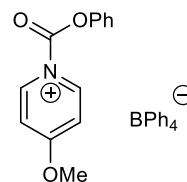
### Preparation of pyridinium salts **2.1b-d**.

These pyridinium salts are prepared according to literature procedures in a fashion similar to that used for pyridinium **2.1a**,<sup>1</sup> with the substituted pyridines used in lieu of pyridine. For pyridinium salt **2.1e**, NaOTf was used in lieu of NaBPh<sub>4</sub>.



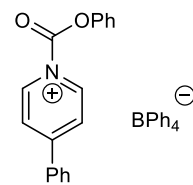
**1-(carbophenoxy)-4-methyl-pyridinium tetraphenylborate 2.1b.**

This cation has been previously reported, but it has been neither isolated nor characterized. <sup>1</sup>H NMR (300 MHz, CD<sub>3</sub>CN, δ): 2.78 (s, 3H, 4-CH<sub>3</sub>C<sub>5</sub>H<sub>4</sub>N), 6.78-6.88 (m, 4H, BPh<sub>4</sub>), 6.93-7.04 (m, 8H, BPh<sub>4</sub>), 7.23-7.33 (m, 8H, BPh<sub>4</sub>), 7.42-7.54 (m, 3H, (O)COPh), 7.55-7.65 (m, 2H, (O)COPh), 7.95-8.02 (d, 2H, **3,5-H** of 4-CH<sub>3</sub>C<sub>5</sub>H<sub>4</sub>N), 9.24-9.29 (d, 2H, **2,6-H** of 4-CH<sub>3</sub>C<sub>5</sub>H<sub>4</sub>N). MS: 214 (M, cation).



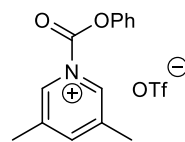
**1-(carbophenoxy)-4-methoxy-pyridinium tetraphenylborate 2.1c.**

This cation has been previously reported, but it has been neither isolated nor characterized. <sup>1</sup>H NMR (400 MHz, CD<sub>3</sub>CN, δ): 4.24 (s, 3H, 4-OCH<sub>3</sub>C<sub>5</sub>H<sub>4</sub>N), 6.78-6.88 (m, 4H, BPh<sub>4</sub>), 6.94-7.03 (m, 8H, BPh<sub>4</sub>), 7.24-7.33 (m, 8H, BPh<sub>4</sub>), 7.38-7.52 (m, 5H, (O)COPh), 7.54-7.62 (m, 2H, **3,5-H** of 4-OCH<sub>3</sub>C<sub>5</sub>H<sub>4</sub>N), 9.18-9.24 (d, 2H, **2,6-H** of 4-OCH<sub>3</sub>C<sub>5</sub>H<sub>4</sub>N). MS: 230 (M, cation).



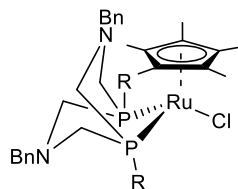
**1-(carbophenoxy)-4-phenylpyridinium tetraphenylborate 2.1d.**

This cation has been previously reported, but it has been neither isolated nor characterized.  $^1\text{H}$  NMR (300 MHz, RT,  $\text{CD}_3\text{CN}$ ): 6.80-6.90 (m, 4H,  $\text{BPh}_4$ ), 6.95-7.05 (m, 8H,  $\text{BPh}_4$ ), 7.23-7.33 (m, 8H,  $\text{BPh}_4$ ), 7.47-7.56 (m, 3H, (O)COPh), 7.58-7.67 (m, 2H, (O)COPh), 7.69-7.85 (m, 3H, 4- $\text{PhC}_5\text{H}_4\text{N}$ ), 8.08-8.16 (m, 2H, 4- $\text{PhC}_5\text{H}_4\text{N}$ ), 8.46-8.52 (m, 2H, **3,5-H** of 4- $\text{PhC}_5\text{H}_4\text{N}$ ) 9.44-9.51 (d, 2H, **2,6-H** of 4- $\text{PhC}_5\text{H}_4\text{N}$ ). Anal. calcd.  $\text{C}_{42}\text{H}_{34}\text{BNO}_2$ , value given as percentage: C 84.71, H 5.75, N 2.35; found C 84.12, H 5.71, N 2.43.



**1-(carbophenoxy)-3,5-dimethylpyridinium trifluoromethanesulfonate 2.1e.**

$^1\text{H}$  NMR (300 MHz,  $\text{CD}_3\text{CN}$   $\delta$ ): 2.61 (s, 6H, 3,5- $(\text{CH}_3)_2\text{C}_5\text{H}_4\text{N}$ ), 7.43-7.54 (m, 3H, (O)COPh), 7.55-7.64 (m, 2H, (O)COPh), 8.59 (s, 1H, 4- $\text{H}$  of 3,5- $(\text{CH}_3)_2\text{C}_5\text{H}_4\text{N}$ ), 9.28 (s, 2H, **2,6-H** of 3,5- $(\text{CH}_3)_2\text{C}_5\text{H}_4\text{N}$ ).



**$\text{Cp}^*\text{Ru}(\text{PPh}_2\text{NBn}_2)\text{Cl}$  2.13-Cl.**

In an inert atmosphere glovebox,  $\text{Cp}^*\text{Ru}(\text{COD})\text{Cl}$  (1.8 mmol),  $\text{PPh}_2\text{NBn}_2$  (1.89 mmol), and a magnetic stir bar were placed in a Schlenk flask. The flask was sealed with a rubber septum, removed from the glovebox, and connected to  $\text{N}_2$  line. To the flask was then added 40 mL of freshly distilled THF, and the reaction proceeded for three hour. THF was then evaporated to

yield a crude material, which was extracted using 3 x 25 mL pentane and collected into another Schlenk flask. Slow evaporation of the pentane solution yielded orange crystalline solid, which was filtered and collected.  $^1\text{H}$  ( $^{31}\text{P}$ -decoupled) NMR (400 MHz,  $\text{CD}_2\text{Cl}_2$ ,  $\delta$ ): 1.29 (s, 15 H,  $\text{Cp}^*$ ), 2.37 and 3.65 (ABq, 4 H,  $J_{\text{AB}} = 11.2$  Hz,  $\text{PCH}_2\text{N}$ ), 3.10 and 3.43 (ABq, 4 H,  $J_{\text{AB}} = 12.4$  Hz,  $\text{PCH}_2\text{N}$ ), 3.42 (s, 2 H,  $\text{NCH}_2\text{Ph}$ ), 4.08 (s, 2 H,  $\text{NCH}_2\text{Ph}$ ), 6.90-6.96 (m, 2H, Ar), 7.13-7.18 (m, 3H, Ar), 7.31-7.54 (m, 11H, Ar), 7.58-7.64 (m, 4H, Ar).  $^{31}\text{P}$  ( $^1\text{H}$ -coupled) NMR (162 MHz,  $\text{CD}_2\text{Cl}_2$ ,  $\delta$ ): 31.9. The  $^1\text{H}$  and  $^{31}\text{P}$  spectra agreed with those reported by DuBois et al.<sup>12</sup> Anal. calcd.  $\text{C}_{40}\text{H}_{47}\text{ClN}_2\text{P}_2\text{Ru}$ , value given as percentage: C 63.69, H 6.28, N 3.71; found C 62.44, H 6.51, N 3.76.

### **Procedure for stoichiometric reaction between pyridinium 2.1b-2.1e and ruthenium hydrides (2.2).**

In an inert atmosphere glovebox, pyridinium salt **2.1** (0.02 mol.) was combined with ruthenium hydride 2.2 (0.02 mol) and placed within a screw-cap NMR tube. To the NMR tube was subsequently added 700  $\mu\text{L}$  of  $\text{CD}_2\text{Cl}_2$  and  $\text{CH}_3\text{CN}$  (0.08 mmol) at room temperature. The reaction was then observed using  $^1\text{H}$  NMR within the domain from  $\delta$  10 to  $\delta$  -15 ppm.

### **Catalytic reduction of pyridinium 2.1b and 2.1d by ruthenium hydride $\text{Cp}^*\text{Ru}(\text{dppe})\text{H}$ 2.2c-H. CAUTION! Always shield pressurized vessels!**

Under an inert atmosphere, pyridinium cation **2.1** (0.50 mmol), **2.2c-H** (0.02 mmol), and a magnetic stirbar were combined in a Fischer-Porter bottle. THF (10 mL) and 2,2,6,6-tetramethylpiperidine (TMP, 0.10 mL, 0.6 mmol) were added and the apparatus was charged with  $\text{H}_2$  (80 psi). The reaction mixture was stirred rapidly at room temperature and stopped after

two hours. From the Fischer-Porter bottle was removed a 2 mL aliquot of the reaction mixture, which was transferred to a flask and evaporated. To the remnant of the reaction mixture was added 0.7 mL  $\text{CDCl}_3$  and 3  $\mu\text{L}$  of  $\text{CH}_3\text{CN}$  as an internal standard to determine NMR yield.

### **Stoichiometric reaction between pyridinium 2.1a and $\text{Cp}^*\text{Ru}(\text{P}^{\text{Ph}}_2\text{N}^{\text{Bn}}_2)\text{H}$ 2.13-H.**

In an inert atmosphere glovebox, pyridinium salt **2.1a** (0.02 mol.) was combined with **2.13-H** (0.02 mol) and placed within a J-Young NMR tube. To the NMR tube was subsequently added 700  $\mu\text{L}$  of  $\text{CD}_2\text{Cl}_2$  and  $\text{CH}_3\text{CN}$  (0.08 mmol) at room temperature. The reaction was then observed using  $^1\text{H}$  NMR within the domain from  $\delta$  10 to  $\delta$  -15 ppm, and the product ratios were determined by  $^1\text{H}$  NMR integration.

### **Catalytic reduction of pyridinium salt 2.1a by $\text{Cp}^*\text{Ru}(\text{P}^{\text{Ph}}_2\text{N}^{\text{Bn}}_2)\text{H}$ 2.13-H. CAUTION!**

*Always shield pressurized vessels!*

Under an inert atmosphere, pyridinium cation **2.1a** (0.50 mmol) and **2.13-H** (0.02 mmol) were combined in a Fischer-Porter bottle. THF (10 mL), hexamethylbenzene (0.166 mmol, as internal standard), and 2,2,6,6-tetramethylpiperidine (TMP, 0.10 mL, 0.6 mmol) were added and the apparatus was charged with  $\text{H}_2$  (80 psi). The reaction mixture was stirred rapidly at room temperature and stopped after two hours. From the Fischer-Porter bottle was removed a 2 mL aliquot of the reaction mixture, which was transferred to a flask and evaporated. The remnant of the reaction mixture was dissolved in 0.7 mL  $\text{CD}_2\text{Cl}_2$  to determine NMR yield.

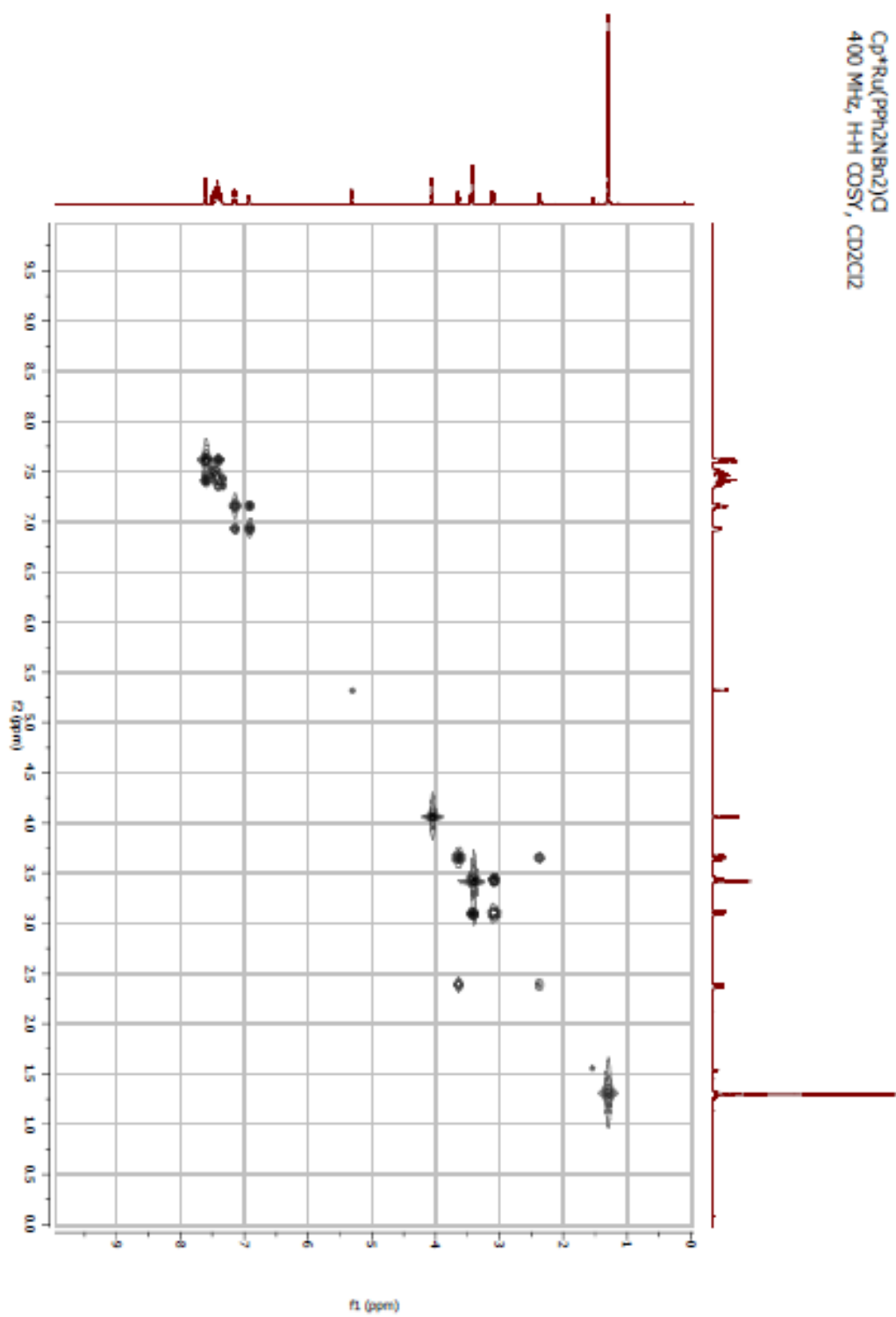


## References

1. Shaw, A. P.; Ryland, B. L.; Franklin, M. J.; Norton, J. R.; Chen, J. Y. C.; Hall, M. L. *J. Org. Chem.* **2008**, *73*, 9668.
2. Eberhart, M. S.; Norton, J. R.; Zuzek, A.; Sattler, W.; Ruccolo, S. *J. Am. Chem. Soc.* **2013**, *135*, 17262.
3. King, J. A.; Bryant, G. L. *J. Org. Chem.* **1992**, *57*, 5136.
4. (a) Guan, H.; Saddoughi, S. A.; Shaw, A. P.; Norton, J. R. *Organometallics* **2005**, *24*, 6358; (b) Smith, K. T.; Roemming, C.; Tilset, M. *J. Am. Chem. Soc.* **1993**, *115*, 8681.
5. Foowler, F. W. *J. Org. Chem.* **1972**, *37*, 1321.
6. Comins, D. L. a. H., James J. *Heterocycles* **1987**, *26*, 2159.
7. Curtis, C. J.; Miedaner, A.; Ciancanelli, R.; Ellis, W. W.; Noll, B. C.; Rakowski DuBois, M.; DuBois, D. L. *Inorg. Chem.* **2003**, *42*, 216.
8. Wilson, A. D.; Newell, R. H.; McNevin, M. J.; Muckerman, J. T.; Rakowski DuBois, M.; DuBois, D. L. *J. Am. Chem. Soc.* **2006**, *128*, 358.
9. Galan, B. R.; Schöffel, J.; Linehan, J. C.; Seu, C.; Appel, A. M.; Roberts, J. A. S.; Helm, M. L.; Kilgore, U. J.; Yang, J. Y.; DuBois, D. L.; Kubiak, C. P. *J. Am. Chem. Soc.* **2011**, *133*, 12767.
10. Liu, T.; Chen, S.; O'Hagan, M. J.; Rakowski DuBois, M.; Bullock, R. M.; DuBois, D. L. *J. Am. Chem. Soc.* **2012**, *134*, 6257.
11. Liu, T.; DuBois, D. L.; Bullock, R. M. *Nat Chem* **2013**, *5*, 228.
12. (a) Tronic, T. A.; Rakowski DuBois, M.; Kaminsky, W.; Coggins, M. K.; Liu, T.; Mayer, J. M. *Angew. Chem. Int. Ed.* **2011**, *50*, 10936; (b) Liu, T.; DuBois, M. R.; DuBois, D. L.; Bullock, R. M. *Energy & Environmental Science* **2014**, *7*, 3630.
13. Liu, T.; Wang, X.; Hoffmann, C.; DuBois, D. L.; Bullock, R. M. *Angew. Chem. Int. Ed.* **2014**, *53*, 5300.
14. (a) Jia, G.; Lough, A. J.; Morris, R. H. *Organometallics* **1992**, *11*, 161; (b) Jia, G.; Morris, R. H. *J. Am. Chem. Soc.* **1991**, *113*, 875.
15. Jia, G.; Lau, C.-P. *Coord. Chem. Rev.* **1999**, *190–192*, 83.
16. Guan, H.; Iimura, M.; Magee, M. P.; Norton, J. R.; Zhu, G. *J. Am. Chem. Soc.* **2005**, *127*, 7805.
17. Belkova, N. V.; Dub, P. A.; Baya, M.; Houghton, J. *Inorg. Chim. Acta* **2007**, *360*, 149.

18. (a) Hu, Y.; Shaw, A. P.; Estes, D. P.; Norton, J. R. *Chem. Rev.* **2016**, *116*, 8427; (b) Ryan, O. B.; Tilset, M.; Parker, V. D. *J. Am. Chem. Soc.* **1990**, *112*, 2618.
19. (a) Braun, L.; Liptau, P.; Kehr, G.; Ugolotti, J.; Frohlich, R.; Erker, G. *Dalton Trans.* **2007**, 1409; (b) Balakrishna\*, M. S.; Panda, R.; Smith Jr, D. C.; Klaman, A.; Nolan\*, S. P. *J. Organomet. Chem.* **2000**, *599*, 159.
20. Boren, B. C.; Narayan, S.; Rasmussen, L. K.; Zhang, L.; Zhao, H.; Lin, Z.; Jia, G.; Fokin, V. V. *J. Am. Chem. Soc.* **2008**, *130*, 8923.
21. Bruce, M. I.; Humphrey, M. G.; Swincer, A. G.; Wallis, R. C. *Aust. J. Chem.* **1984**, *37*, 1747.
22. Bruce, M. I.; Butler, I. R.; Cullen, W. R.; Koutsantonis, G. A.; Snow, M. R.; Tiekink, E. R. T. *Aust. J. Chem.* **1988**, *41*, 963.
23. Belkova, N. V.; Dub, P. A.; Baya, M.; Houghton, J. *Inorg. Chim. Acta* **2007**, *360*, 149.
24. Hembre, R. T.; McQueen, J. S.; Day, V. W. *J. Am. Chem. Soc.* **1996**, *118*, 798.
25. Freedman, L. D.; Doak, G. O. *J. Am. Chem. Soc.* **1952**, *74*, 3414.

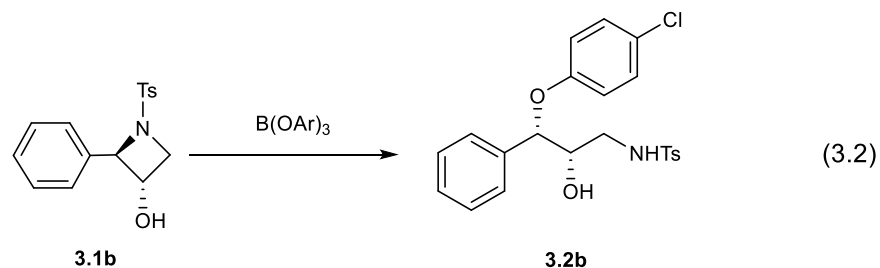
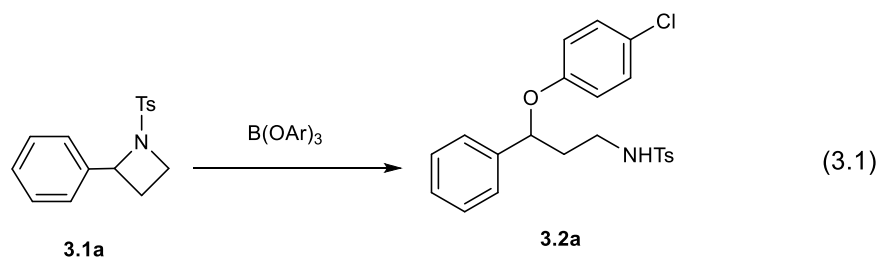
Cp\*Ru(PPh<sub>2</sub>NBr<sub>2</sub>)Cl  
400 MHz, H<sub>2</sub>O, CDCl<sub>3</sub>



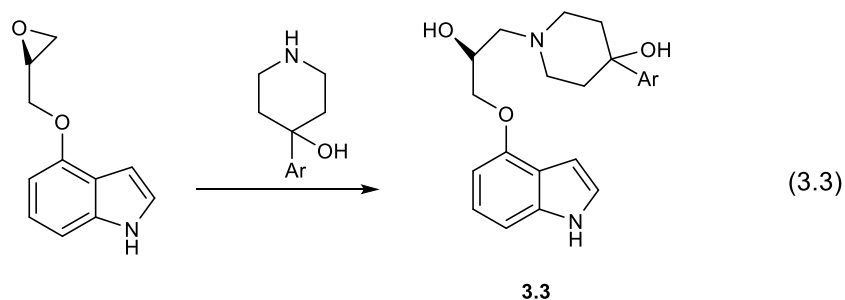
## Chapter 3. Ionic Hydrogenation of Azetidinium Cations

### 3.1. Relevance of ring opening of azetidines and azetidinium cations

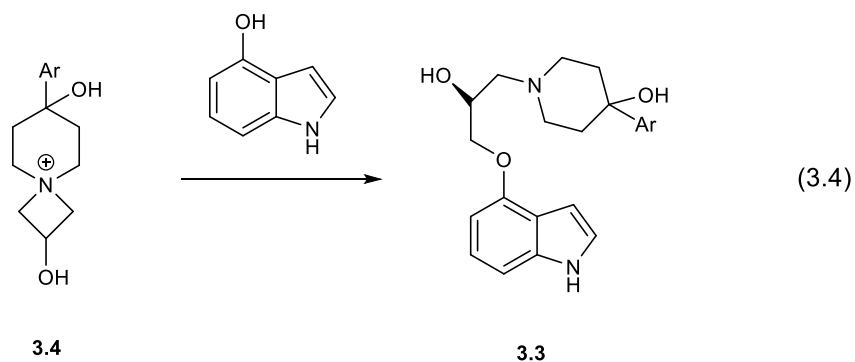
The ring opening of azetidinium rings has practical applications. The class of molecules known as  $\gamma$ -amino ethers has medicinal applications as they may be used to treat psychiatric disorders and other clinical conditions.<sup>1</sup> Bertolini et al. demonstrated that  $\gamma$ -amino ether molecules **3.2a** and **3.2b** may be prepared from the Lewis-Acid-mediated ring opening of azetidines **3.1a** and **3.1b**, respectively (eq. 3.1 and 3.2).<sup>2</sup>



Molecules such as  $\gamma$ -amino ethers **3.3** are known to be biologically active.<sup>3</sup> These compounds have traditionally been made by opening an epoxide with an alkyl amine (eq. 3.3).



An alternate approach to amines such as **3.3** occurs via the attack of a spirocyclic-azetidinium cation **3.4** (eq. 3.4).<sup>3</sup> In addition to phenols, other nucleophiles such as thiols have also been reported to effect ring opening of azetidinium cation **3.4**.<sup>3</sup>



### 3.1.1. General trends for nucleophilic ring opening of azetidinium cations

Azetidines, along with its lower homologue aziridines, represent the two smallest aza-heterocyclic molecules. The nitrogen of azetidine is fairly basic, with its conjugate acid having a  $pK_a$  of 11.29; this value is closer to that of the conjugate of pyrrolidine ( $pK_a$  of 11.31) than to the conjugate of aziridine ( $pK_a$  of 7.98).<sup>4</sup> On the other hand, the ring strain of azetidine at  $25.2 \text{ kcal mol}^{-1}$  is closer to the ring strain of aziridine ( $27.3 \text{ kcal mol}^{-1}$ ) than to the ring strain of pyrrolidine ( $5.8 \text{ kcal mol}^{-1}$ ).<sup>4</sup> The difference in ring strain between azetidine and pyrrolidines leads to divergent reaction pathways in many of the reactions discussed below.<sup>5</sup>

The ring opening of most N-alkyl azetidines requires activation via the protonation, alkylation, or acylation of the azetidine in order to form the corresponding azetidinium cation.<sup>4, 6</sup> Less basic azetidines such as N-sulfonyl azetidines can be activated by a Lewis Acid.<sup>2</sup> However, Lewis acids cannot be used to activate more basic azetidines (*e.g.* N-alkyl azetidines) as the dissociation of the former from the azetidines may be difficult. The ring opening of azetidinium rings by nucleophiles has been reported to be mostly  $S_N2$  in nature,<sup>4, 7</sup> and a variety of

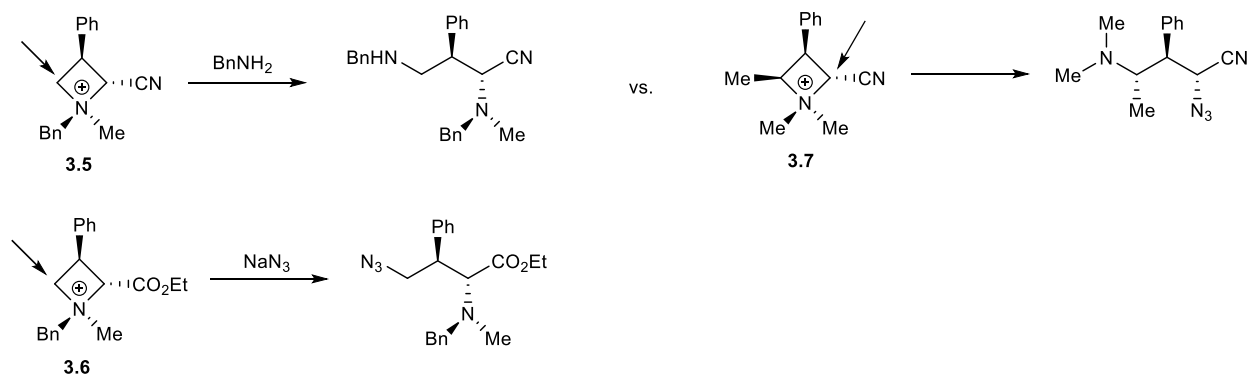
nucleophiles such as amines, azide anions, carboxylates, cyanide anions, halides, and hydrides have been shown to effect the opening of azetidinium rings.<sup>4,8</sup> In a few instances, the opening of azetidinium cations by softer halides has been shown to be reversible, implying that the regioselectivity of these reactions is also influenced by the energies of the products of ring opening.<sup>6</sup>

Strong bases and highly basic nucleophiles such as enolates have been shown to deprotonate  $\alpha$ -carbons that are either part of the azetidinium ring or are located on a substituent on the azetidinium nitrogen atom, resulting in either elimination reactions or the formation of azetidinium ylides (§ 3.1.2, *vide infra*).<sup>9</sup> The presence of an electron withdrawing group on the  $\alpha$ -carbon can stabilize the negative charge generated by the deprotonation, and the ylide thus generated can subsequently participate in reactions that either indirectly<sup>9a, 10</sup> (in cases where  $\alpha$ -carbon within the ring is deprotonated) or directly<sup>9b</sup> (in cases where a substituent on the nitrogen atom is deprotonated) cleave a N-C bond of the azetidinium ring.

### **3.1.1a. Nucleophilic ring opening of C2-substituted azetidinium cations.**

Couty et al. performed extensive studies on the regioselectivity of the opening of azetidinium cations and concluded that steric factors influence the regioselectivity of nucleophilic attack more than electronic factors do (Scheme 3.1).<sup>8, 11</sup> Azetidinium cations bearing nitrile and ester groups on C2 are preferentially attacked at the less substituted C4 by incoming nucleophiles (**3.5** and **3.6**, respectively). While nucleophilic attack does occur at C2 for azetidinium **3.7**, this has been attributed more to a steric effect than to an electronic effect.<sup>4, 8-</sup>

9, 11



**Scheme 3.1.**

Couty et al. have concluded that for azetidinium cations having a quaternary C2, attack at C2 is intrinsically favored.<sup>7</sup> As both the nitrogen and C2 are quaternary, steric crowding due to the substituents on these adjacent atoms weakens the C-N bond by lengthening it, thus leading to a higher positive charge on the  $\alpha$ -quaternary carbon. Couty et al. showed that ring opening occurred at the quaternary C2 for azetidinium cations **3.8a**, **3.8b**, and **3.8c** (**Fig. 3.1**); however, this trend was not observed for the spiroazetidinium **3.8d**, where nucleophilic attack occurred solely at the less hindered carbon.<sup>7</sup>

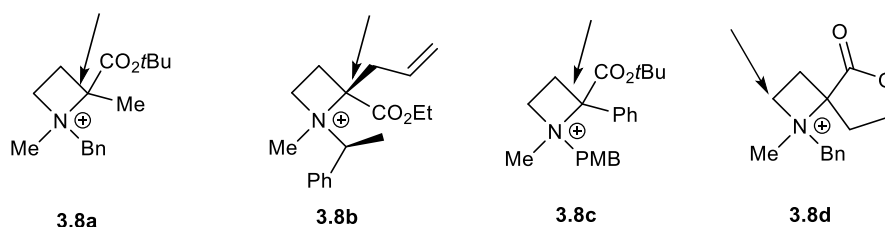
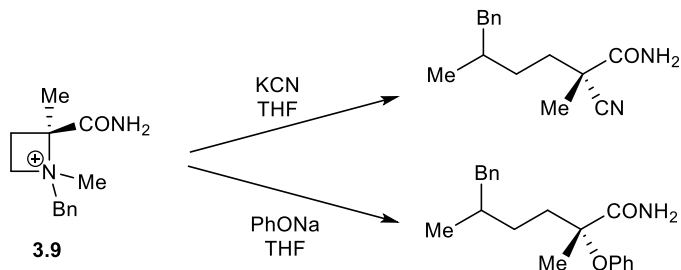


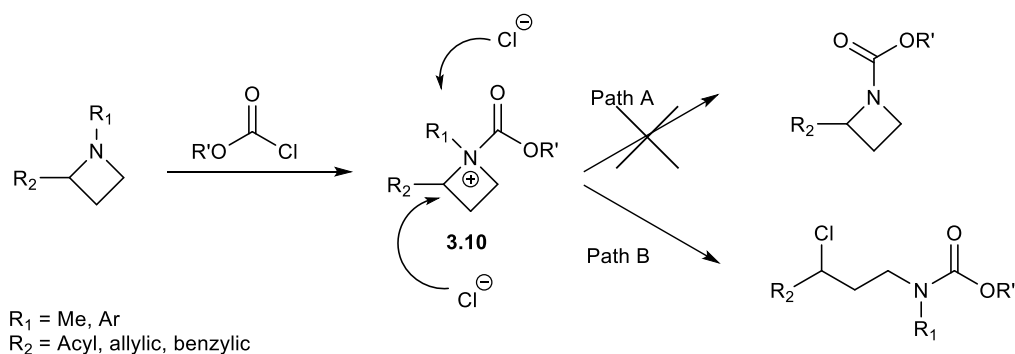
**Fig. 3.1**

The same trend is observed in the work of Leng et al: ring opening occurs at the quaternary C2 of azetidinium **3.9** (Scheme 3.2).<sup>12</sup>



**Scheme 3.2.**

Ring opening occurs at C2 for azetidinium ions **3.10** generated *in situ* from the reaction between chloroformates and azetidines bearing electron withdrawing groups (*e.g.* acyl or nitrile) on C2.<sup>5</sup> In this type of reaction, chloroformate both activates the azetidine for nucleophilic attack and serves as the source of the chloride for the attack (Scheme 3.3, Path B). Nucleophiles attack the substituted C2 of aziridinium cations bearing an allylic, benzylic, or acyl substituent on that carbon; in contrast, nucleophiles attack the unsubstituted C3 in similar aziridinium cations bearing a methyl group on C2.<sup>13</sup> This, in contrast to the reactions in Scheme 3.1, suggests that electronic influences can outweigh steric influences for at least some azetidinium cations.



**Scheme 3.3**

Although the treatment of alkyl amines with a chloroformate is known to be a standard method of removing N-methyl and N-benzyl groups,<sup>14</sup> N-dealkylation reactions (Path A of Scheme 3.3) are not operative for azetidines. On the other hand, the N-dealkylation reactions

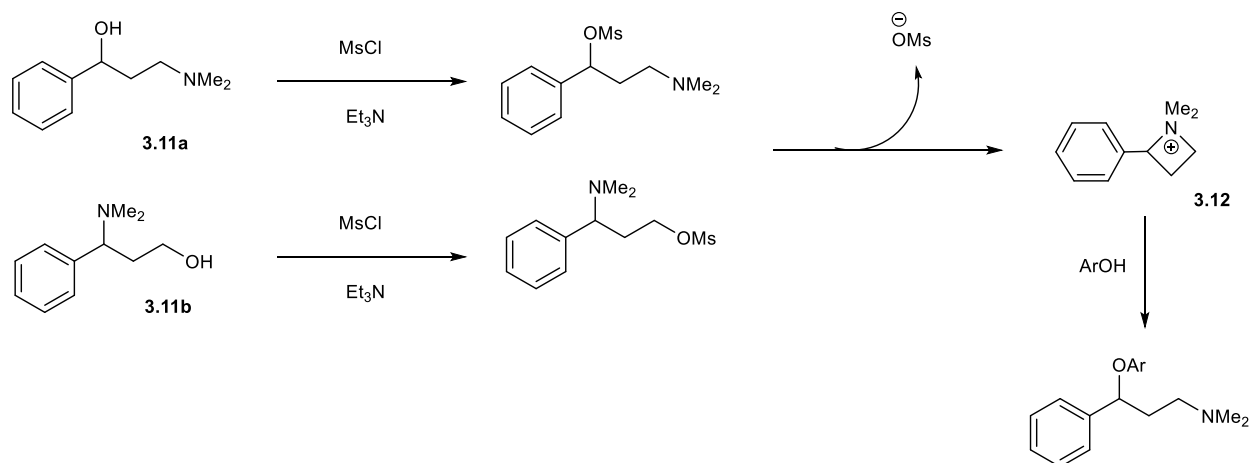


become predominant for pyrrolidines.<sup>5a</sup> Both Couty et al. and Ma et al. attribute this divergence in reaction mechanism to the relief of strain energy upon the opening of the azetidinium ring.<sup>5</sup>

### **3.1.1b. Effect of C2 aromatic substituent on the ring opening of azetidinium cations.**

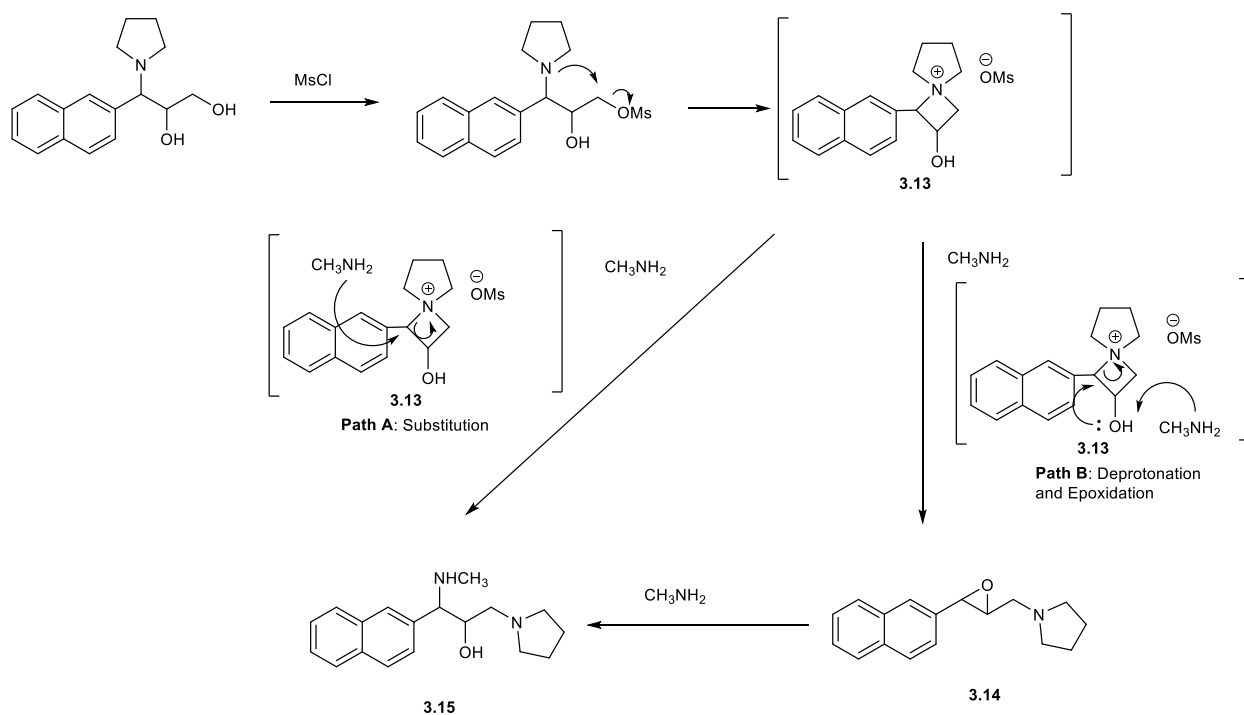
In contrast to the opening of azetidinium cations with electron withdrawing substituents such as nitriles and esters on C2, where electronic effects usually do not predominate over steric effects, the opening of azetidinium cations with aromatic substituents on C2 tends to be more influenced by electronic effects. In all of the known literature examples, incoming nucleophiles such as alcohols,<sup>1, 15</sup> thiols,<sup>16</sup> amines,<sup>17</sup> azides,<sup>12</sup> nitriles,<sup>12</sup> and allyl silanes<sup>18</sup> preferentially attack the aryl-substituted C2 of azetidinium cations or activated azetidines.<sup>14</sup>

Both the works of O'Brien<sup>19</sup> (Scheme 3.4) and Blakemore<sup>17</sup> represent examples where the opening of an *in situ* generated aryl-substituted azetidinium cation is invoked. In the former, the mesylation of the hydroxyl group of an aryl-substituted alkyl amine (**3.11a** or **3.11b**) results in an amino group  $\beta$  to the mesyl group. Subsequent attack of the amino group on the carbon with the mesyl substituent yields an aryl-substituted azetidinium cation (**3.12**), which can be opened at the benzylic C2 by a phenol. The work of Blakemore et al. represents a variation of the principle demonstrated in O'Brien et al. as the incoming nucleophile is an amine as opposed to an aryl alcohol.



### Scheme 3.4.

To the best of our knowledge, the work of Han et al. is the only case where spiro, aryl-substituted azetidinium has been opened.<sup>20</sup> As in the work of Blakemore et al. and O'Brien et al., the azetidinium cation **3.13** of Han et al. is generated *in situ* when a tertiary amine attacks a mesylate intramolecularly to form a four-membered ring. Although Han et al. have proposed that the formation of the product amine **3.15** arises from the opening of azetidinium cation **3.13** (Scheme 3.5), the azetidinium salt has not been isolated. The authors propose two different pathways for the formation of the amine product **3.15**, both of which invoke nucleophilic attack on C2.

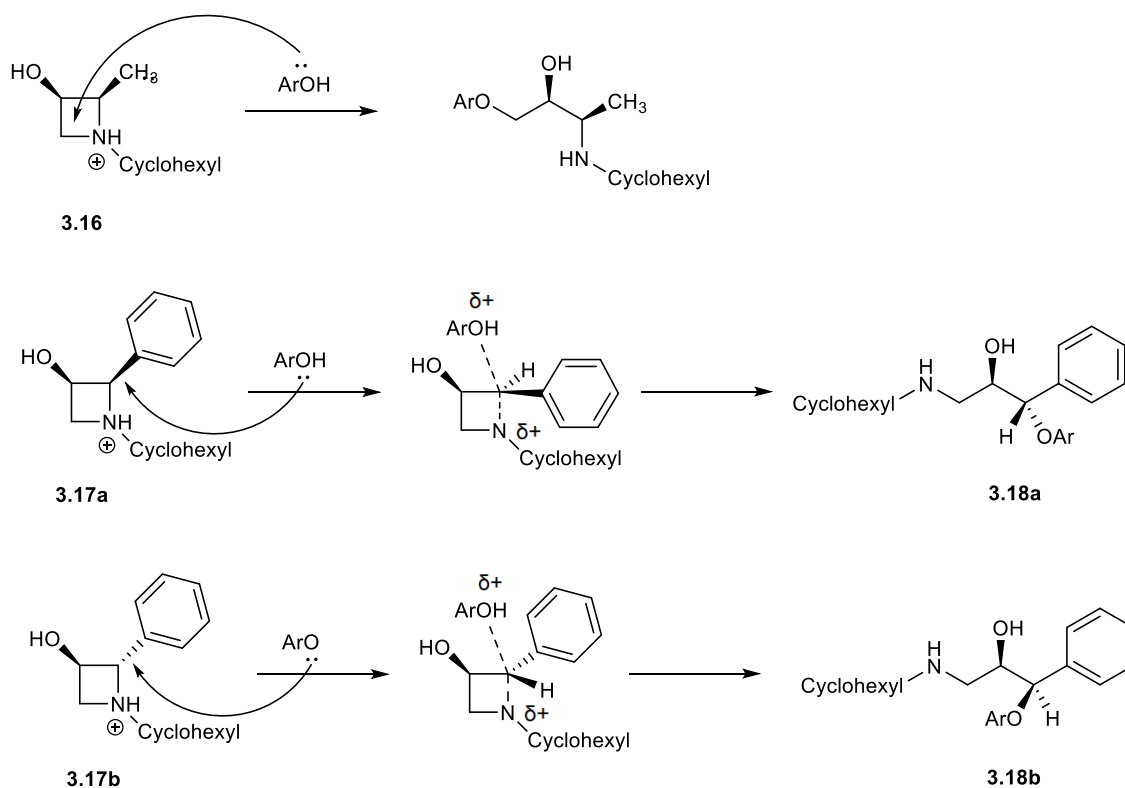


### Scheme 3.5

For Path A, methylamine attacks C2 and directly forms the amine product **3.15**. For Path B, methylamine deprotonates the hydroxyl group, thus leading to the formation of an epoxide ring and the opening of the azetidinium ring. Reaction of epoxide **3.14** with additional methylamine leads to the formation of amine product **3.15**. Han et al. argue that the mechanism in Path B is at least feasible, as the treatment of mesylate ester with triethylamine, a base stronger than methylamine, results in the formation of epoxide **3.14**. In either proposed mechanism, a nucleophile attacks the aromatic substituent bearing C2 of the azetidinium. While the reaction scheme demonstrates that the benzylic carbon on the azetidinium ring is indeed favored, there has been no study of the rate of the ring opening, and no one has determined if Path A, Path B, or both are operative. Nonetheless, this work is of particular interest to the Norton Group as azetidinium cation **3.13** closely resembles the azetidinium cation used in our mechanistic studies (§ 3.3, *vide infra*).

### 3.1.1c. Mechanism of nucleophilic ring opening

Higgins et al. have explored the ring opening of azetidins (**3.16** and **3.17**) that differ only with respect to substituents on C2 and have examined the effects that these substituents have on regioselectivity of ring opening by an aryloxy nucleophile.<sup>21</sup> While the methyl substituent on C2 of azetidinol **3.16** blocks access to the carbon atom due to steric effects and directs an incoming aryloxy nucleophile to C4, the phenyl substituent on C2 of azetidinol **3.17** directs the incoming nucleophile to C2 (Scheme 3.6).



**Scheme 3.6.**

The reaction between azetidinol **3.17** and the aryloxy nucleophile is not only regiospecific but also stereospecific, as nucleophilic attack on **3.17a** and **3.17b** yields solely **3.18a** and **3.18b**, respectively (Scheme 3.6). This result rules out the formation of a

carbocationic intermediate, as such an intermediate would lead to the formation of a racemic mixture of products. Nonetheless, Higgins et al. conclude that the 2-phenyl substituent is able to provide some stabilization to the positive charge on C2 in the transition state, so that the cleavage of the N-C2 bond will occur before the formation of the bond between C2 and the incoming nucleophile.

However, the nucleophilic opening of an azetidinium having an aromatic substituent on C2 does not always proceed via a S<sub>N</sub>2 mechanism. In the study of ring opening of azetidines discussed shown in eq. 3.1 (*vide supra*), Bertolini et al.<sup>2</sup> have shown that the opening of an enantiomerically pure azetidine leads to a racemic product, thus suggesting the reaction proceeding via a carbocation intermediate.

#### **3.1.1d. Ring opening of azetidinium cations by metal hydrides**

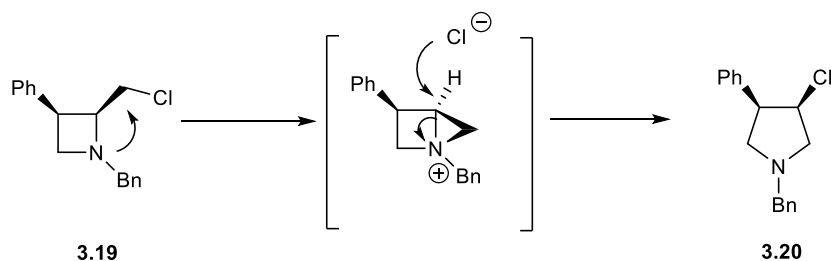
Couty et al. have also examined the reactions of various metal hydrides with azetidinium cations and have shown that steric effects, rather than electronic effects, influence the regioselectivity of the ring opening by sodium borohydride and sodium cyanoborohydride.<sup>11</sup> Ring opening occurs at the unsubstituted C4 in the reaction between borohydrides and azetidinium cations having C2 ester and nitrile groups. For azetidinium cations having substituents on both C2 and C4 (e.g. **3.7**, *vide supra*), ring opening occurs at C2, in line with results discussed above when the incoming nucleophile is an azide.

However, the reactions between aluminum hydrides and azetidinium cations exhibit different regioselectivity. For example, the treatment of azetidinium **3.6** with lithium aluminum hydride results in the concomitant ring opening at C2 and reduction of the C2 ester functional group to an alcohol; however, this difference in regioselectivity is attributed to the directing

effect of the alkoxide group of the intermediate formed during the reduction of the ester group of **3.6**. This study is of particular interest to the Norton Group as we have also attempted to open azetidinium cation with sodium borohydride and lithium aluminum hydride (§ 3.2.x, *vide infra*)

### 3.1.1e. Leaving groups that facilitate intramolecular substitution reactions.

The placement of leaving groups in suitable locations can facilitate intramolecular substitution reaction, which represents another method by which an azetidinium ring may be opened. Couty et al. have shown that azetidine **3.19** may be converted to the pyrrolidine **3.20** via a bicyclic intermediate (Scheme 3.7).<sup>22</sup> As the transformation is the result of two consecutive S<sub>N</sub>2 reactions, it is stereoselective and results in the overall retention of stereochemistry.

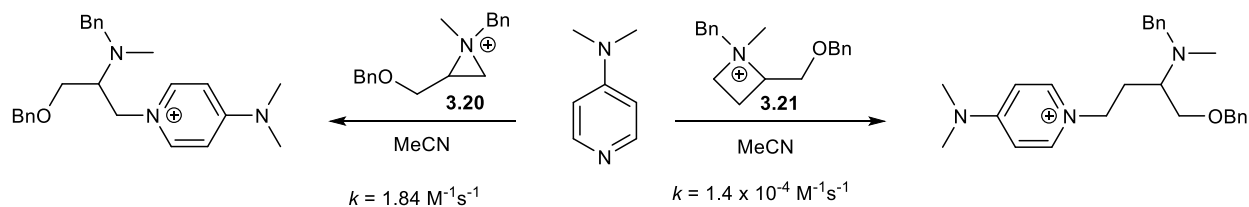


**Scheme 3.7**

### 3.1.1f. Kinetic studies of nucleophilic ring opening of azetidinium

To the best of our knowledge, a study by the Couty group is the sole case in which the rate of ring opening of azetidinium cations has been compared to the rate of ring opening of a corresponding aziridinium cation (Scheme 3.8).<sup>23</sup> The incoming nucleophiles used were 4-dimethylaminopyridine (DMAP) and the more nucleophilic 4-pyrrolidinopyridine (PPY). The ratios of the second-order rate constant for the opening of the aziridinium cation (**3.20**) to that for

the azetidinium cation (**3.21**) are similar for both nucleophiles:  $1.65 \times 10^4$  for DMAP and  $1.75 \times 10^4$  for PPY.



### Scheme 3.8

The difference in activation energy  $\Delta\Delta G^\ddagger$  between the opening of the aziridinium (**3.20**) and azetidinium (**3.21**) cations at 293 K has been extrapolated as  $5.6 \text{ kcal mol}^{-1}$ , which is comparable to that of  $6.8 \text{ kcal mol}^{-1}$  for the ring openings of aziridine and azetidine with ammonia in gas phase, obtained *in silico*.<sup>24</sup> This difference in activation energy is greater than the difference in ring strain between aziridines and azetidines, which has an experimentally determined value of  $1.5 \text{ kcal mol}^{-1}$  and a calculated value<sup>25</sup> of about  $2.1 \text{ kcal mol}^{-1}$ . The authors conclude that the slower opening of the azetidinium ring can not be solely attributed to ring strain.

As the nucleophilicity of DMAP is known, the authors determined the relative electrophilicities of the aziridinium and azetidinium cations by the Mayr-Patz equation (eq. 3.5), wherein  $k$  is the second-order rate constant at  $20^\circ\text{C}$ ,  $N$  and  $E$  are respectively nucleophile and electrophile parameters, and  $s$  is a nucleophile-specific constant.<sup>26</sup> As the values of  $s$  and  $N$  for DMAP in acetonitrile are known to be 0.67 and 14.95, respectively, the values  $E$  for aziridinium and azetidinium cations used in the study are  $-14.4$  and  $-20.7$ , respectively.

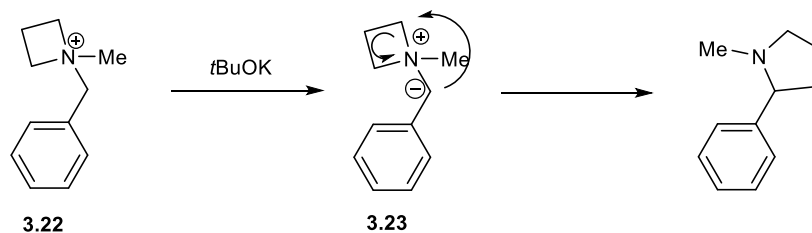
$$\log k_{20^\circ\text{C}} = s(N + E) \quad (3.5)$$

The electrophilicity value for the azetidinium cation at  $-20.7$  is toward the low end of the electrophilicity scale, implying that it is a weaker, more stabilized electrophile than the

corresponding aziridinium cation. While this work sheds understanding on the reactivity of azetidinium cations, the particular substrate studied did not possess an aromatic substituent on C2 that would favor ring opening at the more substituted carbon on the azetidinium ring.

### 3.1.2. Ring opening of azetidinium via the generation of an ylide

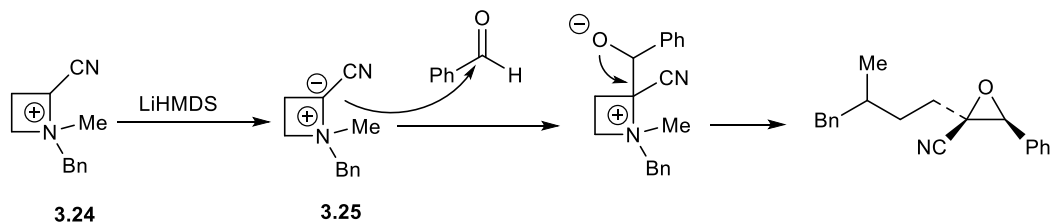
Azetidinium cations having an electron-withdrawing substituent on the carbon adjacent to N1 can be deprotonated to form an azetidinium ylide, which can subsequently open the ring either directly or indirectly. Couty et al. have demonstrated that an azetidinium cation having N-benzyl (**3.22**) or N-benzhydryl substituent on N1 may be deprotonated with a strong base to form an ylide (**3.23**), which can subsequently undergo Stevens rearrangement to form a pyrrolidine ring (Scheme 3.9).<sup>9b</sup>



#### Scheme 3.9

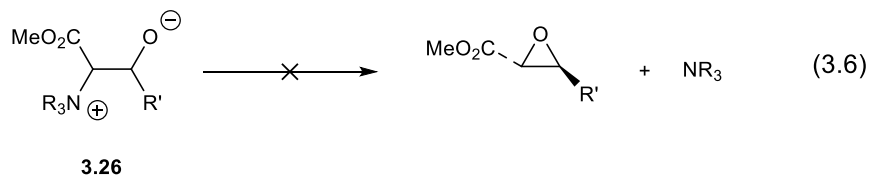
The electron-withdrawing group can also be a substituent on C2 or C4 so that the formal negative charge of the ylide may be assigned to an  $\alpha$ -carbon on the ring.<sup>9a, 10</sup> In one study by Couty et al., azetidinium **3.24** was first deprotonated with a strong base to form ylide **3.25**, which was subsequently treated with benzaldehyde (Scheme 3.10).<sup>9a, 10</sup> That the electron-withdrawing group ends up on a carbon of the epoxide ring suggests that deprotonation occurred C2.<sup>9a, 10</sup> It is noteworthy that while the deprotonation could have also occurred on benzylic carbon of the N-benzyl substituent, reaction products originating from this hypothetical ylide (i.e. similar to that of **3.23**) is not observed.



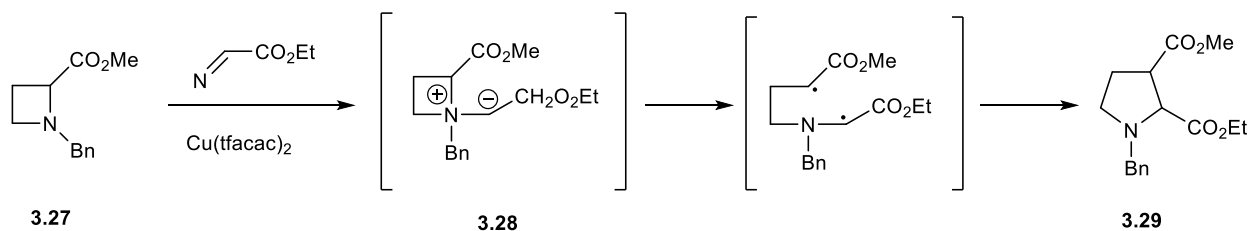


### Scheme 3.10

Couty et al. have concluded that the concomitant formation of an epoxide and opening of an azetidinium is driven by the relief of ring strain, as the formation of an epoxide is not observed when the pyrrolidine homologues of azetidinium (**3.24**) was treated with ketones/aldehydes in the presence of a strong base. This is further bolstered by the observation that tertiary amines in general are poor leaving groups, and that reaction depicted in eq. 3.6 is not known to occur for ylide (**3.26**).<sup>10</sup>



The azetidinium ylide may also be generated from the reaction of an azetidine (e.g. **3.27**) and a carbene (e.g. formed from the decomposition of ethyl diazoacetate), and ylide **3.28** may rearrange to form pyrrolidine **3.29** (Scheme 3.11).<sup>27</sup> The reaction proceeds via a Steven [1,2] shift of the N-C2 bond, which is an exception to what is seen in unstrained molecules as the migration in unstrained molecules usually involve the migration of the most stable radical, which would be the benzyl radical. This difference in reactivity may be explained by the relief of ring strain effected by the migration of the N-C2 bond.<sup>27</sup>



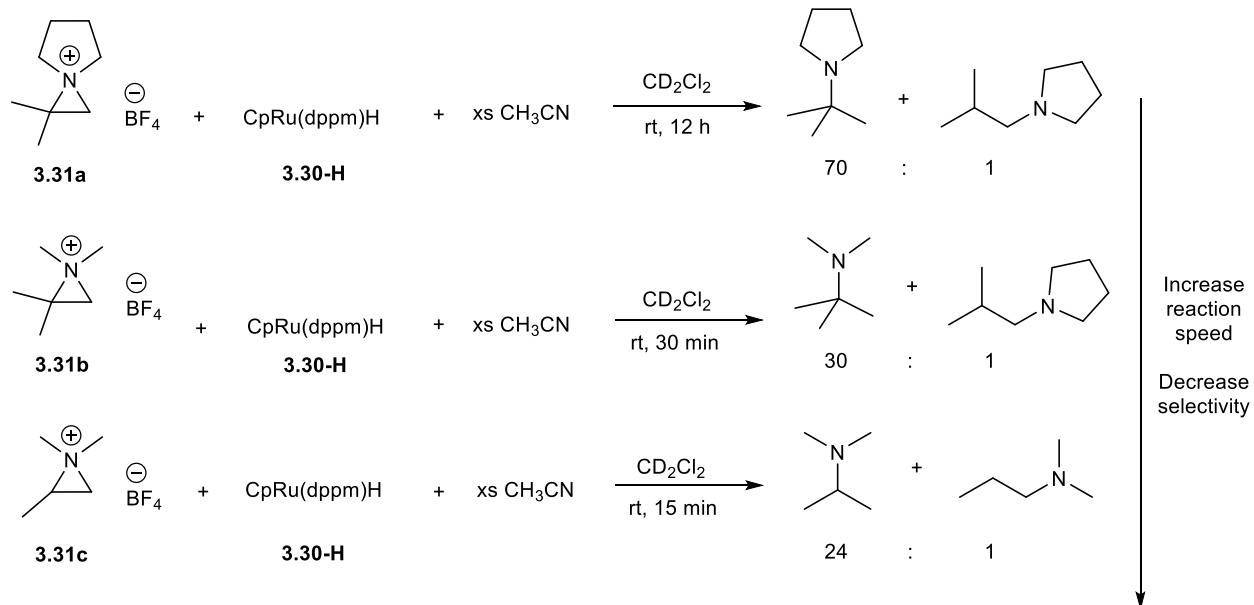
**Scheme 3.11**

### 3.2. Previous studies of hydride transfer to aziridinium cation

The interest of the Norton Group in the opening of azetidinium cations by metal hydrides originates from studies on the opening of aziridinium cations by various ruthenium hydrides, conducted by Dr. Hairong Guan et al. when Dr. Guan was a doctoral student in the Norton Group.<sup>28</sup> One of the key challenges in organometallic catalysis is the production of straight-chain alcohols from terminal alkenes via anti-Markovnikov addition of water,<sup>29</sup> and one approach to this problem is via the hydrogenation of a terminal epoxide. As protonated epoxides are unstable at room temperature,<sup>30</sup> Dr. Guan et al. decided to study hydride transfer to the isoelectronic azetidinium cation.

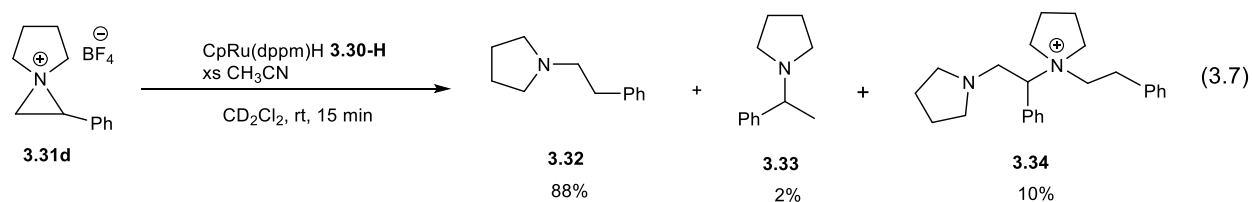
#### 3.2.1. Regioselectivity and kinetics of ring opening of aziridinium cations

Dr. Guan et al. have shown that, in the reaction between CpRu(dppm)H (**3.30-H**) and aziridinium cations having alkyl substituents (**3.31a-c**), hydride transfer occurs at the less substituted carbon to yield branched amines (Scheme 3.12).<sup>28</sup> In contrast, hydride transfer occurs at the more substituted carbon for the aziridinium cation **3.31d** having an aromatic substituent, yielding predominantly a straight-chain amine **3.32** (eq. 3.12). The difference in regioselectivity between aziridinium cations with alkyl and those with aromatic substituents has been previously reported in cases of ring opening by other nucleophiles.<sup>31</sup>



**Scheme 3.12.** After hydride transfer, CH<sub>3</sub>CN traps the resulting 16-electron Ru cation giving a stable complex.

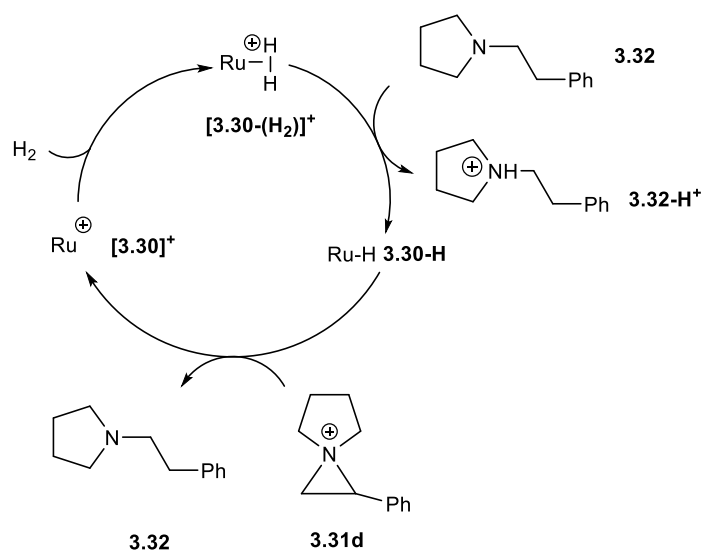
The reaction between aziridinium **3.31d** and hydride **3.30-H** also yielded a third product **3.34**, which is the product of attack on the aziridinium cation **3.31d** by the straight-chain amine **3.32**. Kinetic studies have shown that the reaction of eq. 3.7 is second order overall and first order with respect to **3.31d** and **3.30-H**, with a rate constant  $k = 1.30(2) \times 10^{-3} \text{ M}^{-1}\text{s}^{-1}$  at  $-64 \text{ }^\circ\text{C}$ .



### 3.2.2. Catalytic hydrogenation of aziridinium cations

Dr. Guan et al. have also shown that aziridinium cations **3.31a-3.31d** may be opened with a catalytic amount of hydride **3.30-H** under 50 psi H<sub>2</sub>.<sup>28</sup> The product distribution of the catalytic

reactions is the same as that of the stoichiometric reactions for cations **3.31a-3.31c**; for the aromatic-substituted **3.31d**, the product ratio of the straight chain product **3.32** to the branched product **3.33** is 50:1, and the cationic product **3.34** is not observed. Scheme 3.13 represents the proposed catalytic cycle for the hydride transfer to aziridinium cations from a ruthenium hydride; it is based on the proposed catalytic cycle for the hydrogenation of iminium cations by half-sandwich ruthenium hydrides, in particular **3.30-H**.<sup>32</sup> Absence of the cationic product **3.34** is proposed to be due to the protonation of the straight-chain product amine **3.32**, which makes it unavailable to attack the aziridinium cation **3.30d**.<sup>28</sup>



**Scheme 3.13.**

### 3.2.3. Single electron transfer to aziridinium cation **3.31d**.

Dr. Guan et al. have also confirmed that a single electron may be transferred to aziridinium cation **3.31d** from from Cp\***Ru(dppf)H 3.35-H** (eq. 3.8) using variable temperature <sup>1</sup>H NMR experiments.<sup>28</sup> Like many other half-sandwich ruthenium hydrides, the hydride signal of **3.35-H** is located upfield (at  $\delta$  -12.6). When aziridinium **3.31d** is treated with hydride **3.35H**,

broadening of this upfield hydride signal is observed in the  $^1\text{H}$  NMR spectrum of the reaction mixture (Figure 3.2), indicating rapid one-electron self exchange between the radical cation  $[\mathbf{3.35-H}]^{+\bullet}$  and the hydride  $\mathbf{3.35-H}$  (eq. 3.9).<sup>34</sup> As temperature of the reaction mixture is lowered, the hydride signal sharpens as the electron exchange process becomes slow relative to the NMR time scale. The inability of  $\mathbf{3.35-H}$  to transfer hydride to  $\mathbf{3.31d}$  and the inability of  $[\mathbf{3.35-H}]^+$  to transfer a hydrogen atom to the ring-opened radical are attributed to steric congestion around the Ru complex.

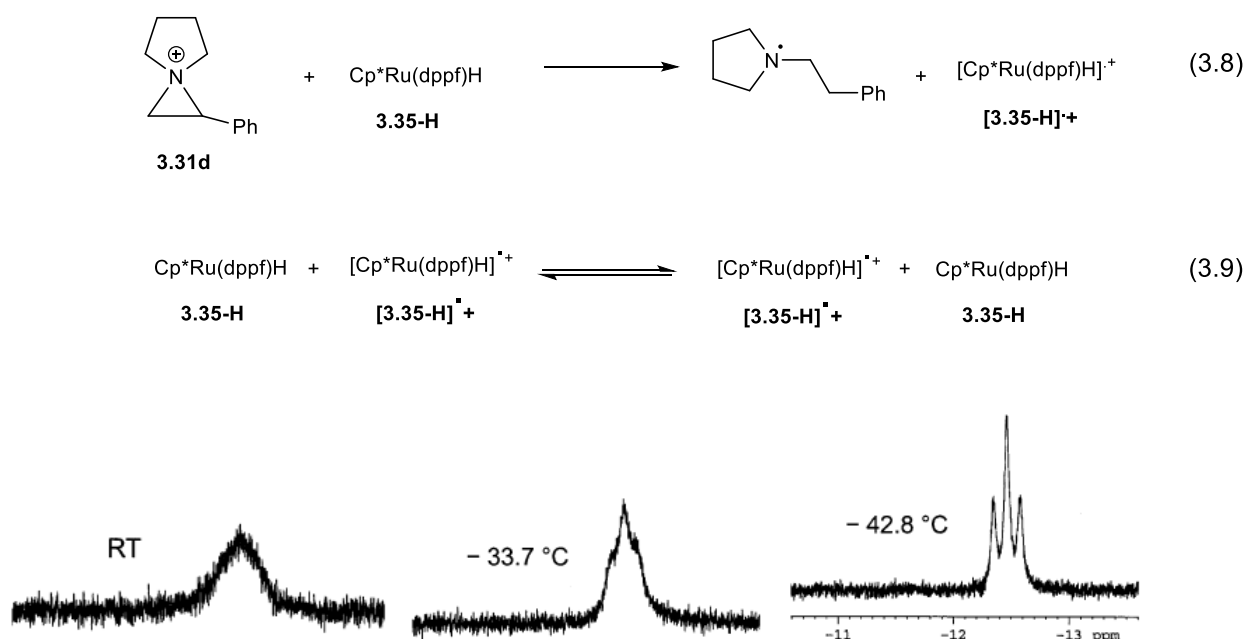
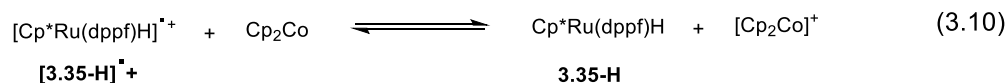


**Figure 3.2.**  $^1\text{H}$  NMR spectra of the hydride signal of  $\mathbf{3.35-H}$  in the reaction mixture of aziridinium cation  $\mathbf{3.31d}$  and hydride  $\mathbf{3.35-H}$  at various temperatures.

The dihydride cation  $[\text{Cp}^*\text{Ru}(\text{dppf})(\text{H})_2]^+$   $[\mathbf{3.35-(H)}_2]^+$  is also observed in the reaction 3.8. As is the case in Chapter 2, disproportionation occurs when two molecules of the radical cation  $[\mathbf{3.35-H}]^{\bullet+}$  yield the coordinative unsaturated cationic complex  $[\text{Cp}^*\text{Ru}(\text{dppf})]^+$   $[\mathbf{3.35}]^+$  and the dihydride  $[\mathbf{3.35-(H)}_2]^+$ .<sup>35</sup> Formation of the cation radical  $[\mathbf{3.35-H}]^{\bullet+}$  was further confirmed by the addition of the 19- $e^-$  complex cobaltocene, which sharpens the upfield hydride signal by reducing  $[\mathbf{3.35H}]^{\bullet+}$  back to the hydride  $\mathbf{3.35-H}$  (eq. 3.10).



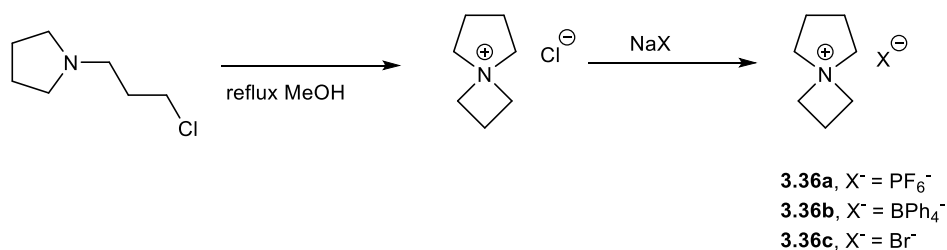
### 3.3. Opening of an azetidinium cation by a transition metal hydride

To the best of our knowledge, the studies most relevant to the work reported in the following sections were conducted by Couty et al as they detailed in separate accounts hydride transfer to an azetidinium cation from a main-group metal hydride and compared the rate of nucleophilic opening of an azetidinium cation to that of an analogous aziridinium cation; however, no work on the rate of hydride transfer to an azetidinium had been reported when the experiments in this section were conducted. As there were only a scant number of studies directed to the hydride opening of azetidinium cations, we decided to extend the scope of the studies described in § 3.2. to azetidinium so that we could ascertain the rate of ring opening of the azetidinium analogue of aziridinium **3.31d** by hydride **3.30-H**. Furthermore, we wished to know if the high regioselectivity for the straight-chain product **3.32** in eq. 3.7) would be observed in the case of an azetidinium.

#### 3.3.1. Preparation of novel azetidinium cation<sup>1</sup>

Azetidinium cation **3.39**, the analogue of aziridinium cation **3.31d**, was an unknown compound when we began our studies. Azetidinium **3.36**, which differs from **3.39** at only the  $\alpha$ -carbon as the former is unsubstituted, had been previously synthesized from 1-(3-chloropropyl)pyrrolidine by Arnott *et al.* (Scheme 3.14).<sup>3</sup>

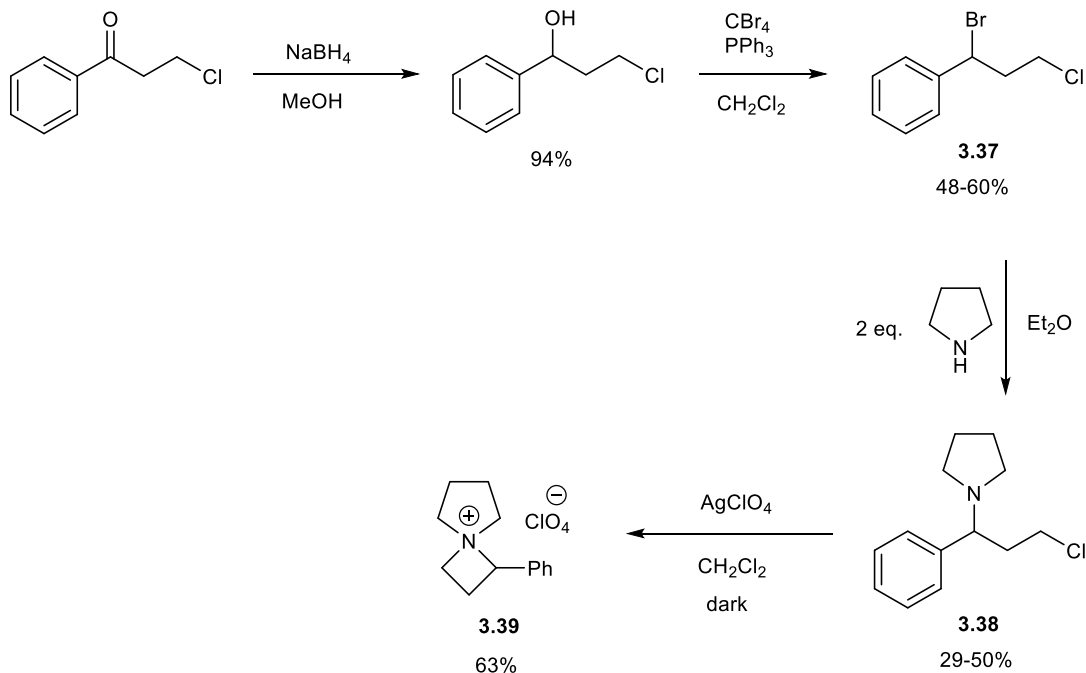
<sup>1</sup> Chapter 2 is a collaboration with Dr. Jason G. Polisar, a former doctoral student in the Norton Group. He optimized the synthetic route to the phenyl azetidinium **3.4**, synthesized and characterized the phenyl azetidinium, synthesized authentic samples of the ring open products, performed a few of the product ratio experiments in Section 2.3.1 and probed one electron chemistry in Section 2.4.



### Scheme 3.14

I proposed that phenyl-substituted azetidinium cation **3.39** can be prepared in a similar fashion. Reduction of the commercially available ketone gives the corresponding alcohol, and this alcohol is subsequently subjected to Appel reaction<sup>36</sup> conditions to yield compound **3.37**. Treating **3.37** with two equivalents of pyrrolidine yields crude **3.38**, which can be purified by chromatography using Florisil.

However, when purified **3.38** is refluxed in methanol, the desired azetidinium cation **3.39** is not obtained. Dr. Polisar suggested an alternate approach to the closure of the ring by using ionic salts having cations that facilitate the leaving of the chloride in **3.38**. In particular, treating **3.38** with silver perchlorate at room temperature gives the best results, and the perchlorate salt of azetidinium (**3.39**) is the azetidinium salt used in all subsequent studies of this section. The overall scheme for the preparation of **3.39** is shown in **Scheme 3.15**.



**Scheme 3.15**

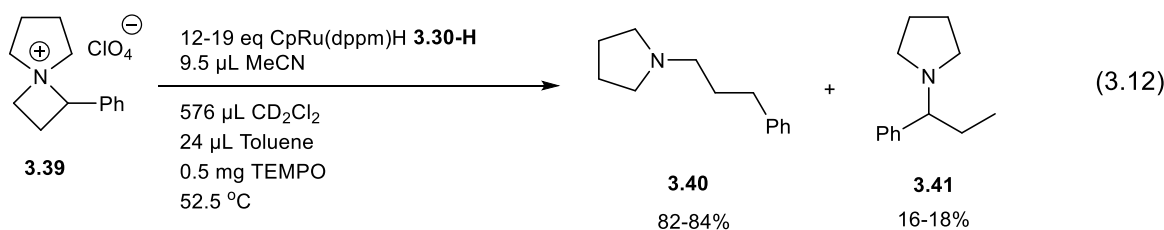
### 3.3.2. Hydride transfer to azetidinium cation from CpRu(dppm)H

Second-order rate constants between CpRu(dppm)H **3.30-H** and azetidinium **3.39** at various temperatures are measured in order to establish an Eyring plot, the extrapolation of which enables the calculation of second-order rate constant between hydride **3.30-H** and azetidinium **3.39** at various temperatures. In particular, we are interested in the rate constant at  $-64\text{ }^\circ\text{C}$  as the rate constant between hydride **3.30-H** and the analogous aziridinium cation **3.31d** (eq. 3.8) was measured at this temperature<sup>28</sup>. We can then determine the ratio between the rate of ring opening of azetidinium cation **3.39** and rate of ring opening of the corresponding aziridinium cation **3.31d**, which in turn allows us to compare it to the only results from the only other known study that reported the ratios of ring opening between analogous aziridinium and azetidinium cations<sup>23</sup>. The opening of **3.39** leads to two isomeric products: the straight-chained product **3.40** and the branch-chained product **3.41** (eq. 3.12, *vide infra*).



### 3.3.2.1. Reaction order of hydride transfer to azetidinium cation from ruthenium hydride.

While we have assumed that the reaction between azetidinium **3.39** and hydride **3.30-H** is second-order overall and first-order with respect to each reactant due to previous experiments between aziridinium **3.31d** and hydride **3.30-H**, the following set of experiments are conducted to support the validity of our assumption. Experiments were carried out at 52.5 °C, and four starting concentrations of hydride **3.30-H** were chosen (eq. 3.12), with at least three trials conducted at each concentration. The concentration of the limiting reagent, azetidinium salt **3.39**, is 0.006 M. After the transfer of hydride from **3.30-H** to **3.39**, a cationic, 16 e<sup>-</sup> ruthenium complex [CpRu(dppm)]<sup>+</sup> [**3.30**]<sup>+</sup> is generated. In our previous studies,<sup>32a, 37</sup> it was observed that **3.30** would coordinate to the lone pair of the amine product, which would complicate the determination of product ratios. In line with what was previously done to address this issue,<sup>28, 32, 37</sup> an excess amount of acetonitrile was added to the reaction mixture so that acetonitrile will coordinate to [**3.30**]<sup>+</sup> to form [CpRu(dppm)(CH<sub>3</sub>CN)]<sup>+</sup>. Toluene was added as an internal standard so that the integral of the azetidinium triplet peak at δ 5.9 may be compared against the toluene methyl peak at δ 2.34.



In all experiments, the ratio of the concentration of hydride **3.30-H** to the concentration of azetidinium **3.39** exceeded 10:1, which ensures the validity of the pseudo-first-order treatment of kinetic data (*viz.* assumption that the concentration of the excess reagent is mostly unchanged).

In all cases, the ratio of the straight-chain product **3.40** to the branched product **3.41** remained constant at ~ 83:17.

A small amount of radical inhibitor TEMPO is added to each reaction mixture in order to prevent the decomposition of Hydride **3.30-H** due to CD<sub>2</sub>Cl<sub>2</sub> by a radical chain mechanism. TEMPO was employed in our previous study of the hydrogenation of iminium cations by CpRu(dppp)H in CD<sub>2</sub>Cl<sub>2</sub><sup>32</sup>, as all hydride in the reaction mixture would otherwise be completely converted to CpRu(dppp)Cl by CD<sub>2</sub>Cl<sub>2</sub> within minutes absent a radical inhibitor. While there was no noticeable decomposition of hydride **3.30-H** by CD<sub>2</sub>Cl<sub>2</sub> in our previous studies of kinetics of hydride transfer to iminium and aziridinium cations, this may be due to the much faster reaction rate between hydride **3.30-H** and the cations studied, which usually take fewer than one hour to reach completion at room temperature. In contrast, the reaction between hydride **3.30-H** and azetidinium **3.39** proceeds much slower, requiring at least nine hours to reach completion at 330K. A control experiment between azetidinium **3.39** and **3.30-H**, conducted without the addition of TEMPO, indicates that presence of TEMPO does not alter the distribution of the product amines **3.40** and **3.41**.

A typical plot of the concentration of azetidinium (*A*) vs time is shown in **Figure 3.3**, and the points of the plot are fitted to equation for exponential decay (eq. 3.13) to extract the pseudo-first-order rate constant. For this particular trial in which the initial concentration of hydride **3.30-H** is 0.118 M, and the pseudo-first-order rate constant is determined to be 0.57(2) hr<sup>-1</sup> or 1.60(6) × 10<sup>-4</sup> s<sup>-1</sup>.

$$A_t = A_\infty + (A_0 - A_\infty)(e^{-k_{obs}t}) \quad (3.13)$$

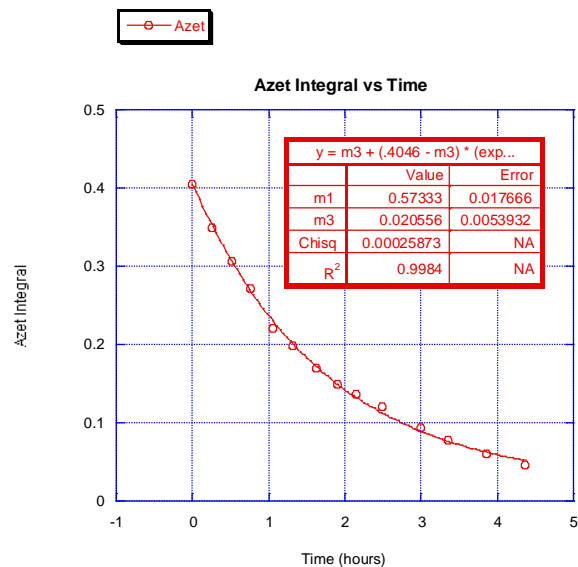


**Figure 3.3.** A representative plot of a kinetic run.  $[\text{Ru-H}] = 0.118 \text{ M}$ ,  $[\text{Azet}] = 0.006 \text{ M}$ .

The pseudo-first-order rate constants obtained for each initial concentrations of hydride **3.30-H** are averaged and plotted against initial concentration of hydride **3.30-H** (**Figure 3.4**). The data points of the plot are fitted using linear regression, and the slope of the best-fit line indicates the second-order rate constant at  $52.5^\circ\text{C}$ , and in this case,  $k_2 = 5.2(2) \text{ M}^{-1} \text{ h}^{-1}$  or  $1.44(6) \times 10^{-3} \text{ M}^{-1} \text{ s}^{-1}$ . The y-intercept of the best-fit line is  $-0.05(2)$ , which means that the intercept is essentially zero.  $R^2$  of the best-fit line is 0.997, which indicates that the points are essentially collinear.

That the value of  $R^2$  for the linear fit of the plot is 0.997 and that the y-intercept is statistically zero indicate that the reaction between Hydride **3.30-H** and azetidinium **3.39** is indeed first order with respect to each reactant.

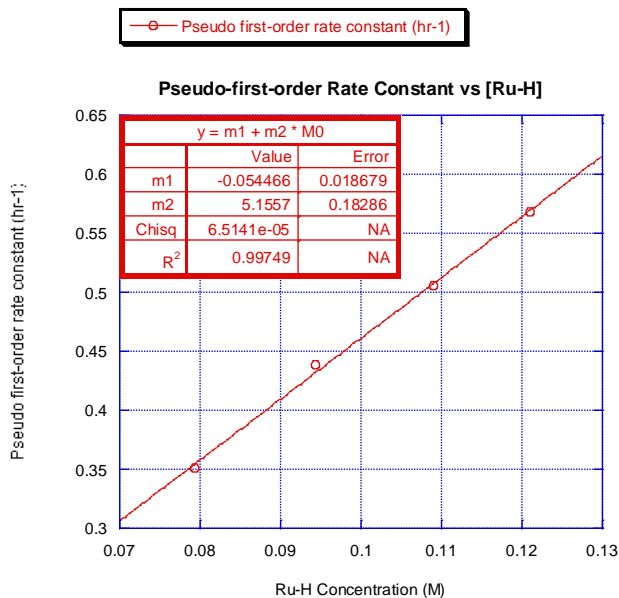
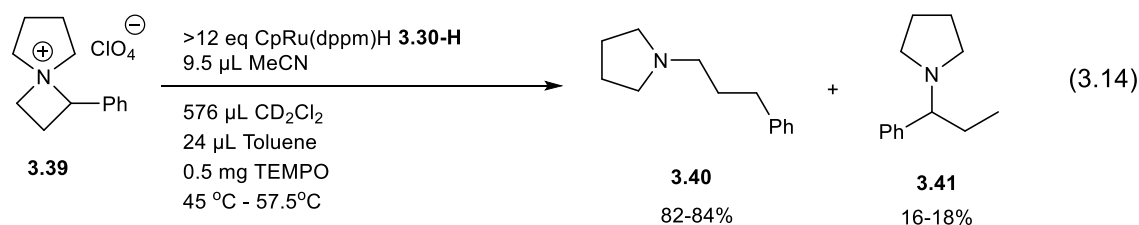


**Figure 3.4.** Pseudo-first-order rate constant vs [CpRu(dppm)H]. The limiting reagent is azetidinium salt **3.39** (0.006 M).

### 3.3.2.2. Temperature dependence of the rate constant of hydride transfer to azetidinium cation.

The second-order rate constant of the reaction between Hydride **3.30-H** and azetidinium **3.39** at 52.5 °C is  $1.44(6) \times 10^{-3} \text{ M}^{-1} \text{ s}^{-1}$ , a value that is comparable to the rate constant of  $1.30(2) \times 10^{-3} \text{ M}^{-1} \text{ s}^{-1}$  for the reaction between hydride **3.30-H** and aziridinium **3.31d** at -64 °C. This suggests that the second-order rate-constant of ring opening of azetidinium **3.39** would be very low at -64 °C, thus making it unfeasible to make a direct comparison of the rate constants of ring opening of the two substrates. As an alternative, the rate constant for the ring opening of azetidinium **3.39** at -64°C would need to be extrapolated using an Eyring Plot, which may be constructed using second-order rate constants of the reaction between azetidinium **3.39** and hydride **3.30-H** at various other temperatures. The temperatures chosen are from 45 °C to 57.5 °C at the increment of every 2.5 °C, and at least three trials are conducted at each temperature (eq. 3.14).



An Eyring plot allows one to obtain the enthalpy of activation ( $\Delta H^\ddagger$ ) and the entropy of activation ( $\Delta S^\ddagger$ ) of a reaction, from which rate constant at any temperature can be extracted. There are two forms of an Eyring plot: a linearized logarithmic form (eq. 3.15) and an exponential form (eq. 3.16).

$$\ln\left(\frac{k}{T}\right) = \ln\left(\frac{k_B}{h}\right) + \frac{-\Delta H^\ddagger}{RT} + \frac{\Delta S^\ddagger}{R} \quad (3.15)$$

$$k = \frac{k_B T}{h} \exp\left(-\frac{\Delta H^\ddagger}{RT} + \frac{\Delta S^\ddagger}{R}\right) \quad (3.16)$$

The linearized logarithmic fit gave a lower  $R^2$  value of 0.989, and the activation parameters calculated from the fit gave  $\Delta H^\ddagger = 16.9(9)$  kcal mol<sup>-1</sup> and  $\Delta S^\ddagger = -20(3)$  cal mol<sup>-1</sup> K<sup>-1</sup> (**Figure 3.5A**). The exponential fit gave a better  $R^2$  value of 0.996, and the activation parameters from the fit gave  $\Delta H^\ddagger = 17.4(7)$  kcal mol<sup>-1</sup> and  $\Delta S^\ddagger = -18(2)$  cal mol<sup>-1</sup> K<sup>-1</sup> (**Figure 3.5B**). The parameters derived from the linearized logarithmic fit were within the uncertainties of values derived from the exponential fit, and vice versa. That the linearized logarithmic fit gave a lower  $R^2$  value was attributed to the bias introduced by taking the logarithm of the rate constant. As such, values from the exponential fit were used to calculate the extrapolated rate constant.

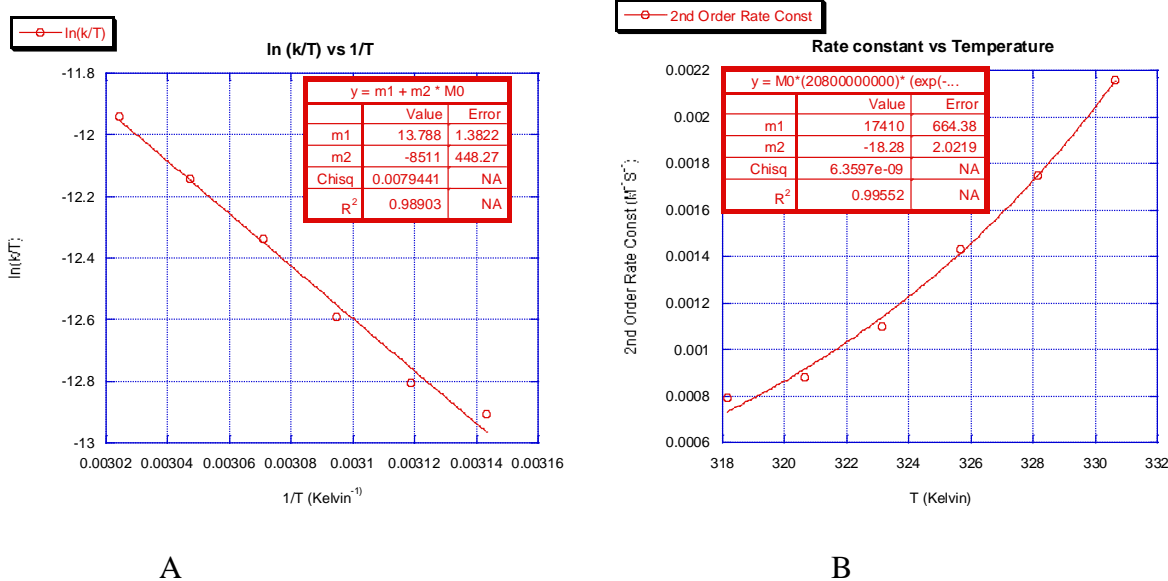


**Figure 3.5.** A) Plot of  $\ln(k/t)$  vs  $1/T$ . B) Plot of  $k$  vs  $T$ .

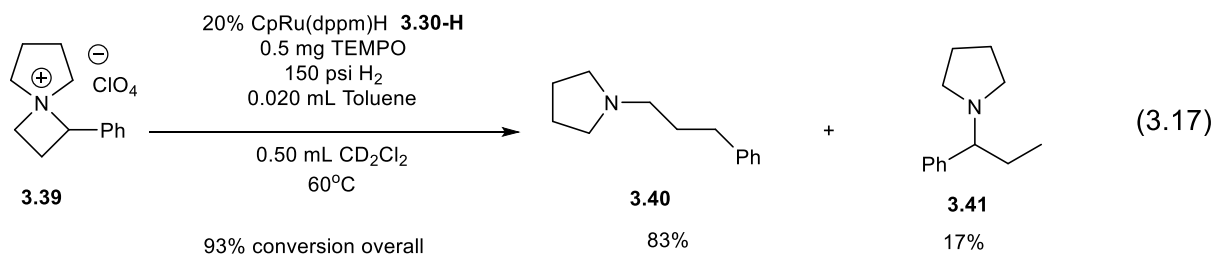
Due to the issue of covariance, extracted activation parameters from eq. 3.16 do not have the correct associated values of uncertainty. As such, the program KinPar,<sup>38</sup> which was developed by former Norton Group student Dr. Richard Jordan to account for covariance in the calculation of  $\Delta H^\ddagger$  and  $\Delta S^\ddagger$  from Eyring Plot data, is used to calculate the correct uncertainty. The second-order rate constant of the reaction between **3.39** and **3.30-H** is determined to be  $4(3) \times 10^{-10} \text{ M}^{-1} \text{ s}^{-1}$ . Compared to the second-order rate constant of  $1.30(2) \times 10^{-3} \text{ M}^{-1} \text{ s}^{-1}$  at  $-64^\circ \text{C}$  for the reaction between hydride **3.30-H** and aziridinium **3.31d**<sup>28</sup>, the second-order rate constant for the reaction between **3.30-H** and azetidinium **3.39** (upper limit of  $7 \times 10^{-10} \text{ M}^{-1} \text{ s}^{-1}$  and lower limit of  $1 \times 10^{-10} \text{ M}^{-1} \text{ s}^{-1}$ ) is six to seven orders of magnitude slower.

This large difference in rate cannot be solely attributed to ring strain energy, as the difference in ring strain between aziridinium and azetidinium cations is only about 2.1 kcal/mol<sup>24</sup>. A similar conclusion was reached in the study by Couty et al.<sup>23</sup> (**Scheme 3.9**), who reported that the rate of ring opening by DMAP for aziridinium **3.20** is about  $1.7 \times 10^4$  times greater than the rate of opening for the corresponding azetidinium **3.21**. Another factor that may affect the rate

of ring opening of aziridinium and azetidinium cations by nucleophiles is the electrophilicity of the ions, which may be determined using the Mayr-Platz Equation (eq. 3.5, *vide supra*). Couty *et al.*<sup>23</sup> determined that azetidinium **3.21** is more stabilized compared to aziridinium **3.20**, and it is likely that the difference in electrophilicity toward ruthenium hydride **3.30-H** between azetidinium **3.39** and aziridinium **3.31d** may be even greater to account for six to seven orders of magnitude difference in the second-order rate constants.

### 3.3.4. Ring opening of azetidinium by a catalytic amount of ruthenium hydride

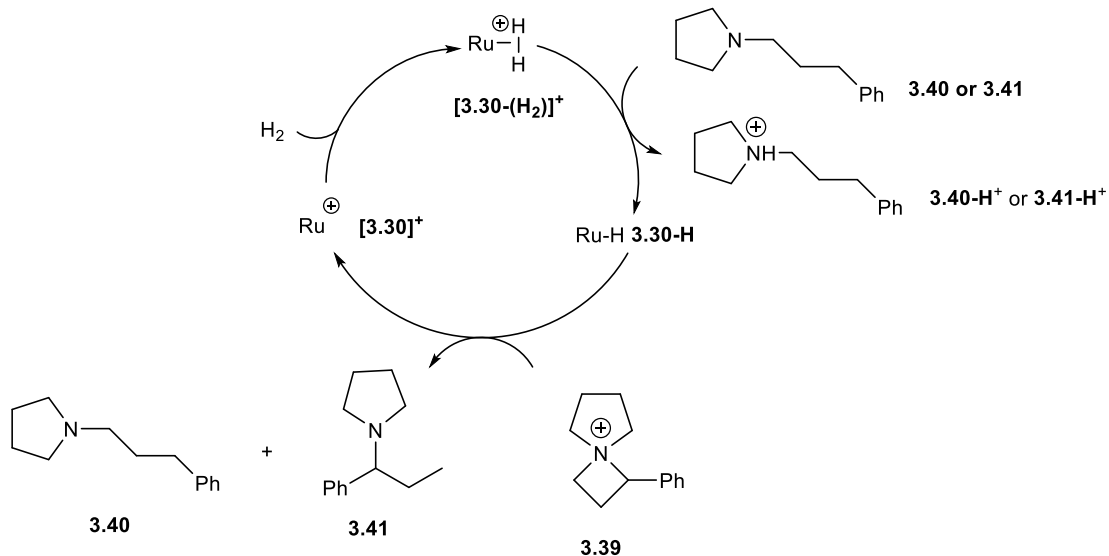
As Hydride **3.30-H** has been previously shown to be able to effect catalytic ionic hydrogenation of iminium<sup>32</sup> and aziridinium<sup>28</sup> cations, we expected **3.30-H** could also effect the catalytic ionic hydrogenation of azetidinium **3.39**. To validate our hypothesis, in a sapphire NMR tube was placed 0.50 mL solution of 0.11 M of azetidinium **3.39** in CD<sub>2</sub>Cl<sub>2</sub>, 20 mol% of ruthenium hydride **3.30-H**, and 0.020 mL toluene as an internal standard. The sapphire NMR tube is then placed under 150 psi H<sub>2</sub>, and the reaction between **3.30-H** and **3.39** proceeded overnight at 60°C, (eq. 3.17). The validity of our hypothesis is confirmed as 93% of **3.39** is converted to products **3.40** and **3.41**, with the ratio of the straight-chain product **3.40** to the branched product **3.41** at 83:17, comparable to what was observed in the stoichiometric kinetic experiments described above.



In contrast to the stoichiometric reaction (eq. 3.13), no acetonitrile is included in the reaction mixture of the catalytic reaction (eq. 3.17). As discussed above, hydride transfer from hydride **3.30-H** results in the 16-electron cationic ruthenium complex  $[\mathbf{3.30}]^+$ , which in the catalytic reaction needs to coordinate to dihydrogen in order to regenerate hydride **3.30-H**. Due to the strong interaction between the lone pairs on nitrogen of acetonitrile and the cationic ruthenium complex  $[\mathbf{3.30}]^+$ , the formation of  $[\text{CpRu}(\text{dppm})(\text{CH}_3\text{CN})]^+$  is not reversible, thus effectively shutting down the catalytic cycle.

We propose that the operating mechanism for the catalytic hydrogenation of azetidinium **3.39** by ruthenium hydride **3.30-H** (Scheme 3.16) is akin to the mechanisms of catalytic hydrogenation of iminium and aziridinium cations by various ruthenium hydrides previously reported by the Norton Group.<sup>28, 32, 37</sup> Hydride transfer from  $\text{CpRu}(\text{dppm})\text{H}$  **3.30-H** to azetidinium **3.39** yields ring-opened amine products (straight chain amine **3.40** or the branched amine **3.41**) and a 16-electron cationic ruthenium complex  $[\text{CpRu}(\text{dppm})]^+$   $[\mathbf{3.30}]^+$ . Complex  $[\mathbf{3.30}]^+$  takes up dihydrogen to form a cationic, 18-electron ruthenium dihydrogen complex  $[\text{CpRu}(\text{dppm})(\text{H}_2)]^+$   $[\mathbf{3.30-(H}_2)]^+$ , which is known to be acidic enough to be deprotonated by tertiary amines such as the ring-opened products **3.40** and **3.41**.<sup>39</sup> The deprotonation of  $[\mathbf{3.30-(H}_2)]^+$  regenerate hydride **3.30-H**, thus completing the catalytic cycle<sup>32b, 40</sup>. To our knowledge, this is the first example of a catalytic ring opening hydrogenation of an azetidinium cation

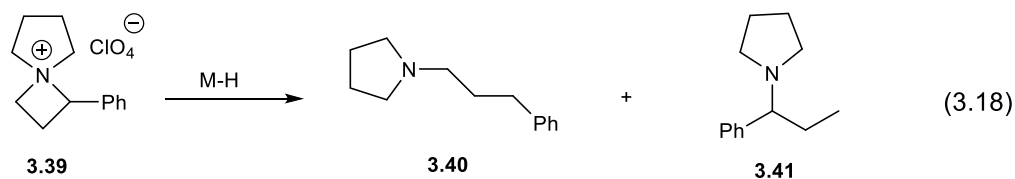




**Scheme 3.16**

### 3.3.5. Hydride transfer to azetidinium cation from other hydride sources

We also wish to determine how the choice of hydrides affects the regioselectivity of the ring opening, and the ring opening of azetidinium **3.39** by five other hydrides (**3.42a-e** in Table 3.1) are studied (eq. 3.18). As expected, CpRu(dppe)H **3.42a** gave a product distribution comparable to that when **3.39** is treated with its analogue **3.30-H**. The distribution of 4:1 favoring the straight-chain amine product **3.40** is comparable to the distribution of 5:1 observed when **3.39** is treated with **3.30-H**. Ring opening effected by main-group hydrides tend to favor the branched product, and selectivity appears to favor the branched amine product **3.41** as more reactive hydride sources (e.g. borohydrides **3.42b** and **3.42c**) are used. Diisobutylaluminum hydride (DIBAL) **3.42e** failed to react with **3.39** at room temperature presumably due to steric congestion of the isobutyl groups around the hydride.



M-H	Product Ratio ( <b>3.40:3.41</b> ) <sup>b</sup>
CpRu(dppm)H ( <b>3.30-H</b> ), 52.5 °C	5:1
20 mol % <b>3.30-H</b> , 150 psi H <sub>2</sub> , 60 °C	5:1
CpRu(dppe)H <sup>c</sup> ( <b>3.42a</b> ), 52.5 °C	4:1
NaBH <sub>4</sub> ( <b>3.42b</b> ), 20 °C	2:1
LiBEt <sub>3</sub> H <sup>d</sup> ( <b>3.42c</b> ), THF, 20 °C	1:1
LiAlH <sub>4</sub> ( <b>3.42d</b> ), 20 °C	< 1:20
DIBAL ( <b>3.42e</b> ), toluene, 20 °C	No Reaction
DIBAL ( <b>3.42e</b> ), CH <sub>2</sub> Cl <sub>2</sub> , 20 °C	No Reaction

**Table 3.1.** Reaction of various metal hydrides with azetidinium **3.39**. <sup>a</sup>All reactions in CH<sub>2</sub>Cl<sub>2</sub> unless otherwise stated. <sup>b</sup>Product ratios estimated by <sup>1</sup>H NMR analysis of the crude mixtures. <sup>c</sup>dpppe = 1,2-bis(diphenylphosphino)ethane. <sup>d</sup>1 M THF of LiBEt<sub>3</sub>H solution added to 0.1 M THF solution of **3.39**

### 3.3.6. Reduction potential of azetidinium cation and single-electron transfer to azetidinium cation

We are aware of no previous electrochemical data for azetidinium cations.  $\alpha$ -aryl aziridinium cations are 0.6 – 0.9 V more easily reduced than  $\alpha$ -alkyl aziridinium cations<sup>41</sup>, and this could be explained by the stabilization provided by the aromatic substituent. Phenyl aziridinium cation **3.31d**<sup>3</sup> undergoes single-electron reduction by Cp\*<sub>2</sub>Ru(dppf)H **3.35-H** (§ 3.2.3),<sup>28</sup> and the reduction potential of **3.31d** was previously measured in aqueous Borax buffer.<sup>41a</sup> Dr. Michael Eberhart, a former graduate student in the Norton Group, had examined the reduction of **3.31d** and determined an irreversible E<sub>pc</sub> of –0.93 V vs FcH<sup>+</sup>/FcH in acetonitrile; however, the difference in reduction potentials between aziridiniums and azetidiniums had not been previously studied. As discussed earlier, there is a pronounced difference in electrophilicity between analogous aziridinium and azetidinium cations despite similarity in strain energy, and

the difference in the reduction potential of aziridinium **3.31d** and azetidinium **3.39** should contribute to the difference in electrophilicity.

Azetidinium **3.39** has proven significantly harder to reduce than the corresponding aziridinium **3.31d**. A mixture of **3.39** and one equivalent of decamethylferrocene ( $E_{1/2} = -0.59$  vs  $\text{FcH}^+/\text{FcH}$ )<sup>42</sup> shows no reaction after one day. A mixture of **3.39** and  $\text{Cp}^*\text{Ru}(\text{dppf})\text{H}$  **3.35-H** ( $E_{1/2} = -0.63$  V) also yields no reaction; the characteristic azetidinium triplet ( $\delta$  5.98) and the hydride triplet ( $\delta$  -12.65) are both unchanged in a  $^1\text{H}$  NMR spectrum taken after 26 hours of reaction (**Figure 3.6**). Though **3.35-H** fails to transfer hydride to **3.39** (eq. 3.19), this is not surprising as **3.35-H** also does not transfer hydride to aziridinium **3.31d**, the cause of which is likely due to the steric bulk on **3.35-H**.

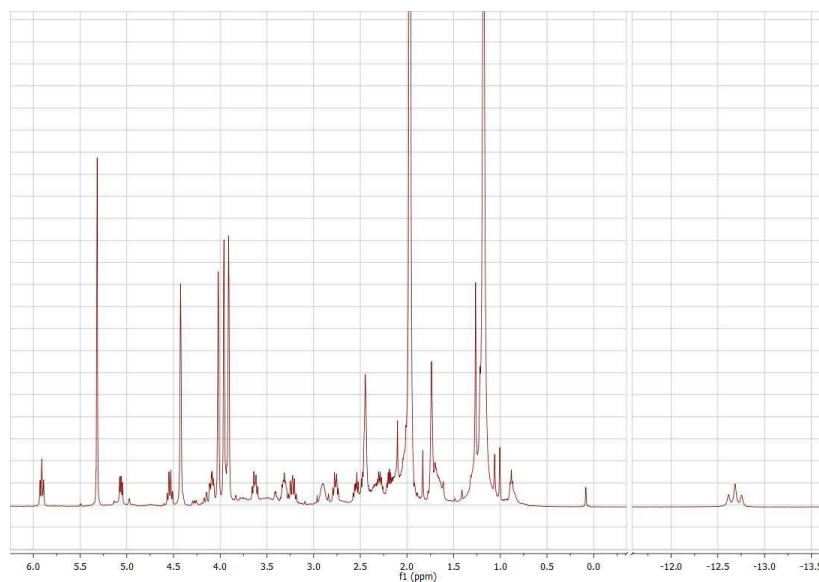
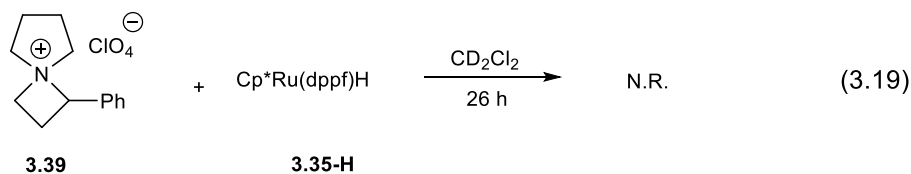


**Figure 3.6.**  $^1\text{H}$  NMR of azetidinium cation **3.39** and  $\text{Cp}^*\text{Ru}(\text{dppf})\text{H}$  **3.35-H** after standing at room temperature for 26 hours in  $\text{CD}_2\text{Cl}_2$ .

Dr. Anthony Shaw, a former Norton graduate student, and Dr. Polisar have obtained cyclic voltammetry data for azetidinium **3.39** (Figure 3.7). We presume that the peak at  $E_{pc} = -1.43$  V (vs  $FcH^+/FcH$ ) corresponds to the irreversible reduction of **3.39**. This finding indicates that azetidinium **3.39** is indeed less likely to undergo reduction than its aziridinium analogue **3.31d**, and agrees with our observation that the azetidinium does not react with hydride **3.35-H**. The irreversible  $E_{pc}$  of **3.39** at  $-1.43$  V is comparable to the irreversible reduction peak of phenyliminium cation **3.43** ( $E_{pc} = -1.42$  V vs  $FcH^+/FcH$ , Table 3.2), which is another ion that fails to react with hydride **3.35-H**.<sup>40</sup>

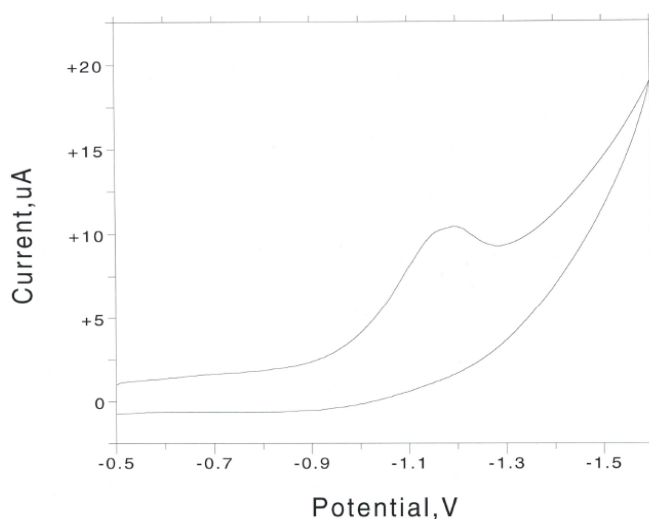
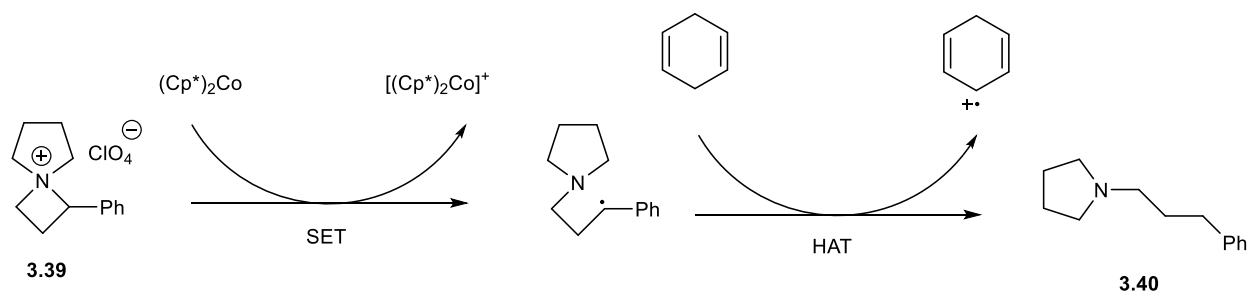


**Figure 3.7.** Cyclic voltammetry of phenyl substituted azetidinium cation **3.39**. Azetidinium **3.39** (0.004 M) in  $CH_2Cl_2$  with  $n-Bu_4NPF_6$  (0.1 M) as the supporting electrolyte measured with platinum electrodes and a  $Ag^+/Ag$  reference electrode.  $FcH^+/FcH$  is + 0.24 V vs  $Ag^+/Ag$ . Scan rate = 200 mV/s.

Azetidinium **3.39** is next treated with  $(Cp^*)_2Co$  ( $E_{1/2} = -1.94$  V vs  $FcH^+/FcH$ , which suggests that the latter should be able to reduce **3.39** with ease).<sup>42</sup> Though **3.39** is consumed, no organic products could be identified in the spectrum of the complex reaction mixture. The experiment is then repeated in the presence of excess 1,4-cyclohexadiene, a hydrogen-atom donor (Scheme 3.17). Analysis of the  $^1H$  NMR spectrum indicates the formation of unidentified

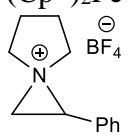
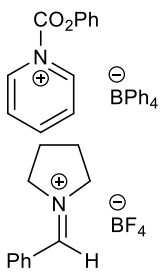
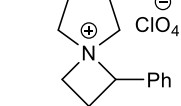
byproducts as well as the presence of the straight-chain amine **3.40** identifiable by its characteristic peak ( $\delta$  2.65,  $J = 7.7$  Hz); characteristic peaks of the branched product **3.41** are not detected. Regioselectivity of the reaction confirms our hypothesis that the straight-chain product will be generated if the hydride transfer occurs by a two step process in which single electron transfer (SET) is followed by hydrogen atom transfer (HAT).



### Scheme 3.17

The potential of  $CpRu(dppm)H$  **3.30-H** in  $CH_2Cl_2$  is also determined, and its potential ( $E_{pa} = -0.13$ ) means that **3.30-H** is less reducing than other half-sandwich Ru-hydrides studied by the Norton group (Table 3.2).<sup>40</sup> A correlation between decreasing bisphosphine bite angles and (a) decreasing one-electron reduction potentials concomitant (b) increasing rates of hydride transfer was previously suggested.<sup>43</sup> The magnitude of the oxidation potentials of all ruthenium hydrides in Table 3.2 are at least 0.8 V less than the magnitude of the reduction potential of azetidinium **3.39**, suggesting that the hydride transfer from these hydrides to azetidinium **3.39** is not a two step process as single electron transfer from these hydrides to **3.39** would be highly unlikely.

**Table 3.2.** Summary of the relevant electrochemical potentials of various hydrides and cations<sup>a</sup>.

Compound	Volts (vs FcH <sup>+</sup> /FcH) <sup>a</sup>
CpRu(dppm)H ( <b>3.30-H</b> ) <sup>b</sup>	$E_{pa} = -0.13$
CpRu(dppe)H ( <b>3.42a</b> ) <sup>b</sup>	$E_{pa} = -0.16^c$
CpRu(dppf)H <sup>b</sup>	$E_{1/2} = -0.31^c$
Cp*Ru(dppe)H <sup>b</sup>	$E_{1/2} = -0.51^c$
Cp*Ru(dppf)H ( <b>3.35-H</b> ) <sup>b</sup>	$E_{1/2} = -0.63^c$
(Cp*) <sub>2</sub> Fe	$E_{1/2} = -0.59^d$
 <b>3.31d</b>	$E_{pc} = -0.93^{e,f}$
 <b>3.43</b>	$E_{pc} = -0.87^c$
 <b>3.39</b>	$E_{pc} = -1.42^c$
(Cp*) <sub>2</sub> Co	$E_{1/2} = -1.43$
(Cp*) <sub>2</sub> Co	$E_{1/2} = -1.94^d$

<sup>a</sup>Measured in CH<sub>2</sub>Cl<sub>2</sub>,<sup>40</sup> unless otherwise stated. Organic cations are measured at 200 mV/s, and the ruthenium hydrides are measured 50 mV/s. <sup>b</sup>Previously measured in THF.<sup>34, 44</sup> <sup>c</sup>Literature value. <sup>d</sup>Literature value.<sup>42</sup> <sup>e</sup>Previously measured in aqueous borax buffer.<sup>41a</sup> <sup>f</sup>Measured in CH<sub>3</sub>CN.

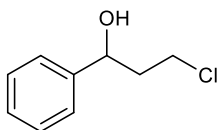
### 3.4. Experimental Procedures

#### General Procedures.

Toluene, diethyl ether, methanol (MeOH) and dichloromethane (CH<sub>2</sub>Cl<sub>2</sub>) were purified by a Grubbs system.<sup>45</sup> CD<sub>2</sub>Cl<sub>2</sub> used in the kinetic runs was dried over activated molecular sieves, degassed by three freeze-pump-thaw cycles and stored in an inert atmosphere glovebox. CpRu(dppm)H<sup>46</sup>, CpRu(dppe)H<sup>46</sup> and Cp\*Ru(dppf)H<sup>34</sup> were prepared as previously described.

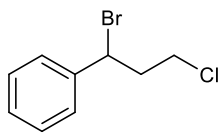
MS refers to low resolution mass spectroscopy performed on a JEOL JMS-LCmate liquid chromatography mass spectrometer using the CI+ (MeOH) or FAB+ technique. Characterization NMR spectra were recorded with a 300, 400 or 500 MHz Bruker spectrometer in CDCl<sub>3</sub> and are referenced to TMS or CDCl<sub>3</sub> (<sup>13</sup>C δ 77.16). <sup>1</sup>H NMR spectra taken in CD<sub>3</sub>CN and CD<sub>2</sub>Cl<sub>2</sub> are referenced to residual solvent peaks: δ 1.94 and δ 5.32, respectively, for CD<sub>2</sub>HCN and CDHCl<sub>2</sub>. Copies of NMR are in the appendix. IR spectra were obtained neat as a thin film on a NaCl salt plate.

The general electrochemistry procedure using CH<sub>2</sub>Cl<sub>2</sub> as the solvent was previously described.<sup>40</sup>



#### 3-Chloro-1-phenylpropan-1-ol.

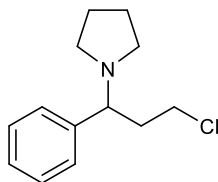
Sodium borohydride (1.8 g, 1.1 equiv) was added in 4 portions to a 0 °C suspension of 3-chloro-1-phenylpropan-1-one (7.4 g) in MeOH (110 mL, 0.4 M). After stirring 2-3 h, the reaction mixture was quenched with an equal volume of brine and extracted 2× with CH<sub>2</sub>Cl<sub>2</sub>. The combined CH<sub>2</sub>Cl<sub>2</sub> layers were washed with brine, dried over MgSO<sub>4</sub> and evaporated to give 7 g (93%) of a pale yellow liquid.<sup>47</sup>



3.37

**(1-Bromo-3-chloropropyl)benzene.**

Triphenylphosphine (9.97 g, 1 equiv) was added in 3 portions to a  $\text{CH}_2\text{Cl}_2$  solution (115 mL, 0.33 M) of 3-chloro-1-phenylpropan-1-ol (6.5 g) and carbon tetrabromide (12.6 g, 1 equiv) at room temperature. After stirring 1 h, the reaction mixture was concentrated and then loaded onto a silica gel flash column. Elution with hexanes, followed by  $\text{CH}_2\text{Cl}_2$  gave 5.3 g (60%) of a pale yellow liquid.<sup>47</sup>

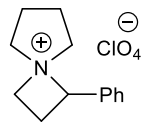


3.38

**1-(3-Chloro-1-phenylpropyl)pyrrolidine.**

Pyrrolidine (0.59 mL, 2 equiv) was added dropwise to a solution of **3.37** (935 mg) in ether (5.5 mL, 0.65 M). After stirring overnight the reaction mixture was extracted 3× with 1 M HCl. The aqueous layer was washed 2× with 5 mL  $\text{CH}_2\text{Cl}_2$ , 2× with 5 mL hexanes, neutralized with 6 M NaOH and then extracted 4× with ether. The combined ether layers were dried over  $\text{MgSO}_4$ , filtered, concentrated and loaded onto a Florisil flash column. Elution with 15:1 hexanes:ethyl acetate gave 0.27 mg (34 %) of a colorless oil.  $^1\text{H}$  NMR (300 MHz,  $\text{CDCl}_3$ ,  $\delta$ ): 1.71-1.76 (m, 4H,  $\text{N}_{\text{ring}}\text{CH}_2\text{CH}_2\text{CH}_2\text{CH}_2$ ), 2.14-2.21 (m, 1H), 2.34-2.55 (2 × m, 5H), 3.11-3.44 (2 × m, 3H, Ph-CH and Cl- $\text{CH}_2$ ), 7.25-7.35 (m, 5H, Ar).  $^{13}\text{C}$  NMR (100 MHz,  $\text{CDCl}_3$ ,  $\delta$ ): 23.39, 38.72, 42.19, 52.67, 68.06, 127.53, 128.24, 128.52, 141.71. MS: 224/226 ( $\text{M}+1$ ), 188 ( $\text{M}-35 = \text{M}-\text{Cl}$ ). IR ( $\text{cm}^{-1}$ ): 2965, 2787, 1492, 1453.





**1-Phenyl-4-azaspiro[3.4]octan-4-ium perchlorate.**

**3.39**

To a suspension of silver perchlorate (1 equiv) in CH<sub>2</sub>Cl<sub>2</sub> (3 M) was added a solution of **3.38** (0.3 M) via pipette in the dark (two washes of **3.38** were added, each 1 M). After stirring overnight, the reaction mixture was passed through a glass fiber filter and then evaporated to give a clear colorless oil. Several runs on this scale gave yields 55-91%, 70% average. <sup>1</sup>H NMR (500 MHz, CDCl<sub>3</sub>, δ): δ= 1.59-1.63 (m, 1H), 2.00-2.07 (m, 2H), 2.12-2.19 (m, 1H), 2.79-2.94 (2 × m, 2H), 3.20-3.29 (m, 1H), 3.39-3.43 (m, 1H), 3.65-3.71 (m, 1H), 4.01-4.06 (m, 1H) 4.14-4.19 (m, 1H), 4.67 (q, *J*=9.4 Hz, 1H), 5.98 (t, *J*=9.4 Hz, 1H), 7.54-7.55 (m, 5H, Ar). <sup>13</sup>C NMR (100 MHz, CDCl<sub>3</sub>, δ): 20.0, 20.59, 21.17, 56.31, 60.98, 63.34, 76.45, 129.48, 129.79, 130.15, 131.73. MS: 188 (M, cation). IR (cm<sup>-1</sup>): 1461, 1059.

Authentic samples of the straight-chain amine product **3.40** and branched amine product **3.41** were prepared by literature methods.<sup>48</sup>

**General Procedure for the Kinetic Runs.**

In an inert atmosphere glovebox a stock solution of the azetidinium **3.39** (*ca.* 0.05 M) with 40 μL toluene (as an internal standard) in CD<sub>2</sub>Cl<sub>2</sub> was prepared. An aliquot of known volume was added to a 1 mL volumetric flask followed by MeCN (9 μL), CpRu(dppm)H **3.30-H**, 1% TEMPO and the remaining solvent. Most of the solution was transferred to a J-Young tube and removed from the glovebox. The reaction was placed in a constant temperature bath. Periodically, it was cooled in ice water before obtaining NMR data on a Bruker 500 MHz

spectrometer. As the reaction produces two amine products, the disappearance of the azetidinium was monitored by integrating the triplet at  $\delta$  5.9 against the toluene methyl peak at  $\delta$  2.34. Data were plotted and fitted on KaleidaGraph software.

The data used to generate plot used to generate Fig. 3.4 (which confirmed that the reaction between azetidinium cation and ruthenium hydride is second-order overall and first-order with respect to each reactant) is from the following set of experiments. At least three runs were conducted at each temperature; each points used to generate Fig. 3.4 was obtained by averaging the starting concentration and pseudo-first-order rate constant for the particular temperature.

Ru-H Concentration [ <b>3.30-H</b> ] (M)	Pseudo first-order rate constant (hr <sup>-1</sup> )
0.0780	0.371
0.0800	0.348
0.0802	0.334
0.0926	0.470
0.0953	0.423
0.0953	0.424
0.107	0.496
0.107	0.481
0.111	0.512
0.111	0.533
0.122	0.591
0.122	0.508
0.118	0.553
0.120	0.618

## Sample Error Analysis

As the reaction kinetics may be treated as pseudo-first-order, the direct measurements having an effect on the measured second-order rate constants are as follows: a) integral of the azetidinium triplet peak (to obtain the pseudo-first-order rate constant) and b) the average concentration of ruthenium hydride. Item a) is determined by measuring a1) integral of the azetidinium triplet peak and normalizing it against the c) integral of the toluene methyl peak. Item b) is derived from b1) initial concentration of ruthenium hydride and b2) final concentration of ruthenium hydride. As the calculation require only concentrations and not the absolute measurements, the accuracy of the 600  $\mu\text{L}$  reaction mixture does not affect accuracy of the aforementioned parameters.

For example, for the reaction at 50  $^{\circ}\text{C}$ ,  $45.6 \pm 0.5$  mg of Ru-H and  $40 \pm 1$   $\mu\text{L}$  of toluene were added to make  $1.00 \pm 0.01$  mL of stock solution, from which  $0.60 \pm 0.01$  mL of the solution were drawn into a J-Young NMR tube for the study.

For a) the integral of azetidinium triplet peak, as the value used the plot is derived from referencing the integrals of the azetidinium triplet against that of the toluene methyl peak (as an internal standard), the overall relative error for each value is  $(\frac{3}{100} + \frac{3}{100}) = 0.06$  (assuming  $\pm 3\%$  precision for each NMR integral). The pseudo-first-order rate constant from the exponential regression fit of the data is  $0.310 \text{ hr}^{-1}$ , or  $(8.6 \pm 0.4) \times 10^{-5} \text{ s}^{-1}$ ; and the associate standard deviation is  $0.015 \text{ hr}^{-1}$  or  $0.4 \times 10^{-5} \text{ s}^{-1}$ , representing 4.6% of the pseudo-first-order rate constant. Therefore, using the standard deviation as the associate error would appear to be reasonable.

For b1), the initial concentration of Ru-H is computed as

$$\frac{45.6 \pm 0.5 \text{ mg}}{(551.56 \text{ g/mol}) \times (1.00 \pm 0.01 \text{ mL})} = 0.0827 \pm 0.0827 \times (\frac{0.5}{45.6} + \frac{0.01}{1.00}) = 0.0827 \pm 0.002 \text{ M.}$$

For b2), the final concentration is determined by comparing the integral of the Ru-H peak to that of the internal standard used. The volume of the internal standard, 40  $\mu\text{L}$  of Toluene, is  $40 \pm 1 \mu\text{L}$ . NMR integration of the toluene peak and the ruthenium hydride peak is assumed to be  $\pm 3\%$ , which suggests that the relative error is  $(\frac{1}{40} + \frac{6}{100}) = 8.5\%$ . This means that the concentration of Ru-H in the last data point of the run has a spread that is 8.5% of 0.0742 M, or  $0.0742 \pm 0.0063 \text{ M}$ . The corresponding average concentration from the initial point of  $0.0827 \pm 0.0002 \text{ M}$  and the final point of  $0.0742 \pm 0.0063 \text{ M}$  is thus  $0.0785 \pm 0.0033 \text{ M}$ , thus suggesting an upper bound of 0.0818 M and a lower bound of 0.0752 M.

By dividing the pseudo-first-order rate constant of  $(8.6 \pm 0.4) \times 10^{-5} \text{ s}^{-1}$  by  $0.0785 \pm 0.0033 \text{ M}$ , one obtains

$$\frac{8.60 \pm 0.41 \text{ s}^{-1} \times 10^{-5}}{(0.0785 \pm 0.0033) \text{ M}} = (1.10 \pm 1.10 \times (\frac{41}{860} + \frac{33}{785})) \times 10^{-3} \text{ M}^{-1} \text{ s}^{-1} = 1.1 \pm 0.1 \times 10^{-3} \text{ M}^{-1} \text{ s}^{-1}.$$

### Catalytic Hydrogenation of Azetidinium **3.39** by CpRu(dppm)H.

*CAUTION: Always Shield Pressurized Vessels.* Inside an inert atmosphere glovebox, into an 1 mL volumetric flask vial was placed 0.11 mol. azetidinium perchlorate **3.39**, 0.022 mol. ruthenium hydride **3.30-H**, and 1 mg TEMPO. The reagents were dissolved in  $\text{CD}_2\text{Cl}_2$  to make 1.0 mL of solution, and 0.50 mL of this solution was transferred via syringe into a sapphire NMR tube, to which was subsequently added 0.020 mL toluene as an internal standard. The sapphire NMR tube was then pressurized to 150 psi  $\text{H}_2$  and subsequently placed in a 60  $^\circ\text{C}$  bath to proceed overnight. Reaction was stopped after 24 hours.

## References

1. Ghorai, M. K.; Shukla, D.; Bhattacharyya, A. *J. Org. Chem.* **2012**, *77*, 3740.
2. Bertolini, F.; Crotti, S.; Bussolo, V. D.; Macchia, F.; Pineschi, M. *J. Org. Chem.* **2008**, *73*, 8998.
3. ARNOTT, E., Alexander; CROSBY, J.; EVANS, M., Charles; FORD, J., Gair; JONES, M., Francis; LESLIE, K., William; MCFARLANE, I., Michael; SEPENDA, G., Joseph *WIPO Patent Application WO/2008/053221* **2008**.
4. Couty, F.; Drouillat, B.; Evano, G.; David, O. *Eur. J. Org. Chem.* **2013**, *2013*, 2045.
5. (a) Vargas-Sanchez, M.; Lakhdar, S.; Couty, F.; Evano, G. *Org. Lett.* **2006**, *8*, 5501; (b) Ma, S.-h.; Yoon, D. H.; Ha, H.-J.; Lee, W. K. *Tetrahedron Lett.* **2007**, *48*, 269.
6. Kenis, S.; D'hooghe, M.; Verniest, G.; Dang Thi, T. A.; Pham The, C.; Van Nguyen, T.; De Kimpe, N. *J. Org. Chem.* **2012**, *77*, 5982.
7. Drouillat, B.; Wright, K.; David, O.; Couty, F. *Eur. J. Org. Chem.* **2012**, *2012*, 6005.
8. Couty, F.; David, O.; Durrat, F.; Evano, G.; Lakhdar, S.; Marrot, J.; Vargas-Sanchez, M. *Eur. J. Org. Chem.* **2006**, *2006*, 3479.
9. (a) Couty, F.; David, O.; Drouillat, B. *Tetrahedron Lett.* **2007**, *48*, 9180; (b) Drouillat, B.; d'Aboville, E.; Bourdreux, F.; Couty, F. *Eur. J. Org. Chem.* **2014**, *2014*, 1103.
10. Alex, A.; Larmanjat, B.; Marrot, J.; Couty, F.; David, O. *Chem. Commun.* **2007**, 2500.
11. Couty, F.; David, O.; Durrat, F. *Tetrahedron Lett.* **2007**, *48*, 1027.
12. Leng, D.-H.; Wang, D.-X.; Pan, J.; Huang, Z.-T.; Wang, M.-X. *J. Org. Chem.* **2009**, *74*, 6077.
13. Lee, B. K.; Kim, M. S.; Hahm, H. S.; Kim, D. S.; Lee, W. K.; Ha, H.-J. *Tetrahedron* **2006**, *62*, 8393.
14. Bott, T. M.; West, F. G. *Heterocycles* **2012**, *84*, 223.
15. (a) Ghorai, M. K.; Das, K.; Kumar, A. *Tetrahedron Lett.* **2007**, *48*, 4373; (b) Ghorai, M. K.; Das, K.; Kumar, A.; Das, A. *Tetrahedron Lett.* **2006**, *47*, 5393.
16. Dwivedi, S. K. *Tetrahedron Lett.* **2007**, *48*, 5375.
17. Blakemore, D. C.; Chiva, J.-Y.; Thistlethwaite, I. *Synlett* **2011**, *2011*, 1101.
18. Domostoj, M.; Ungureanu, I.; Schoenfelder, A.; Klotz, P.; Mann, A. *Tetrahedron Lett.* **2006**, *47*, 2205.

19. O'Brien, P.; Phillips, D. W.; Towers, T. D. *Tetrahedron Lett.* **2002**, *43*, 7333.
20. Han, M.; Hahn, H.-G. *Bull. Korean Chem. Soc.* **2012**, *33*, 3867.
21. Higgins, R. H.; Faircloth, W. J.; Baughman, R. G.; Eaton, Q. L. *J. Org. Chem.* **1994**, *59*, 2172.
22. Durrat, F.; Sanchez, M. V.; Couty, F.; Evano, G.; Marrot, J. *Eur. J. Org. Chem.* **2008**, *2008*, 3286.
23. De Rycke, N.; David, O.; Couty, F. *Org. Lett.* **2011**, *13*, 1836.
24. Banks, H. D. *J. Org. Chem.* **2006**, *71*, 8089.
25. Dudev, T.; Lim, C. *J. Am. Chem. Soc.* **1998**, *120*, 4450.
26. (a) Brotzel, F.; Kempf, B.; Singer, T.; Zipse, H.; Mayr, H. *Chem. Eur. J.* **2007**, *13*, 336; (b) Mayr, H.; Patz, M. *Angewandte Chemie International Edition in English* **1994**, *33*, 938.
27. Bott, T. M.; Vanecko, J. A.; West, F. G. *J. Org. Chem.* **2009**, *74*, 2832.
28. Guan, H.; Saddoughi, S. A.; Shaw, A. P.; Norton, J. R. *Organometallics* **2005**, *24*, 6358.
29. Dong, G.; Teo, P.; Wickens, Z. K.; Grubbs, R. H. *Science* **2011**, *333*, 1609.
30. Olah, G. A.; Szilagyi, P. J. *J. Org. Chem.* **1971**, *36*, 1121.
31. (a) Ghorai, M. K.; Sahoo, A. K.; Kumar, S. *Org. Lett.* **2011**, *13*, 5972; (b) Ghorai, M.; Tiwari, D.; Kumar, A.; Das, K. *Journal of Chemical Sciences (Bangalore, India)* **2011**, *123*, 951; (c) Ghorai, M. K.; Nanaji, Y.; Yadav, A. K. *Org. Lett.* **2011**, *13*, 4256; (d) Bernhard, H. O.; Snieckus, V. *Tetrahedron* **1971**, *27*, 2091; (e) Ghorai, M. K.; Das, K.; Kumar, A.; Ghosh, K. *Tetrahedron Lett.* **2005**, *46*, 4103; (f) Ghorai, M. K.; Kumar, A.; Tiwari, D. P. *J. Org. Chem.* **2010**, *75*, 137.
32. (a) Guan, H.; Iimura, M.; Magee, M. P.; Norton, J. R.; Janak, K. E. *Organometallics* **2003**, *22*, 4084; (b) Guan, H.; Iimura, M.; Magee, M. P.; Norton, J. R.; Zhu, G. *J. Am. Chem. Soc.* **2005**, *127*, 7805.
33. Sixt, T.; Fiedler, J.; Kaim, W. *Inorg. Chem. Commun.* **2000**, *3*, 80.
34. Hembre, R. T.; McQueen, J. S.; Day, V. W. *J. Am. Chem. Soc.* **1996**, *118*, 798.
35. (a) Smith, K. T.; Roemming, C.; Tilset, M. *J. Am. Chem. Soc.* **1993**, *115*, 8681; (b) Ryan, O. B.; Tilset, M.; Parker, V. D. *J. Am. Chem. Soc.* **1990**, *112*, 2618.
36. Appel, R. *Angewandte Chemie International Edition in English* **1975**, *14*, 801.
37. Magee, M. P.; Norton, J. R. *J. Am. Chem. Soc.* **2001**, *123*, 1778.

38. Jordan, R. F.; Norton, J. R.
39. (a) Jessop, P. G.; Morris, R. H. *Coord. Chem. Rev.* **1992**, *121*, 155; (b) Heinekey, D. M.; Oldham, W. J. *Chem. Rev.* **1993**, *93*, 913.
40. Shaw, A. P.; Ryland, B. L.; Franklin, M. J.; Norton, J. R.; Chen, J. Y. C.; Hall, M. L. *J. Org. Chem.* **2008**, *73*, 9668.
41. (a) Kass, M. B.; Borsetti, A. P.; Crist, D. R. *J. Am. Chem. Soc.* **1973**, *95*, 959; (b) Crist, D. R.; Borsetti, A. P.; Kass, M. B. *J. Heterocycl. Chem.* **1981**, *18*, 991.
42. Connelly, N. G.; Geiger, W. E. *Chem. Rev.* **1996**, *96*, 877.
43. Shaw, A. P.
44. (a) Smith, K. T.; Røemming, C.; Tilset, M. *J. Am. Chem. Soc.* **1993**, *115*, 8681; (b) Jia, G.; Morris, R. H. *J. Am. Chem. Soc.* **1991**, *113*, 875; (c) Belkova, N. V.; Dub, P. A.; Baya, M.; Houghton, J. *Inorg. Chim. Acta* **2007**, *360*, 149.
45. Pangborn, A. B.; Giardello, M. A.; Grubbs, R. H.; Rosen, R. K.; Timmers, F. J. *Organometallics* **1996**, *15*, 1518.
46. Bruce, M.; Humphrey, M.; Swincer, A.; Wallis, R. *Aust. J. Chem.* **1984**, *37*, 1747.
47. Silvestri, R.; Artico, M.; La Regina, G.; Di Pasquali, A.; De Martino, G.; D'Auria, F. D.; Nencioni, L.; Palamara, A. T. *J. Med. Chem.* **2004**, *47*, 3924.
48. (a) Russell Bowman, W.; Stephenson, P. T.; Terrett, N. K.; Young, A. R. *Tetrahedron* **1995**, *51*, 7959; (b) Saidi, M. R.; M., N. *Monatshefte fuer Chemie* **2004**, *135*, 309.